PEOPLE'S DEMOCRATIC REPUBLIC OF ALGERIA

MINISTRY OF HIGHER EDUCATION AND SCIENTIFIC RESEARCH

FERHAT ABBAS UNIVERSITY-SETIF-1

INSTITUTE OF OPTICS AND PRECISION MECHANICS

THESIS

Submitted to obtain

3rd Cycle LMD DOCTORATE

Domain: Science and Technology

Faculty: Optics and Precision Mechanics

Specialty: Materials for optics and optoelectronics.

By

Abbas Farouq

Title

Contribution to the optimization of nano polishing process of optical materials

Discussed publicly : 25/09 /2025

Members of the assessment committee:

Chairman	**Ferria Kuider**	**Prof**	**F.A.U. Setif1**
Supervisor	**Nabil BELKHIR**	**Prof**	**F.A.U. Setif1**
Co-supervisor	**Edda Radlein**	**Prof**	**TU Ilmenau**
Examiner	**Christine Wünsche**	**Prof**	**TH Deggendorf**
Examiner	**Guessoum Assia**	**MCA**	**F.A.U. Setif1**

Acknowledgement

First and foremost, I would like to thank **Allah** for granting me the strength, patience, and perseverance to continue believing in myself throughout the challenges and obstacles I faced during my PhD journey.

I express my deep gratitude to **Professor Belkhir Nabil** for offering me the opportunity to work on this topic, for his valuable supervision, insightful advice, and for the enriching scientific discussions that guided me throughout this work.

My sincere thanks also go to all my professors at the **Institute of Optics and Precision Mechanics** for equipping me with strong theoretical knowledge and for their continuous support during my academic formation.

A special acknowledgment goes to **Professor Eddar Radlein** for her co-supervision of this thesis, for providing access to the necessary equipment and facilities, and for generously sharing her professional network and opportunities, which were instrumental in the successful realization of this study.

I would also like to express my thanks to **Professor Ferria Kouider**, who supervised me during my master's thesis. It was under his guidance that I was first introduced to the world of scientific research, a turning point that shaped the course of my academic and professional path.

I would like to sincerely thank all the jury members for accepting to be part of my thesis defense committee: **Professor Ferria Kuider, Professor Edda Rädlein, Professor Christine Wünsche, Professor Hamdi Amine and Dr. Guessoum Assia**. I also thank Professor **Christine Wünsche**, as part of this work was carried out within her research group.

Finally, I would like to thank my friend **Dr. Ilyas Bensalem** for his friendship and for all the valuable discussions we shared, both professionally and personally.

Dedication

I would like to dedicate this work to my **beloved family members**, especially my **parents**, for their unlimited and unconditional support, and for all the positive values they instilled in me since childhood. I am deeply grateful to my **two sisters, Rafika and Wafaa**, and to my **wife** for always being there for me and supporting me through every step of this journey.

Abstract

In Chemical Mechanical Polishing of optical glass (CMP) using ceria-based abrasives, maintaining particle stability and understanding the relationship between chemical and mechanical interactions are crucial for achieving consistent and reproducible polishing results. This study explores how glass composition, abrasive particle size, slurry aggregation, and polishing duration affect the slurry's behavior and polishing performance. Three types of optical glass: soda-lime-silicate, borosilicate, and fused silica, representing high, medium, and zero alkali content, were polished using 400 nm and 80 nm ceria abrasives. A significant increase in slurry pH was observed during the polishing of alkali-containing glasses with 400 nm abrasives, suggesting chemical dissolution of glass components into the slurry. In contrast, no measurable pH shift occurred when using 80 nm abrasives or polishing fused silica, indicating a strong dependence on both glass composition and abrasive size. Zeta potential analysis, particle size distribution, and SEM imaging revealed notable changes in particle aggregation behavior as a function of these parameters. To investigate the role of slurry aggregation, three slurries with controlled aggregation states (low, medium, and high) were prepared and used to polish fused silica and N-BK7. Material removal rate (MRR), surface roughness, and real-time electrical power consumption were monitored. Results showed a clear correlation between slurry aggregation and polishing performance, with higher aggregation generally leading to reduced MRR and poorer surface quality. Furthermore, extended polishing experiments demonstrated that ceria abrasives lose their sharpness over time, resulting in decreased removal efficiency and increased surface roughness. These findings highlight the importance of controlling not only the initial abrasive properties but also their evolution during polishing.

Keywords: Chemical Mechanical Polishing, Optical Glass, Ceria Abrasives, Particle Stability, Particle Size, Slurry Aggregation, Glass Composition, pH Variation, Material Removal Rate, Surface Roughness, Polishing Efficiency, Abrasive Evolution.

Résumé

Dans le polissage chimico-mécanique (CMP) du verre optique avec des abrasifs à base de cérium, la stabilité des particules et l'interaction entre effets chimiques et mécaniques sont essentielles pour des résultats reproductibles. Cette étude analyse l'influence de la composition du verre, de la taille des abrasifs, de l'agrégation du slurry et du temps de polissage. Trois verres (silicate sodocalcique, borosilicate et silice fondue) ont été polis avec des particules de 400 nm et 80 nm. Une augmentation du pH a été observée uniquement pour les verres contenant des alcalins avec des particules de 400 nm, indiquant une dissolution chimique. Aucun changement n'a été constaté avec les particules de 80 nm ou la silice fondue. Les analyses ont montré que l'agrégation influence fortement les performances: une agrégation élevée réduit le taux d'enlèvement de matière (MRR) et dégrade la qualité de surface. De plus, les abrasifs perdent leur efficacité avec le temps, augmentant la rugosité. Ces résultats soulignent l'importance de contrôler l'évolution des abrasifs durant le polissage

Mots-clés : Polissage chimico-mécanique, Verre optique, Abrasifs à base de cérium, Stabilité des particules, Taille des particules, Agrégation du slurry, Composition du verre, Variation du pH, Taux d'enlèvement de matière, Rugosité de surface, Efficacité du polissage, Évolution des abrasifs.

ملخص

في التلميع الكيميائي الميكانيكي للزجاج البصري باستخدام مواد كاشطة قائمة على السيريوم، تُعد استقرار الجسيمات والتفاعل بين التأثيرات الكيميائية والميكانيكية أمرين أساسيين لتحقيق نتائج قابلة للتكرار .تحلل هذه الدراسة تأثير تركيب الزجاج، وحجم المواد الكاشطة، وتجمع الملاط، ومدة التلميع. تم تلميع ثلاثة أنواع من الزجاج)سيليكات الصودا والجير، البوروسيليكات، والسيليكا المنصهرة (باستخدام جسيمات بحجم أربعمائة نانومتر وثمانين نانومتر .لوحظت زيادة في قيمة الأس الهيدروجيني فقط في الزجاج المحتوي على القلويات عند استخدام جسيمات بحجم أربعمائة نانومتر، مما يشير إلى حدوث ذوبان كيميائي .لم يُلاحظ أي تغير عند استخدام جسيمات بحجم ثمانين نانومتر أو عند تلميع السيليكا المنصهرة ,أظهرت التحليلات أن التجمع يؤثر بشكل كبير على الأداء، حيث يؤدي التجمع العالي إلى تقليل معدل إزالة المادة وتدهور جودة السطح .بالإضافة إلى ذلك، تفقد المواد الكاشطة كفاءتها مع مرور الوقت، مما يزيد من خشونة السطح .تسلط هذه النتائج الضوء على أهمية التحكم في تطور المواد الكاشطة أثناء التلميع..

الكلمات المفتاحية: التلميع الكيميائي الميكانيكي، الزجاج البصري، مواد كاشطة من السيريوم، استقرار الجسيمات، حجم الجسيمات، تجمع الملاط، تركيب الزجاج، معدل إزالة المادة، خشونة السطح، كفاءة التلميع، تطور المواد الكاشطة.

Table of contents

General Introduction *4*

Chapter1. Theoretical background *8*

1.1 Introduction 8

1.2 Common Polishing Methods 9

1.2.1 Contact Polishing 8

1.2.2 Non-contact polishing 13

1.3 Why chemical mechanical polishing? 16

1.3.1 Effect of slurry properties on polishing 18

1.3.2 Ceria-ceria particle interactions. 23

1.3.3 Dissolution of glass compounds on the polishing slurry 26

1.4 Conclusion 30

Chapter2. Background on polishing slurries and their characterization *31*

2.1 Introduction 31

2.2 POLISHING POWDERS 32

2.2.1 COLLOIDAL SILICA SLURRY 32

2.2.2 Diamond-based slurry 33

2.2.3 Alumina-based slurry 34

2.2.4 Cerium oxide 35

2.3 Characterization techniques of polishing powders 39

2.3.1 Dispersing and Deagglomeration 39

2.3.2 Particle size distribution 42

2.3.3 Large particle count 42

2.3.4 Zeta potential measurements 44

2.3.5 Sedimentation method 47

2.4 Conclusion 49

Chapter3. Investigation of the Impact of Optical Glass composition on Ceria Slurry Stability during Chemical Mechanical Polishing process. *50*

3.1 Introduction 50

3.2 Materials and Methods 52

3.2.1 Borosilicate glass production 52

3.2.2 The polishing process 55

3.3 Material removal and surface roughness 59
3.3.1 Effect of Particle Size on Material Removal 59
3.3.2 Effect of Abrasive Size on Surface Roughness 61
3.4 pH MEASUREMENTS 61
3.4.1 pH Stability using 80 nm ceria abrasives. 62
3.4.2 pH modification using 400nm ceria abrasives. 62
3.4.3 pH calculation. 64
3.5 Zeta potential measurements 64
3.5.1 Zeta potential of 400 nm particles. 64
3.5.2 Zeta potential of 80 nm particles 65
3.5.3 Zeta potential of 400 nm ceria particles after fused silica glass polishing 66
3.5.4 Effect of electrolyte nature on zeta potential 69
3.6 Particle size distribution measurements 71
3.6.1 Particle size distribution measurements of the 80 nm particles 71
3.6.2 Particle size distribution measurements of 400 nm particles 72
3.7 Correlation between the sedimentation, particle size distribution (PSD), and SEM images. 71
3.8 Conclusion 76
Chapter4. Effect of slurry parameters on the polishing results 76
4.1 Introduction 76
4.2 Investigation of Slurry Aggregation Effects on CMP Process with Electrical Power Sensor Utilization. 77
4.2.1 Preparation of slurries with different aggregation states 77
4.2.2 Machine and Polishing Process 80
4.2.3 Material Removal Rate 83
4.2.4 Surface Roughness 85
4.2.5 Power measurement 86
4.2.6 Correlation between power measurements and polishing results measurements 91
4.3 Effect of the long-time polishing on particle size 92
4.3.1 Experimental procedure 92
4.3.2 PH measurement of the slurry 94
4.3.3 Surface roughness and material removal measurements throughout the polishing process 97
4.3.4 Particle size distribution measurements 99
4.4 Conclusion 100

General conclusion *100*
References ……..…….*102*

General introduction

Optical materials, in the most general sense, can be defined as materials whose function is to alter or control electromagnetic radiation in the ultraviolet (UV), visible, or infrared (IR) spectral regions. Such materials are fabricated into optical elements such as lenses, mirrors, windows, prisms, polarizers, detectors, and modulators, etc. They can be used to refract, reflect, transmit, disperse, polarize, detect, and transform light.[1]

With the extensive application of optical parts in many high-tech fields such as high-power lasers, space optics, and aerospace, the requirements for the surface quality of optical parts are also increasing, which requires not only high surface qualities but also low defects, including low subsurface damage and strict wavefront errors. As an essential link in precision and ultraprecision optical manufacturing, various surface polishing methods and techniques have always attracted researchers' continuous study and exploration. [2]

Chemical-mechanical polishing (CMP) of optical glasses is extensively used and serves as the foundation for numerous high-precision polishing procedures. The pads, slurries, and glass materials utilized in the polishing process possess diverse properties. In particular, the slurry is comprised of various components, such as abrasive particles, chemical additives, and slurry liquids, which can be altered over time. Consequently, it significantly influences the CMP performance, including the material removal rate (MRR), accuracy, and scratch behavior [3].

Cerium oxide (CeO_2) stands out as one of the most effective agents for polishing optical glass, producing high-quality surfaces [4, 5], those particles are widely used in precision chemical mechanical polishing (CMP) fields, such as thin film transistor liquid crystal display (TFT-LCD) glass substrates and integrated circuits [6-12]. Its polishing performance surpasses that of other materials, including typical abrasive materials like SiO_2 and Al_2O_3; it delivers a higher MRR while maintaining excellent material surface quality. [13]. The high polishing efficiency of cerium oxide stems not only from mechanical abrasion but also from its chemical properties. The polishing of glass and certain other surfaces is not only a purely mechanical process; it also involves a complex set of chemical interactions between the polishing agent, the polished surface, and the polishing medium [14-17].

The high chemical reactivity of ceria particles improves the material removal of the polished substrates. This chemical reactivity remains difficult to quantify and control because it depends on multiple factors. Including the nature and concentration of additives to the slurry [18-21], the concentration of Ce^{3+} ions and oxygen vacancy sites on the particle's surface [18,5,22, 23], and the size of abrasives [24, 25]. Those factors will affect directly affect the dispersion behaviors of ceria (CeO_2) particles in polishing slurries, which directly influence surface quality [26]. Therefore, bad dispersion behavior will lead abrasives to aggregate and precipitate, negatively affecting the polishing results.

Many researchers have tried to understand the role of slurry properties and their effect on the material removal rate and surface roughness. Cao et al. [27] connected slurry pH to material removal rate (MRR) by explaining that under both acidic and alkaline conditions, chemical reactions disrupt the glass structure, leading to increased MRR. In alkaline slurries, higher pH promotes the breakdown of Si-O bonds in silicate glasses and the displacement of metal ions in phosphate glasses, accelerating surface dissolution and material removal. Softer glasses like Nd-doped phosphate glass exhibit higher MRR due to their weaker structure, while harder glasses like fused silica show lower MRR. Thus, MRR increases with pH, especially when the slurry reaches a pH of 9. In their study, the authors focused primarily on the interaction between slurry pH and the workpiece surface without examining the effects of pH on key slurry properties such as stability, particle size distribution, and particle concentration. However, numerous other studies have emphasized the importance of optimizing the initial slurry parameters to enhance abrasive performance. These studies have explored the use of a wide variety of additives to stabilize the slurry, control particle aggregation, and maintain a consistent particle concentration, ultimately aiming to achieve optimal polishing efficiency across different glass types. The study of Venkataronappa et al. [28] investigated methods for improving the dispersion stability of micron-sized ceria particles in glass polishing processes by using polyacrylic acid (PAA) as a dispersant. PAA effectively stabilizes ceria particles in slurries, preventing aggregation and ensuring even particle distribution on the glass surface, which is critical for achieving smooth, high-quality finishes in precision glass manufacturing. [29, 30]. As an anionic surfactant, PAA interacts with the positively charged ceria particles through electrostatic attraction. Upon adsorption onto the ceria surface, the carboxylic groups (–COOH) in PAA deprotonate, forming negatively charged

carboxylate (–COO–) groups. This deprotonation increases the repulsive forces between particles, improving dispersion stability.

Similar dispersants, such as poly methyl methacrylate (PMMA), have also been shown to stabilize ceria particles by providing a steric hindrance that prevents agglomeration, resulting in a stable slurry and effective polishing [31]. Additionally, non-ionic surfactants like polyvinylpyrrolidone (PVP) and polyethylene glycol (PEG) have been used for their broad material compatibility and ability to prevent particle clustering [18]. Organic acids, such as acetic acid, propionic acid, lactic acid, and phytic acid, are often used as pH-adjusting agents to enhance slurry stability further [5-22].

These large variations of additives demonstrate the critical effect of slurry parameters in the polishing process and their role in achieving good and predictable results.

This thesis is divided into four chapters. In the first chapter, a theoretical background was presented, where we demonstrated the main techniques used for the polishing process. Furthermore, the choice of CMP polishing over other CMP techniques, the effect of slurry parameters on the polishing process, particle-particle interaction, and the solubility of optical glass compounds were all demonstrated with the goal of having a theoretical overview and making a link between slurry parameters and its chemistry and how it can affect the polishing results.

In the second chapter, we present the common polishing powders used for optical glass polishing, with a specific focus on cerium oxide-based abrasives, to understand what makes them one of the best and most effective polishing powders. For this purpose, different characterization techniques are employed to analyze the behavior of particles before, during, and after the polishing process. Consequently, this chapter introduces the most significant methods for powder characterization.

The third chapter represents the first part of the experimental work, where the impact of optical glass composition on ceria slurry stability during the chemical mechanical polishing process was investigated, in this study, a correlation between glass compositions, the amount of the material removed during the process and the variation of slurry chemistry was established.

While the third chapter showed that glass composition can, under certain conditions, affect slurry stability by changing its initial chemical configuration, the first part of the fourth chapter investigates how variations in slurry chemistry affect polishing results. Additionally, collaboration with the Campus for Optical Technology in Teisnach was conducted to complement the study by using a motor power sensor, aiming to compare slurry performance under different aggregation states during the process.

To further explore slurry parameters and their impact on polishing results, the wear behavior of ceria particles is analyzed in the second part of the fourth chapter. Glass was polished for extended periods, and comparisons between polishing results and particle size distribution measurements over time provided valuable insights into how abrasive wear influences polishing efficiency.

Finally, in the general conclusion of the thesis, a global overview of the contribution of our work in the field of optical material finishing is demonstrated, with some suggestions for further optimizations.

Chapter1. Theoretical background

1.1 Introduction

Nowadays, the surface quality of the material is crucial for industry and science. With the development of microelectronics and optics, the demand for surface quality has become more and more rigorous, making optical surface polishing more and more critical [32].

With the extensive application of optical parts in many high-tech fields such as high-power laser, space optics, and aerospace, the requirements for the surface quality of optical parts are also increasing, which requires not only high surface qualities but also low defects, including low subsurface damage and strict wavefront errors. As an essential link in precision and ultra-precision optical manufacturing, various surface polishing methods and techniques have always attracted researchers' continuous study and exploration [2]

In this chapter, various techniques and methods used for polishing are explored. These methods are classified based on whether they involve contact or non-contact modes between the polishing tool and the workpiece. The texts highlight the importance of the chemical mechanical polishing (CMP) process in the optical elements industry, glass-ceria slurry interactions during CMP, and ceria-ceria particle interactions to review existing research on particle aggregation and slurry stability. The chapter also covers the limited studies that have addressed changes in slurry parameters during the polishing process.

1.2 Common Polishing Methods

1.2.1 Contact Polishing

Contact polishing refers to the processing method in which the polishing pad contacts the polished surface in the processing process. During processing, the mechanical, chemical, or electrochemical action is used to reduce the roughness of the surface to obtain a bright and smooth surface. Contact polishing usually exerts a certain pressure on the polished surface, which can achieve high material removal efficiency. It is the most common application form in traditional polishing.

1.2.1.1 Bowl Feed Polishing

Bowl feed polishing (BFP) is an ultrasmooth surface processing method proposed by Dietz and Bennett based on traditional polishing equipment and techniques to develop UV optics in the United States in the 1960s, and the ultrasmooth surface of RMS 0.3 nm is obtained on fused quartz.

As shown in Figure 1, the contact surface between the polishing pad and the workpiece is immersed in the polishing fluid, the polishing pad rotates, and the workpiece moves horizontally while rotating to ensure that each point of the polished surface is in random contact with each point of the working surface of the polishing pad. The stirrer keeps stirring to ensure that nearly all of the polishing mixture particles remain suspended which makes the abrasive particles precipitate continuously on the polishing pad to form a tiny blade to cut the workpiece [33].

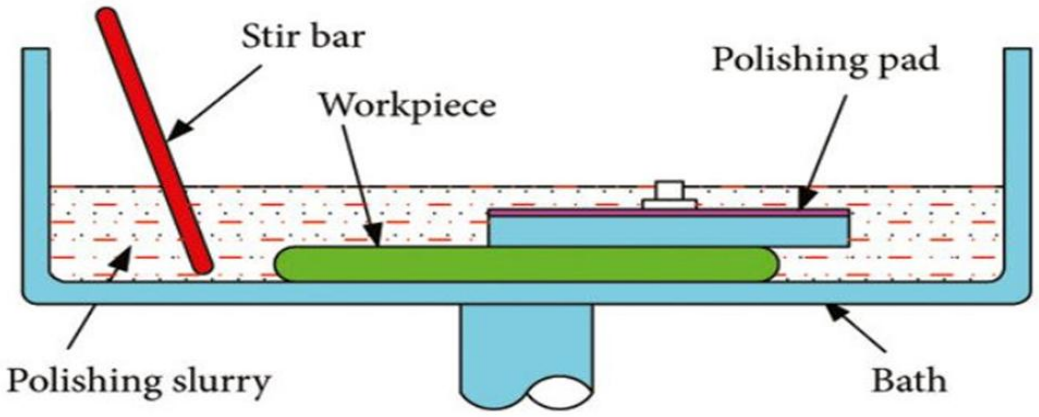


Figure 1: Bowl feed polishing principle.

1.2.1.2 Bonnet Polishing

Bonnet polishing is a computer controlled sub-aperture polishing process that actively controls the position and orientation of a spinning, inflated, membrane tool (the 'bonnet') as it sweeps through the polished surfaces [2]

In 2000, Zeeko Company and Walker et al. in the UK put forward bonnet-polishing technology and produced the IRP-200 polishing machine tool. The surface profile accuracy and surface roughness can reach 80 nm (PV) and 3 nm (Ra), respectively, and the material removal rate of rough polishing can reach 2 mm^3 /min. The processing principle is shown in Figure 2. (The technology uses a spinning, bulged, and compliant tool covered with a suitable polishing surface (cloth, polyurethane, etc.). By controlling the axial position of the tool and its internal pressure, the tool contact area (“spot size”) and polishing pressure can be modulated independently and the process requirements of workpieces with different curved surfaces and sizes can be met, which not

only ensures the polishing efficiency but also improves the machining accuracy. It is especially suitable for machining aspheric or freeform surfaces [34]

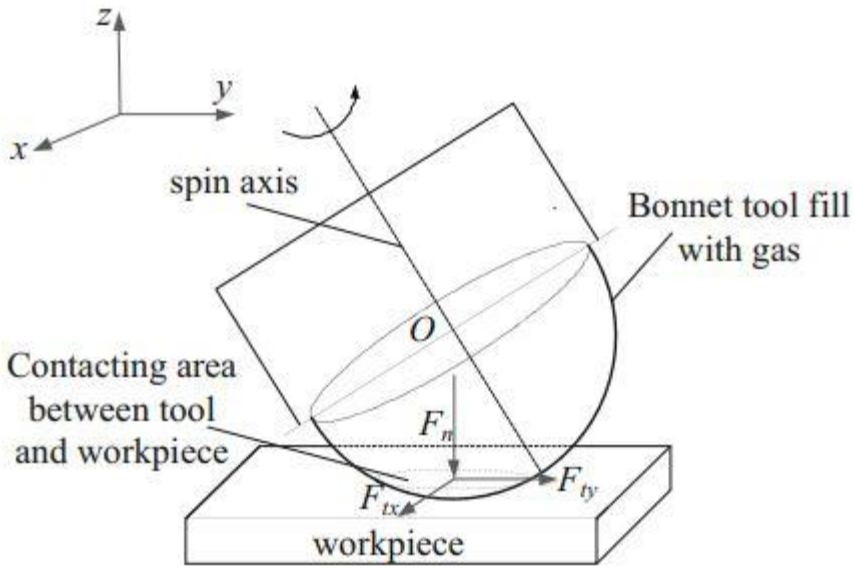


Figure 2: Typical bonnet polishing process. [35]

1.2.1.3 Magnetorheological polishing

Magnetorheological finishing (MRF) is an advanced precision polishing technology that utilizes magnetorheological fluids to achieve ultra-smooth surfaces on various materials, particularly optical components. The process involves the use of a magnetorheological fluid, which consists of magnetic particles suspended in a carrier liquid. When subjected to a magnetic field, the viscosity of the fluid changes, allowing it to behave like a solid under pressure while flowing like a liquid when not under stress. This unique property enables precise control over the material removal process, facilitating deterministic polishing that can achieve nanometer-scale surface finishes. MRF is particularly effective for complex geometries and can be adapted to various materials, including glass and ceramics, making it a versatile choice in manufacturing high-performance optical elements. The technology has garnered significant attention in recent years, with ongoing research focusing on optimizing process parameters and expanding its applications in ultra-precision machining. [36-38].

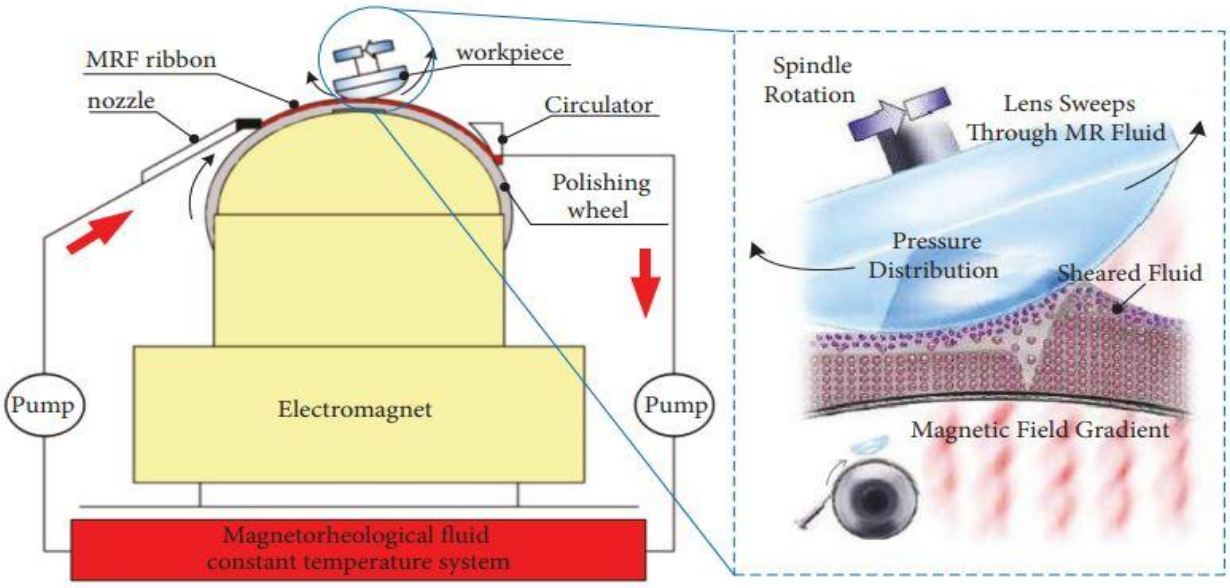


Figure 3: Magnetorheological finishing principle. [2]

The principle of magnetorheological finishing (MRF) is shown in Figure 3. As a quasi-contact polishing, magnetorheological finishing (MRF) is developed from magnetic medium-assisted polishing, which can realize the flexible polishing of workpieces. In the process of polishing, the abrasive particles in the magnetorheological fluid adhere to the magnetic medium and form a chain-like structure under the action of magnetic fields, which will turn the polishing liquid into a viscoelastic Bingham medium and form a ribbon bulge. When the medium moves relative to the workpiece driven by the polishing pad, the shearing force is generated on the surface of the workpiece, and the material on the workpiece surface is removed by the combined action of the chemical and rheological forces. [2]

1.2.1.4 Chemical mechanical polishing

Chemical Mechanical Polishing (CMP) is a sophisticated surface finishing technique that combines both chemical and mechanical processes to achieve exceptionally smooth and flat surfaces, particularly in the manufacturing of optical glass and semiconductor devices. The CMP process utilizes a slurry composed of abrasive particles, often cerium oxide or silica, suspended in a chemical solution that interacts with the substrate material. During polishing, a rotating polishing pad applies pressure to the glass surface (Figure 4), allowing the mechanical action of the abrasives to physically remove material while the chemical components facilitate the etching or softening of the glass, enhancing the overall removal efficiency. Research has shown that variations in slurry

composition, such as ceria concentration, can significantly affect the material removal rate and surface quality; for instance, higher concentrations of ceria have been linked to improved polishing performance due to enhanced chemical interactions with the glass surface [39]. Moreover, optimizing process parameters such as pad type, pressure, and rotational speed is essential for minimizing defects and maximizing yield rates during CMP operations. Research indicates that the characteristics of polishing slurries, including the size and type of abrasive particles, play a pivotal role in determining the overall polishing performance. Adjustments to slurry properties can lead to significant variations in material removal rates and defect densities. The interplay of chemical interactions between the slurry components and mechanical actions from the abrasives is vital for achieving high-quality finishes while maintaining production efficiency. [40, 41]

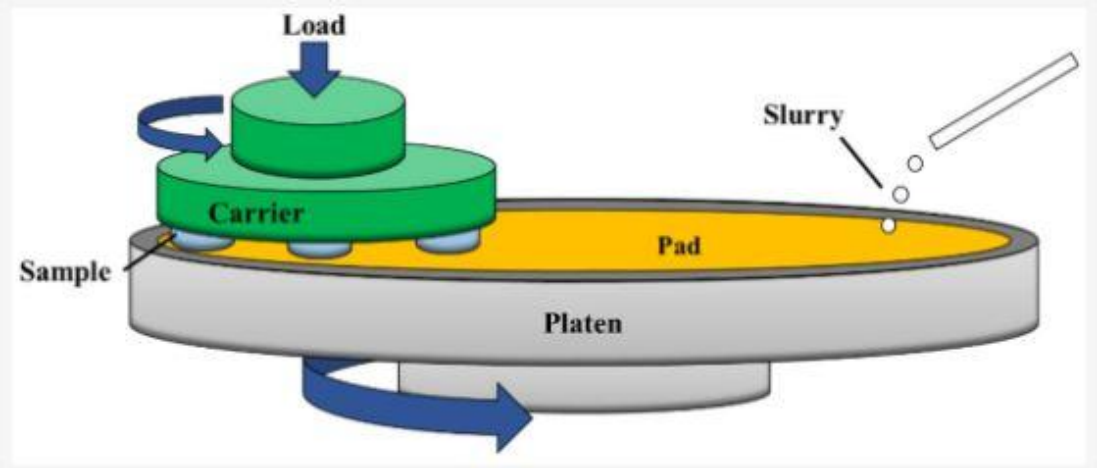


Figure 4: Polishing schematic diagram. [42]

1.2.1.5 Bounded Abrasive Polishing

Bound abrasives are a key component of fixed abrasive polishing processes. These abrasives are embedded within a matrix, such as a resin or metal, which provides a stable and controlled environment for the polishing process. The matrix material can also influence the polishing performance by affecting factors like particle distribution, abrasive exposure, and the overall mechanical properties of the polishing wheel.

By using bound abrasives, it is possible to achieve a more consistent and predictable polishing process. The matrix material helps to maintain the abrasive particles in a specific arrangement, ensuring that they are evenly distributed across the polishing surface. This can lead

to improved surface quality and reduced defects. Additionally, the matrix can provide a certain level of support to the abrasive particles, preventing them from becoming dislodged or damaged during the polishing process [43].

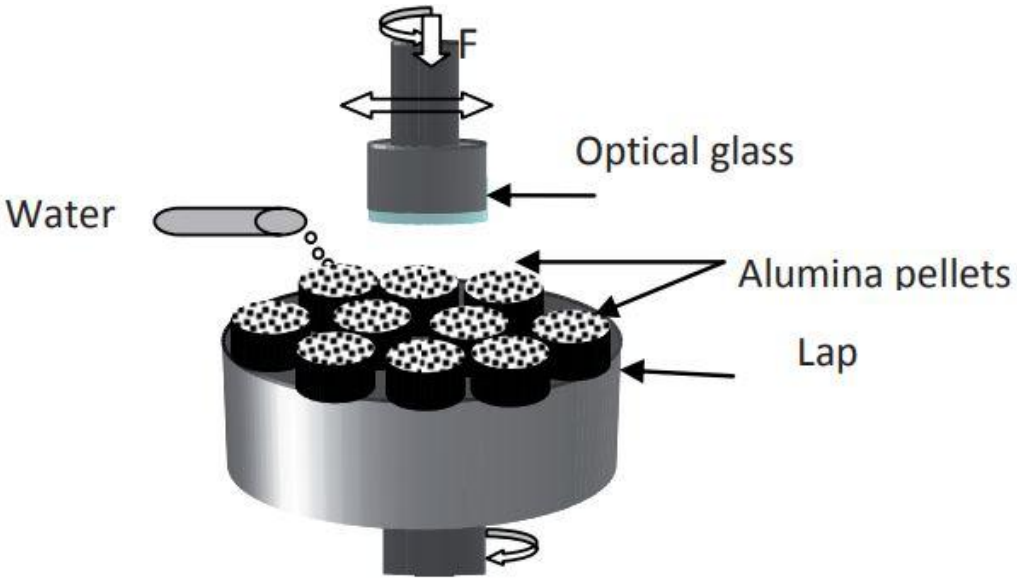


Figure 5: Fixed abrasives polishing illustration. [44]

1.2.2 Non-contact polishing

Noncontact polishing refers to a polishing method in which the polishing pad does not come into contact with the polished surface. It mainly depends on the polishing fluid or ions to erode the machined surface to obtain high surface accuracy and improve subsurface damage. This type of technology is characterized by getting a complete final structure without mechanical damage, low surface roughness, and high surface precision.

1.2.2.1 Ion Beam Polishing

Ion beam polishing (IBP) is a process of deterministic shape modification polishing through surface shape error corrections, which is developed based on atomic sputtering theory. Its principle is shown in Figure 6. In the vacuum environment, the ion source controlled by the numerical control system emits ions with a specific energy to bombard the polished surface. These ions continuously collide with the atoms of the polished surface for energy exchange. When the

polished surface atoms obtain the energy to get rid of the lattice binding, the physical sputtering effect occurs to realize the atomic level machining of the workpiece. [2]

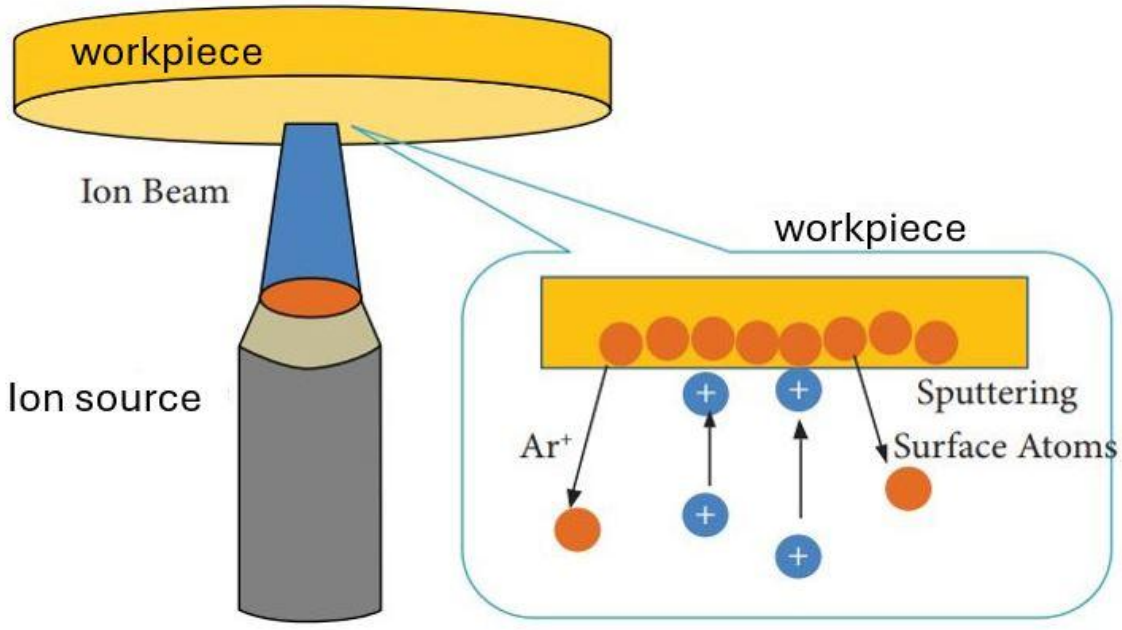


Figure 6: Ion beam polishing principle. [2]

1.2.2.2 Laser polishing

This technique is based on melting a thin layer of the material surface and smoothing it under surface tension. Lasers are applied to the surface of the material and melt the mountains and valleys on it to make a flat surface. The depth of the melted zone is 20-100 micrometers, and the surface tension of the melted material ensures that it will reset evenly. The peak-to-valley of the roughness should not be higher than the depth of the melted zone, and the surface should be kept molten for a long time. The result is a shiny surface, but not as smooth as what may be achieved by hand polishing.

There are many applications for this technique, but it is mainly developed for use simply on the inside surfaces of the molds that cannot be polished by hand or other techniques. The molds can be polished by lasers ten times faster than polishing by hand, which has a rate of 0.1 cm^2/min

[45]. It is also suitable for glass materials, which can be polished quickly compared to other techniques. This process requires no abrasives or surface-adapted tools for polishing [46].

1.2.2.3 Atmospheric pressure plasma polishing

Atmospheric pressure plasma polishing (APPP) is an innovative technique that utilizes atmospheric pressure plasma jets to achieve high-precision surface finishing on optical components. The process is particularly effective for generating optical freeform surfaces and correcting figure errors, making it a promising alternative to traditional mechanical-abrasive polishing methods. The process involves the generation of plasma containing reactive species, which chemically react with the surface atoms of the material being processed, leading to material removal and a polished finish. This technique offers several advantages, such as non-contact processing, fine-scale control, and a wide range of applications [47]. The principle of atmospheric pressure plasma polishing is shown in Figure 7

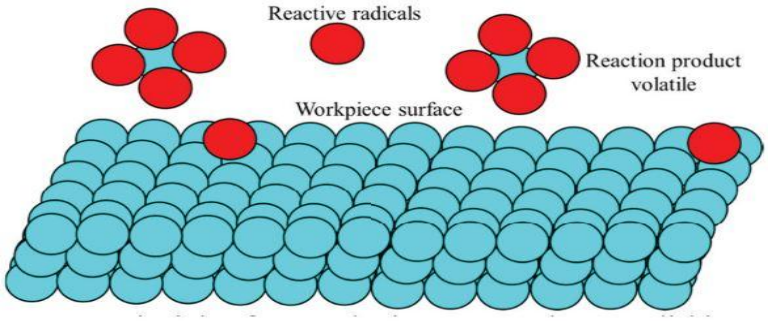


Figure 7: Principle of atmospheric pressure plasma polishing. [48]

1.2.2.4 Fluid jet polishing (FJP)

In fluid jet polishing, two main techniques are used. the abrasive water jet AWJ where the abrasive is added to the fluid when it is passing through the nozzle to form a jet of the mixture. Water is used as the fluid, and various kinds of abrasives with different weight percentages are added to it. The optical glass can be polished by this technique to decrease the roughness to 25 nm RMS. [49] Figure 8 shows the principal entrainment of AWJ. The second technique is the Abrasive slurry jet (ASJ). The principle of the two techniques is similar, and the difference is that the abrasives and water are premixed to form a suspension (slurry) to increase the power density compared to the AWJ process. The increasing power density is due to the fact that the momentum

transfer between the water and the abrasives is more efficient making it 5 times faster than AWJ [50].

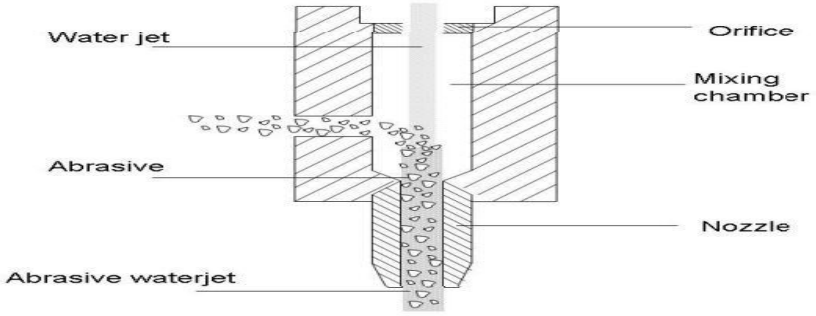


Figure 8: Principle of AWJ. [51]

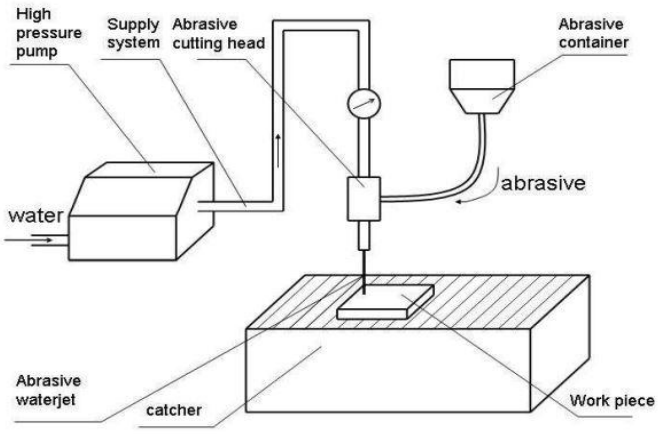


Figure 9: Major components of AWJ. [51]

1.3 Why chemical mechanical polishing?

At the time CMP was invented, it was a revolutionary technology that solved two major issues and would enable future generations of technology [52]. Chemical mechanical polishing is considered one of the most prominent and most efficient methods of glass polishing, it is an ultra-precision polishing technique for hard and brittle materials [53-57]. The efficiency and effectiveness of CMP are entirely based on the processing parameters to which it is subjected to including polishing pressure, rotation speed of the tool, slurry parameters, slurry fed rate, and the polishing pad [55, 58, and 59]. Polishing involves chemical and mechanical actions taking place at the workpiece–polisher interface, which leads to material removal. Hence, optimizing the process parameters improves the efficiency of polishing and makes the process economically

viable [60]. In the five years between 2014 and 2019; Lee and Sung summarized the research topics related to CMP published in Elsevier DB and Springer DB (243 papers in 64 journals) [61] see (table 2).

Research topic	Papers	
	No.	%
Process analysis/development, theoretical model, MRR (material removal rate)	59	24.3
Chemical effect, Slurry composition/ properties	58	23.9
Abrasive/Particle (material, structure, properties)	56	23.0
Film/Substrate (material, structure, properties)	28	11.5
Post-processing, Cleaning	19	7.8
Tribological approach (friction, wear, lubrication, scratch, contact mechanics)	13	5.3
Pad (material, structure, properties)	10	4.1
Total	243	100

Table 1: CMP research topics published in some major academic journals in the last 5 years (2014~2019; Total 243 papers in 64 journals). [61]

Most of the studies consist of understanding the mechanisms of material removal and improving CMP efficiency. However, recent changes in the global climate environment have increased interest in the sustainability of the semiconductor and CMP industries. Academics are also researching various methods to assess the impact of CMP processes on the environment and reduce the environmental burden. Further, the interest in improving process efficiency for reducing energy consumption in the processes is increasing.

In another study by Lee et al [62], the future of the CMP process was discussed, and more than 100 studies were examined including 17 % of the studies on the environmental burden and 38% on CMP wastewater treatment. Therefore, they summarized the future of CMP on three keywords: expansion, digitalization, and sustainability as shown in Figure 15.

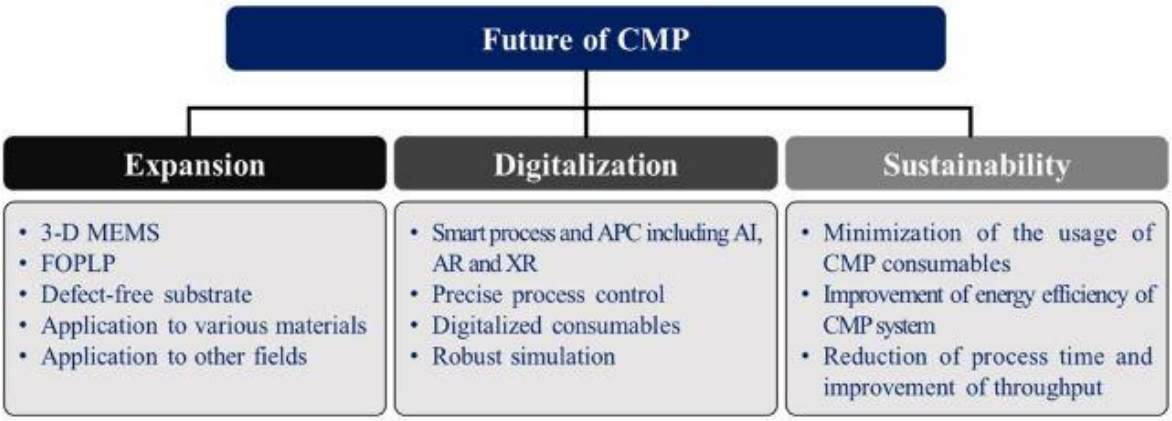


Figure 10: Summary of the future of CMP where 3-D MEMS is three-dimensional microelectromechanical systems, FOPLP is the fan-out panel level packaging, APC (Advanced Process Control), AR (Augmented Reality) and XR (Extended Reality). [62]

As a general overview, **C**hemical Mechanical Polishing (CMP) remains a critical technology for achieving ultra-precision surfaces in various materials. It involves a combination of mechanical and chemical actions to remove material, enabling the production of high-quality components. Key factors influencing CMP performance include polishing pressure, rotation speed, slurry parameters, and polishing pad. While recent research has focused on improving efficiency and sustainability, CMP remains a vital technology for industries like semiconductors and optics.

1.3.1 Effect of slurry properties on polishing

Abrasive CMP slurry particles provide the mechanical action during the polishing process. The chemically modified surface layer of the sample is abraded continuously with the submicron size slurry abrasives, resulting in material removal. To achieve an optimal polishing performance with minimal deformations and good planarity, it is necessary to optimize the rates of chemical modification and mechanical abrasions. The intensity of the mechanical abrasion also varies with the slurry particle size and concentration as these factors determine the load applied per particle. Furthermore, the frequency of abrasion depends on the number of slurry abrasives in contact with the sample surface. Therefore, slurry particle size and concentration, as well as the particle size distribution are very important factors in determining the polishing performance and should be studied carefully to understand the CMP process. A small variation in the slurry particle size distribution by oversize particle contamination or due to slurry aggregation may result in major

changes in the particle-substrate interactions. Consequently, the material removal rate response may vary, resulting in poor process control and an increase in the number of surface deformations. [63]

1.3.1.1 Effect of particle size

The size of polishing particles has a significant effect on the material removal rate (MRR) in the chemical mechanical polishing (CMP) process. As particle size increases, the MRR generally increases as well due to the larger particles applying higher localized pressure on the glass surface, leading to more efficient material removal. However, once the particle size reaches a certain threshold (e.g., 2.6 μm in the provided study), the MRR begins to decrease, as shown in Figure 11. This is likely because larger particles tend to settle quickly in the slurry, reducing the number of active particles making contact with the surface, which in turn diminishes the overall material removal efficiency. Therefore, optimizing particle size is crucial for maintaining a high MRR over extended polishing times.[27]

In terms of surface roughness, particle size plays a pivotal role in scratch formation and surface roughness. Larger particles have a higher removal ability, which increases the likelihood of generating scratches on the surface of the glass, particularly brittle and mixed scratches that include both plastic modifications and cracks. As the particle size increases, the surface roughness also tends to increase, with larger particles creating more pronounced surface irregularities [64]. For instance, rough structures appear on K9 glass and Nd-doped glass when polished with larger particles, while fused silica, being harder and more resistant, shows fewer scratches and a smoother surface despite the larger particles. Reducing the particle size is, therefore, an effective way to minimize scratch density and improve surface smoothness.[27]

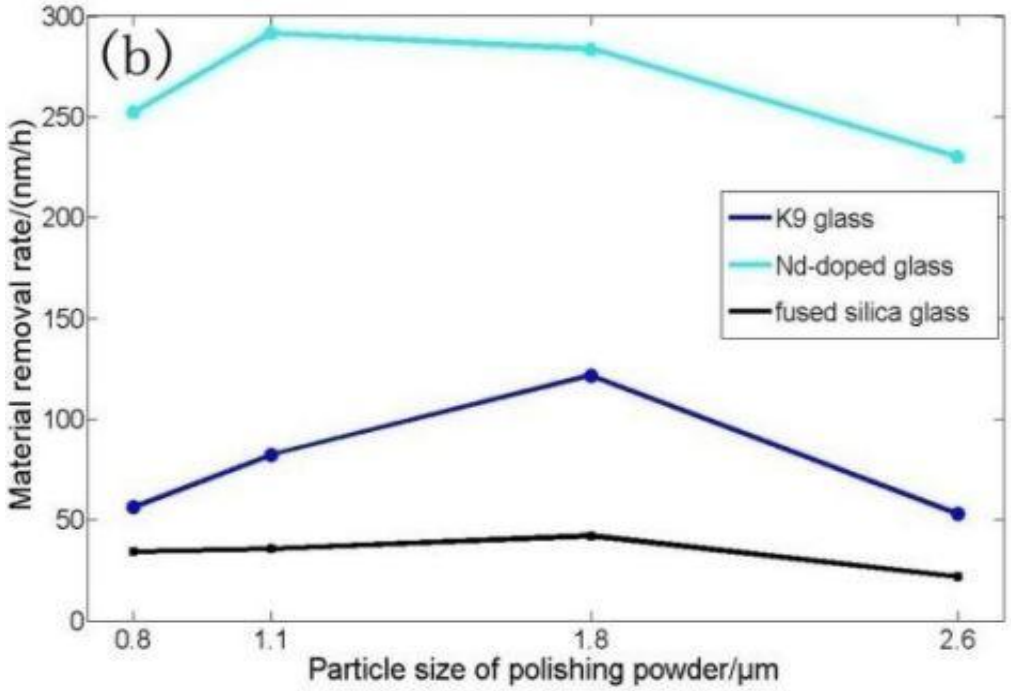


Figure 11: MRR of three kinds of glass polished by different sizes of powder. [27]

1.3.1.2 Effect of particle concentration

The concentration of abrasives in the Chemical Mechanical Polishing (CMP) process significantly influences the polishing performance of glass substrates as the concentration of abrasive particles increases, the material removal rate rises steadily due to the greater number of active particles interacting with the glass surface as shown in Figure 12, which enlarges the contact area and enhances the polishing process. However, this effect plateaus at higher concentrations as the increased contact area reduces the pressure exerted by individual particles, balancing out the benefit of more abrasives. The efficiency per particle declines after a certain concentration because non-active particles dilute the overall removal effectiveness. In terms of surface roughness, lower concentrations lead to rougher surfaces, as fewer abrasives are available to effectively polish and remove surface irregularities. At higher concentrations, the surface becomes significantly smoother, as the increased abrasive interaction leads to more efficient polishing and reduced roughness. [64]

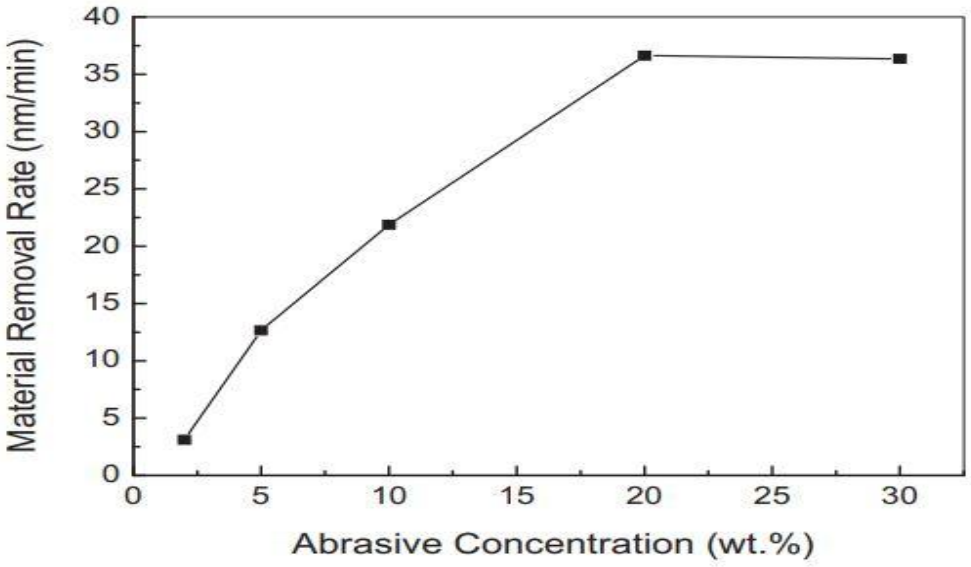


Figure 12: MRR as a function of abrasive concentration. [64]

On the other hand, at very low concentrations of ceria, the material removal rate (MRR) surprisingly increases rather than decreases, which contradicts the conventional expectation that fewer abrasives should lead to reduced MRR. This is primarily due to improved particle dispersion and uniformity at lower concentrations, which enhances the efficiency of the abrasives. As concentration decreases, smaller particles are more uniformly dispersed and active in the process, leading to higher MRR. Additionally, lower concentrations promote more Ce^{3+} formation on the abrasive surface, which enhances chemical interactions with the glass surface, further increasing MRR. Regarding surface roughness, lower concentrations also yield smoother surfaces due to better particle distribution and a uniform polishing process. This results in the effective removal of surface irregularities, as evidenced by AFM images (figure 13) showing significant reductions in surface roughness after polishing with ceria slurries at concentrations between 0.25 and 1 wt.%. [39]

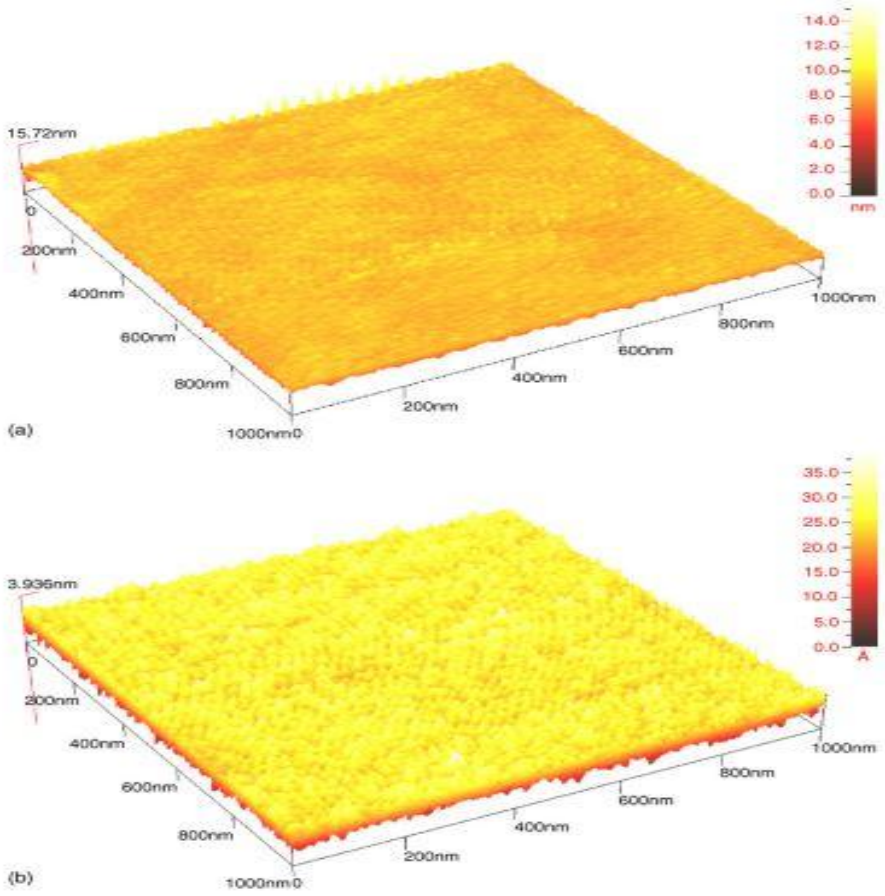


Figure 13: Typical AFM images of the optical glass surface: (a) Pre-CMP; (b) Post-CMP. [39].

1.3.1.3 Effect of slurry pH.

At pH levels near the isoelectric point (IEP) of the polishing agent, the surface charge of the abrasive particles is neutral or nearly neutral, reducing electrostatic interactions between the abrasive and the glass surface. While this might suggest weaker adhesion, the reduction in repulsive forces allows for increased abrasive-to-surface contact without significant electrostatic interference. This can enhance mechanical polishing efficiency, as the particles engage more freely with the glass surface, leading to higher material removal rates (MRR) despite minimized electrostatic interactions. The combination of mechanical contact and chemical activity around the IEP supports efficient material removal. For example, in the case of CeO_2 polishing BK7 glass, the maximum MRR was observed at pH 7, which is close to the IEP of CeO_2. However, pH levels above the IEP create negative surface charges on both the polishing agent and glass, leading to repulsive forces that prevent particle agglomeration. This improves surface smoothness by reducing the likelihood of deep scratches but may lower the MRR due to less efficient mechanical

interaction. Therefore, an optimal pH range exists where polishing efficiency and surface quality are balanced, depending on the type of glass and polishing agent used. [65] At higher pH (around 10), while adhesion forces decrease, the enhanced dissolution rate of materials like silica contributes to a much higher MRR, with improved surface finish and reduced roughness [66]. The surface roughness begins to increase when the pH becomes too high. This is because, under highly alkaline conditions, the polishing slurry can over-corrode the surface, leading to uneven material removal and the formation of pits, thus increasing surface roughness. Therefore, while higher pH improves MRR, overly alkaline conditions can degrade surface quality by causing defects. [67]

1.3.2 Ceria-ceria particle interactions.

Cerium oxide powders are widely used and are of fundamental importance in catalytic pollution control and energy, solid oxide fuel cells, oxygen sensors, catalysts, ultraviolet absorbents and filters, and polishing media for micro-electronics and optical glass [68, 69-74]. The useful properties of ceria are a consequence of the physical and chemical characteristics of these particles and their reactivity, which can vary greatly with the size, shape, charge, and surface coating. Many of the unique features are linked with the dual oxidation state of cerium (switching between Ce^{3+} and Ce^{4+}) [75]. The formation of an oxygen vacancy results in the reduction of cerium ions within the lattice, transitioning from Ce^{4+} to Ce^{3+}. Ce^{3+} plays a pivotal role in initiating the reaction with the oxide surface, forming strong Ce-O-Si chemical bonds. This strong adhesion accelerates the generation of Ce-O-Si bonds, subsequently enhancing the removal rate of SiO_2 [76-78]. Under the combined action of mechanical wear and chemical reaction, CeO_2 abrasives have a high material removal rate (MRR) and superior surface finishes compared to other polishing agents. However, due to their high surface activity, ceria particles tend to aggregate quickly, which reduces both the efficiency and precision of the polishing process. [79].

To improve slurry efficiency, many scientists have focused on incorporating various chemical additives to ensure proper particle dispersion and prevent aggregation during the process. The dispersion behavior of ceria particles in polishing slurries has a direct impact on surface quality [25], making it a crucial factor for achieving optimal results. The techniques used for this purpose are cited as follows:

1.3.2.1 Addition of sodium citrate ($Na_3C_6H_5O_7 \cdot 2H_2O$)

The study of Liang et al. [80] showed that Sodium citrate plays a crucial role in enhancing slurry stability, material removal rate (MRR), and surface roughness during the chemical mechanical polishing (CMP) process. As an organic electrolyte, sodium citrate improves the hydrophilicity of cerium oxide particles by increasing the thickness of the solvent film on their surface, as shown in Figure 14, leading to reduced particle agglomeration and better slurry stability. This stabilization effect is particularly pronounced at optimal concentrations, preventing large particles from forming and thereby minimizing surface defects, such as corrosion pits. In terms of MRR, while lower concentrations of sodium citrate may cause a slight reduction in MRR compared to slurries without additives, it effectively balances between stable polishing performance and reduced surface roughness. As the concentration of sodium citrate increases beyond a threshold, it can lower MRR significantly due to reduced transport of material and decreased particle-glass contact strength. Overall, sodium citrate proves beneficial for achieving smoother surfaces with fewer defects, contributing to both efficient polishing and improved surface quality.

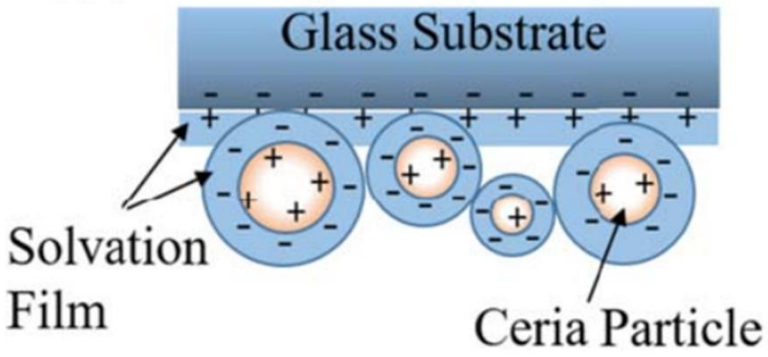


Figure 14: Schematic diagram of the interaction between the CeO_2 particles and the glass surface, note that the solvation film in this picture does not indicate the zeta potential layer [80].

1.3.2.2 Addition of polyacrylic acid (PAA)

The effect of different additives on ceria slurry stability can be understood through the changes in zeta potential and adsorption behavior as shown in the study of Kang et al [81]. Without additives, the zeta potential of the ceria slurry changes from positive to negative as the pH increases, with an isoelectric point (IEP) around pH 5.6. The addition of 1 wt. % PAA (polyacrylic

acid) significantly enhances slurry stability by increasing the negative charge on both ceria particles and substrates (3 wt. % in the study of Muskan et al [82]), with a maximum negative zeta potential of -52.4 mV for ceria at pH 7. This enhanced negative charge creates strong electrostatic repulsion between ceria particles and the substrate, reducing particle aggregation and increasing stability. In contrast, lactic acid, which lacks the excessive carboxylate groups of PAA, causes minimal changes in zeta potential and thus has a negligible effect on slurry stability. The PAA additive also drastically reduces the removal rate of silicon nitride. At the same time, the addition of RE-610 (a phosphate-ester-based chemical compound used as a wetting agent) to the PAA-containing slurry accelerates silicon oxide hydration, increasing the removal rate of silicon oxide while maintaining ceria slurry stability [81].

1.3.2.3 Addition of poly (acrylic acid-co maleic acid) sodium salt (PAMS)

Kim et al [83] proved that the addition of PAMS dispersant to ceria slurry significantly improves slurry stability and polishing performance. Without PAMS, the slurry rapidly separates into water and sediment layers, indicating poor stability. At an optimal concentration of 3 wt. % PAMS see (Figure 15), the slurry remains stable for up to 48 hours, with a large dispersed layer and minimal sedimentation. This is attributed to the adsorption of PAMS on ceria particles, providing steric hindrance and electrostatic repulsion that prevent particle agglomeration. Polishing results using the optimized slurry show enhanced performance, with a high removal rate of 1 μm/min and improved surface roughness (0.67 nm), which is superior to previous studies. The higher pH (10) induced by PAMS enhances SiO_2 removal, as the surface becomes softer under alkaline conditions. However, particle contamination remains a concern.

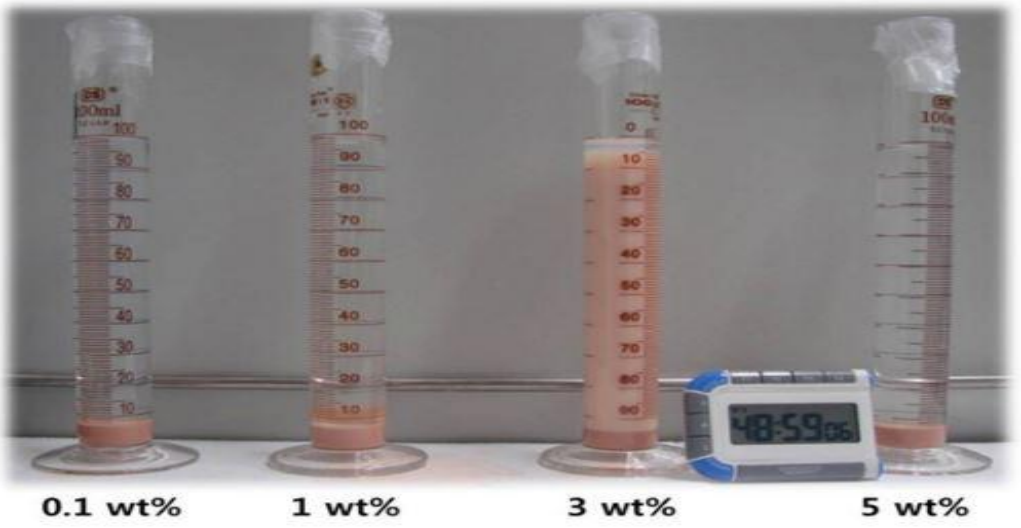


Figure 15: Photograph of ceria slurry dispersions at various PAMS concentrations. [83]

1.3.3 Dissolution of glass compounds on the polishing slurry

The dissolution of glass compounds in the polishing slurry is a critical factor in the chemical mechanical polishing (CMP) process. During polishing, the interaction between the slurry and the glass surface leads to the dissolution of certain glass compounds, altering the chemical composition of the slurry. This dissolution can affect both the chemical reactivity and mechanical behavior of the slurry, directly influencing material removal rates and surface quality. Furthermore, it may contribute to changes in the slurry pH, which in turn affects the stability and performance of the abrasive particles, as well as the overall efficiency and precision of the CMP process. Despite the significance of this phenomenon, few studies have explicitly addressed glass dissolution during CMP. Therefore, relevant research on glass dissolution in aqueous media will be reviewed, along with the limited studies that explore its effect on slurry chemistry.

1.3.3.1 Glass dissolution in aqueous solution

The dissolution of glass in aqueous solutions is a complex process influenced by various factors, including temperature, pH, and the composition of the glass itself. In the study of Vienna et al [84], the forward dissolution rate of EWG-C (enhanced waste glass) was investigated under different conditions. The results showed that the dissolution rate increases with increasing temperature and pH as shown in Figure 16. Additionally, the composition of the glass also plays a

significant role in the dissolution process, with certain glass compositions exhibiting higher dissolution rates than others.

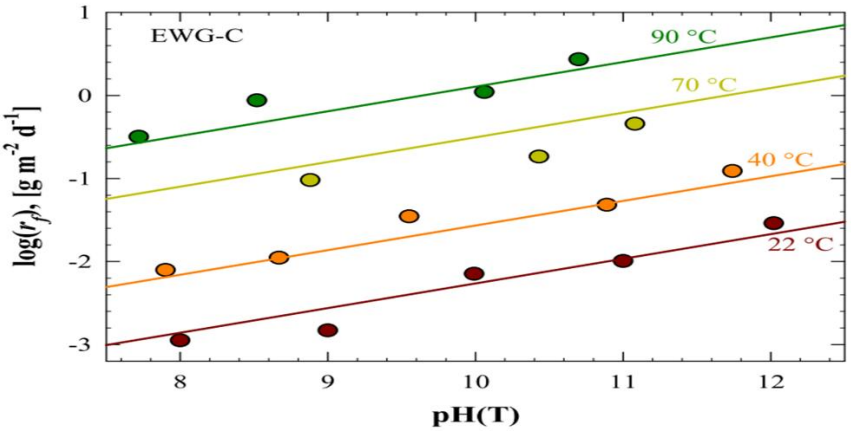


Figure 16: Normalized forward dissolution rates, rf, calculated from releases as a function of pH at various temperatures [84].

Furthermore, the study of Jollivet et al. [85] showed that the dissolution of SON68 glass (nuclear borosilicate glass) in various aqueous solutions is influenced by temperature, pH, leaching solution composition, and glass composition. Higher temperatures and neutral to slightly basic pH conditions generally lead to increased dissolution rates. The presence of specific ions, especially calcium, significantly enhances the dissolution, while higher ionic strengths of the leaching solution further accelerate the process. Glass composition also affects its dissolution susceptibility, with alkaline earth cations, excluding magnesium, generally promoting higher dissolution rates compared to alkali metal cations. The dissolution mechanism is linked to the hydrolysis of silicon-oxygen bonds, which can be weakened by certain cations on the glass surface.

1.3.3.2 Relationship between glass dissolution and slurry chemistry

Research on the impact of glass dissolution on slurry chemistry is very limited, with only a few studies addressing this phenomenon. One notable example is the work by Becker et al. [86], where they discussed the impact of glass composition and chemical interactions on the chemical mechanical polishing (CMP) process, focusing on how the dissolution of various glass ions can destabilize the polishing suspension and significantly affect material removal rates. Key findings are presented through experiments with three different suspensions used to polish BaK 4, a reference optical glass. The authors show how variations in the suspension's chemical composition, particularly the presence of dissolved ions like Si, Ca, and Zn, can lead to instabilities in the

polishing process. These instabilities manifest as changes in removal rates. Additionally, the authors used HSC Chemistry software to model how different glass constituents dissolve and interact in a polishing suspension, highlighting the effects of additives like NaF, as shown in Figure 17. The simulation showed that NaF can cause precipitates like CaF2, leading to higher surface roughness.

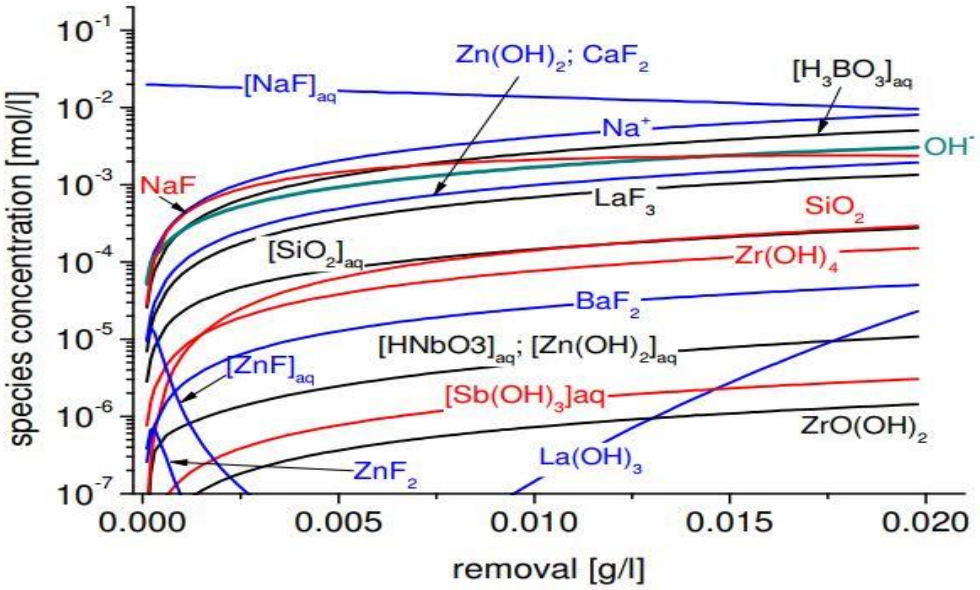


Figure 17: Concentration of species in aqueous solution as a function of the amount of dissolved glass (removed from the polished glass) for a typical optical glass N-LaK 8 with the prior addition of NaF. [86]

In another study, Surtwala et al. [87] added glass products to the slurry to simulate the potential effect of the dissolution of the polished glass in the slurry. They found that the chemical compounds of glass can significantly affect the slurry chemistry and polishing efficiency during the polishing process. The dissolution of glass products into the slurry can alter the electrostatic characteristics of the slurry particles, influencing their spatial distribution and interactions with the workpiece and pad surfaces see (Figure 18), which can lead to changes in the polishing forces, removal rates, and ultimately, the surface roughness of the polished workpiece. For example, the addition of glass products from phosphate glass can create a strong attractive force between the slurry particles and the workpiece at high pH, leading to increased slurry buildup and potentially

affecting the polishing process. Understanding these chemical interactions is crucial for optimizing polishing processes and achieving desired surface quality.

In particular, the dissolution of glass products can influence the pH of the slurry, which in turn affects the surface charge of the particles and the interactions between them. Additionally, the presence of specific ions from dissolved glass can alter the equilibrium between different components in the slurry, leading to the formation or dissolution of precipitates. These precipitates can act as abrasive particles, affecting the removal rate and surface finish.

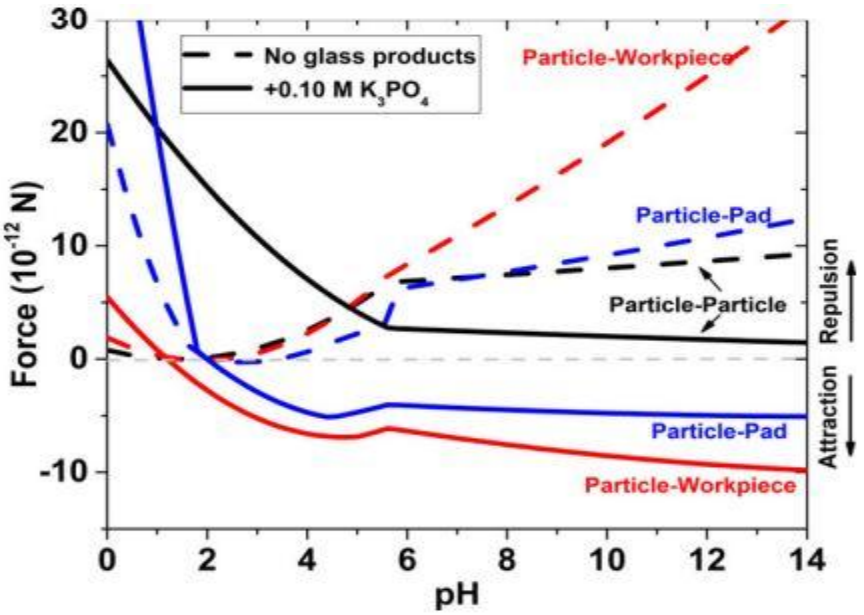


Figure 18: Calculated particle-particle, particle–pad, particle– workpiece forces with and without glass products for polishing phosphate glass. [87]

Furthermore, the composition of the glass itself can play a role in its dissolution behavior and the subsequent impact on the slurry. Glasses with different chemical compositions may release different ions into the slurry, leading to varying effects on the polishing process.

Therefore, it is essential to consider the chemical interactions between glass compounds and slurry when optimizing polishing processes. By understanding these interactions, it is possible to select appropriate polishing slurries and additives to achieve the desired surface quality and minimize potential problems associated with slurry instability and reduced polishing efficiency.

1.4 Conclusion

In this chapter, the main polishing methods were highlighted, including chemical mechanical polishing, which is a vital technology for ultra-precision polishing of hard and brittle materials, combining mechanical and chemical actions to remove material at the workpiece-polisher interface. Its efficiency depends on key parameters such as polishing pressure, tool rotation speed, slurry properties, feed rate, and polishing pad selection. Recent studies, particularly between 2014 and 2019, have highlighted advancements in understanding material removal mechanisms and optimizing process efficiency. CMP's relevance in the semiconductor and optical industries remains strong, with growing research interest in sustainability and environmental impacts, including wastewater treatment and energy reduction. Looking forward, CMP is expected to evolve with a focus on expansion, digitalization, and sustainability. Studies have examined the impact of slurry properties like particle size, concentration, and pH on polishing results, with larger particles generally increasing material removal rate (MRR) until a certain level, beyond which aggregation reduces efficiency. Optimizing these factors can improve surface quality and minimize defects, making CMP a critical process in various industrial applications.

Few studies discussed the impact of glass chemistry on the polishing results, however, its impact on the slurry parameters in terms of particle size distribution, particle concentration, and slurry pH has not been discussed so far.

Chapter2. Background on polishing slurries and their characterization

2.1 Introduction

Polishing powders used in Chemical Mechanical Polishing (CMP) are essential for achieving the high precision required in semiconductor manufacturing. CMP combines mechanical abrasion with chemical reactions to remove material from polished samples, ensuring a smooth and planar surface. The most common polishing powders include silica (SiO_2), ceria (CeO_2), and alumina (Al_2O_3), each selected based on the specific substrate and desired finish. Silica slurries are often used for softer polishing applications, while ceria is favored for its unique properties that enhance both chemical reactivity and mechanical performance. Alumina powders, characterized by their high hardness and controlled particle size distribution, are effective for polishing harder materials like tungsten [88]. In addition, diamond abrasive is widely used in the grinding and polishing of hard glass, chips, sapphire substrates, and other materials because of their high hardness and high wear resistance [89].

Many factors determine the performance of the polishing process, expressed by criteria like removal rate, planarity, yield, and defect number. It is generally acknowledged that the efficiency of polishing and planarizing is closely related to the slurry properties [90-94]. The slurry quality is characterized by parameters such as stability, pH value, temperature, and viscosity of the suspension. Slurry quality is affected by particle properties (type, size, shape, and concentration of primary particles and agglomerates), zeta potential, and components of the liquid phase (oxidizers, complexing agents, and pH adjustment). Moreover, the state of the CMP slurry can be changed by mechanical stress [95].

In this chapter, the commonly used polishing powders for optical glass polishing are discussed, with a special focus on ceria abrasives, given their recent prominence in the field and their application in this study. Various characterization methods essential for evaluating slurry performance are presented, including pH, zeta potential, particle size distribution, large particle content, and sedimentation analysis. These methods provide a comprehensive understanding of slurry stability and effectiveness, supporting the optimization of polishing processes for optical glass.

2.2 POLISHING POWDERS

2.2.1 COLLOIDAL SILICA SLURRY

Silica-based slurries are essential consumables in chemical mechanical polishing (CMP) applications. Among the common types, colloidal silica and fumed silica are widely used for their distinct properties. Colloidal silica slurries uniquely offer both dispersing and CMP actions, making them effective in intermediate polishing of metals and in achieving high-quality surfaces by minimizing subsurface damage. These slurries are often chemically stabilized to form nearly ideal suspensions and may contain additives to reduce particle aggregation and crystallization effects. The particle size distribution of colloidal silica notably influences the polishing rate and surface roughness of polished materials [43].

In contrast, fumed silica, created via flame pyrolysis of silicon tetrachloride, is appreciated for its low cost, high purity, and straightforward synthesis. However, due to weak hydrogen bonding, it tends to agglomerate in aqueous solutions, which necessitates extra processing such as microfluidization and filtration to ensure consistency in CMP applications. Colloidal silica, typically synthesized through the hydrolysis of metal-organic precursors, allows for controlled particle size and uniformity. Although certain forms of silica, like sodium-containing silicic acid, can cause gate oxide damage in sensitive applications, ion exchange processes or the use of organic silicate can produce high-purity silica that mitigates these concerns. With rising standards for defect-free surfaces as device dimensions decrease, colloidal silica has largely replaced fumed silica in CMP applications that demand superior surface quality [88].

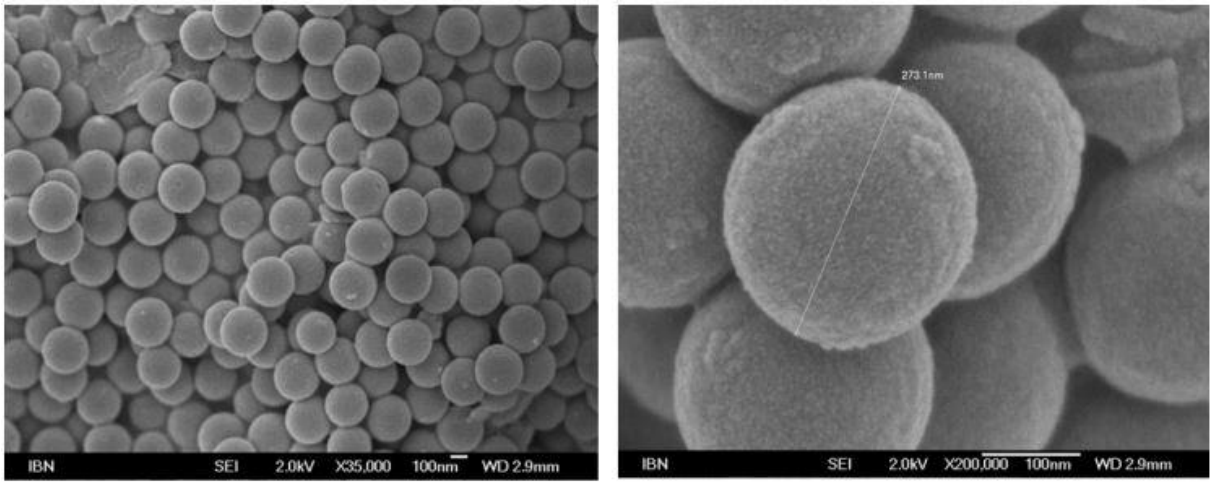


Figure 19: SEM photos of as-synthesized silica nanoparticles [96]

2.2.2 Diamond-based slurry

Diamonds can be found in the earth in their natural form or can be manmade. It is the hardest and the sharpest abrasive known. Because of its hardness, it is normally used to work with very hard materials such as tungsten carbide and ceramics. Soft materials should not be lapped with diamond abrasives because of their embedding tendency. A lapping plate charged with diamond abrasives cuts fast and produces a fine finish. Recent developments in man-made abrasives have made synthetic fine diamond powders increasingly available for industrial applications. Their use is limited due to their high cost. Two types of diamond abrasives are commonly used: polycrystalline and monocrystalline diamond. The features and advantages of polycrystalline diamond include the following:

• Higher cutting rates.

• Very uniform surface finish.

• More uniform particle size distribution.

• Higher removal rates (self-sharpening abrasives).

• Surface area is 300% greater than monocrystalline diamond. [97]

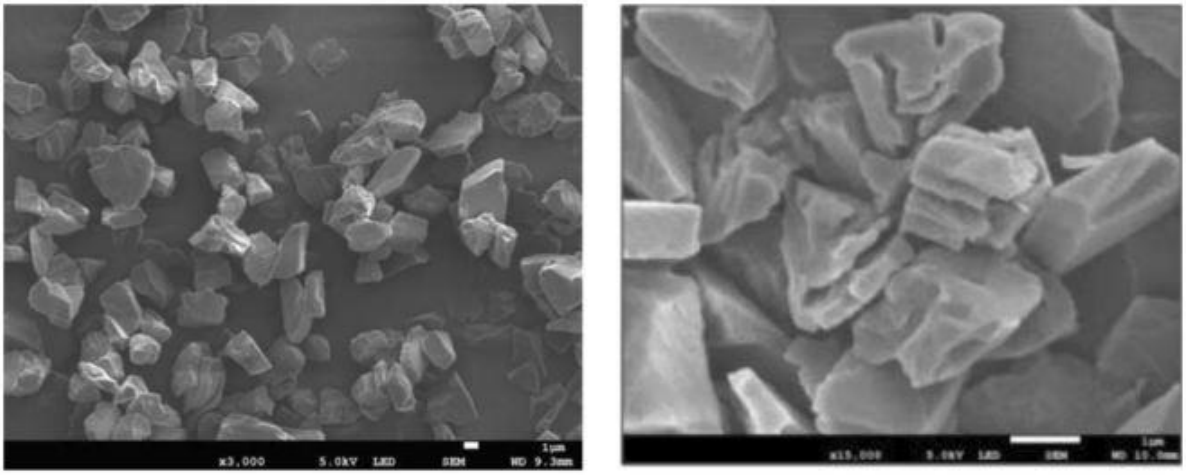


Figure 20: SEM images of diamond abrasives, scale 1µm. [98]

2.2.3 Alumina-based slurry

Alumina abrasives are widely used in chemical mechanical polishing (CMP) due to their strong mechanical abrasion, making them effective in removing materials like copper (Cu). However, alumina alone lacks the selectivity required for materials such as tantalum (Ta) and oxide layers. When used in mixed abrasive slurries (MAS) with silica, alumina's selectivity improves as silica particles coat the alumina, enhancing interactions with Ta and oxide layers. This combination offers a balanced approach in CMP for various materials by optimizing selectivity and surface quality [99].

Achieving an optimal material removal rate (MRR) with alumina abrasives requires a balance between chemical and mechanical actions. Alumina slurries are generally alkaline to encourage chemical reactions, especially with the heat generated during polishing. Particle size and concentration affect MRR, with moderate sizes enhancing removal, while excessive size or concentration may reduce effectiveness. Dispersants are added to stabilize the slurry, aiding in particle dispersion and MRR, but over-stabilization can limit surface interaction. Oxidants may be included to further boost MRR by facilitating chemical reactions [100].

Alumina's durability, heat resistance, and structural variety make it useful across industries. Different forms of alumina, like calcined, fused, and tabular, have unique structures that affect their behavior in polishing. Calcined alumina is typically fine-grained and structurally uniform,

while fused and tabular types are larger and less uniform, reflecting differences in their production processes. These structural characteristics influence their abrasive properties and are useful in various CMP applications [101].

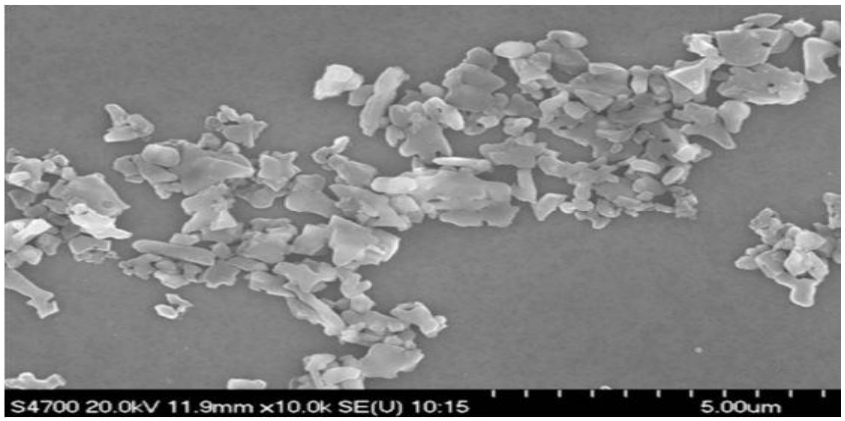


Figure 21: SEM image of alumina particles. [102]

2.2.4 Cerium oxide

Cerium oxide (CeO_2), a rare-earth metal oxide, is recognized for its remarkable properties and diverse applications, particularly in polishing and catalysis. It exhibits high hardness and a unique fluorite crystal structure, which provides oxygen vacancies that enhance its catalytic activity and effectiveness as an abrasive material in glass polishing. The dual oxidation states of cerium (Ce^{3+} and Ce^{4+}) facilitate redox cycling, contributing to its enzyme-like activities, including scavenging reactive oxygen species, making it valuable in biomedical applications as well [103,104]. Additionally, cerium oxide effectively neutralizes impurities in glass production, improving clarity and quality by eliminating discoloration caused by elements like iron and chromium [105].

2.2.4.1 Ceria structure.

Ceria (CeO_2) adopts a fluorite (CaF_2) crystal structure with a space group of Fm3m. In this structure, Ce cations form a face-centered cubic (FCC) arrangement, while O anions are positioned in a simple cubic pattern within the unit cell. The lattice constant of the cubic unit cell is 0.541 nm. Each Ce atom is coordinated with eight oxygen atoms, while each oxygen atom is tetrahedrally coordinated with four Ce atoms. Despite the FCC-like arrangement of the Ce cations, they are not close-packed. The low index surfaces of ceria, such as (111), (110), and (100) see (figure 22), are

characterized by different stabilities, with the (111) surface being the most stable and (100) the least stable. This stability is influenced by the surface energy and the degree of relaxation between the atomic layers, with the (100) surface exhibiting the greatest degree of contraction among its surface atoms. [106]

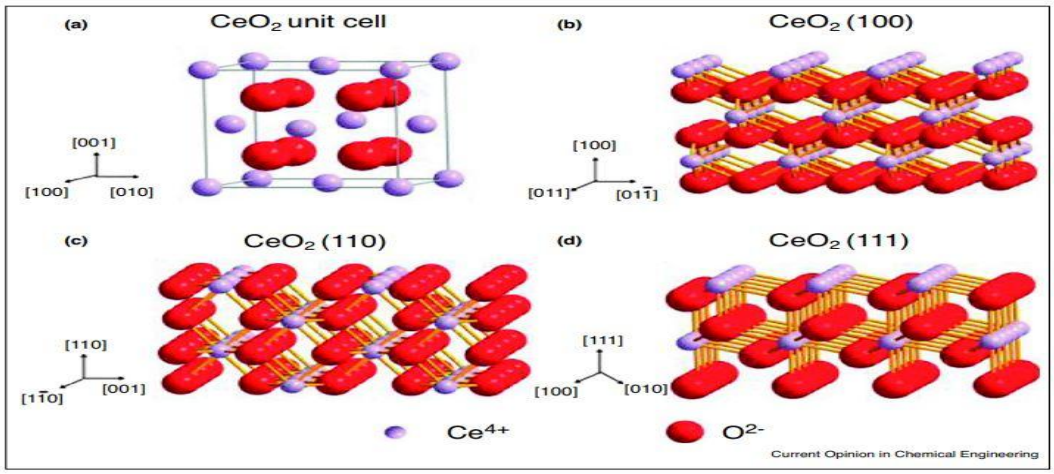


Figure 22: Atomic configurations of the unit cell and the (001), (111), and (110) facets of CeO_2. [107]

2.2.4.2 Ceria synthesis methods

2.2.4.2.a Precipitation method

The solution precipitation method is a widely used technique for synthesizing nanoparticles, including ceria (CeO_2) particles. In this process, a soluble metal precursor, such as cerium nitrate, is dissolved in an aqueous solution. A precipitating agent, typically a base like ammonia [108] or hexamethylenetetramine (HMTA) leading to the gradual release of ammonia and other basic species at high temperatures [109,110], is then added to adjust the pH of the solution, promoting the formation of metal hydroxides or oxides. This triggers the nucleation and growth of nanoparticles within the solution. Continuous stirring and controlled temperature help ensure uniform particle size distribution. To enhance oxidation, oxygen may bubble through the mixture, converting Ce (III) to Ce (IV). The precipitated particles are collected through processes like centrifugation, followed by repeated washing with water and ethanol to remove impurities. Finally, the particles are dried and characterized by their size, morphology, and crystallinity. This method allows control over particle size and purity, making it suitable for various applications. [111]

2.2.4.2.b Hydrothermal and Solvothermal Methods

Hydrothermal or solvothermal synthesis is a widely used method for the preparation of pure ceria (CeO_2) nanocrystals, offering precise control over crystal size, shape, and growth. Traditionally, early solvothermal methods operated at high temperatures (T > 300°C) in the supercritical regime to produce large ceria crystals, which are challenging to form due to the high melting point of CeO_2. However, more recent approaches utilize milder, subcritical conditions (T < 250°C) to achieve control over nanoscale crystals. A variety of cerium salts, including Ce^{3+} and Ce^{4+} compounds, as well as elemental cerium, are used as precursors. Oxidation often occurs during synthesis, especially with Ce^{3+} salts, resulting in ceria crystals with potential mixed valency and surface defects. Solvent choice, additives, and reaction conditions are crucial for controlling morphology, with water being frequently replaced by alcohol to obtain monodisperse particles [112]. Additives such as organic molecules or bases further influence particle dispersion and shape, with the formation of unique structures like nanorods, nanotubes, and spherical crystallites [113]. This method also enables the production of fine ceria powders with applications in areas such as sintering and ionic conductivity.

2.2.4.2.c Sol gel method

The sol-gel method is a well-established approach for the synthesis of inorganic oxides. The formation of the metal oxide via this approach involves several different consecutive steps. The first involves forming a dispersion of colloidal powders within a solution (the sol). This sol then becomes a ‘gel’ through simultaneous hydrolysis and polycondensation of the organometallic precursors (generally metal acetates, nitrates or metal alkoxides etc.). The formed gel is an interconnected three-dimensional network of oxide- or alcohol-bridged metal ions within a liquid medium. The third step involves the water and/or other volatile liquids being removed from the gel network, either by thermal evaporation or extracted under supercritical conditions. The choice of this drying process in some cases has a direct result on the pore radii as well as the structure of the product. [114]

To synthesize ceria particles using the sol-gel method, cerium nitrate hexahydrate ($Ce(NO_3)_3 \cdot 6H_2O$) is first dissolved in deionized water along with a buffer such as urea ($CO(NH_2)_2$) and a dispersant like polyvinylpyrrolidone (PVP) [115- 117]. The resulting solution is stirred

continuously while its temperature is gradually increased to a predetermined level and maintained for about an hour. Ammonia is then added dropwise, triggering a rapid reaction that causes a noticeable color change from purple to pale yellow, indicating the oxidation of Ce^{3+} to Ce^{4+}. The synthesized solution undergoes further aging and drying, leading to the formation of ceria colloids. These colloids can be characterized for structural properties using techniques like X-ray diffraction (XRD) and transmission electron microscopy (TEM) to confirm their crystallinity and particle size [117].

2.2.4.2.d Mechanochemical Synthesis

The synthesis of ceria (CeO_2) nanoparticles can be achieved through various techniques, each tailored to optimize particle size and properties. One approach involves Mechanochemical synthesis, where CeO_2 powder is milled in different dispersing media, including aqueous basic (ammonia, pH 10) and acidic (propionic acid, pH 3) solutions, as well as non-polar media (xylene with stearic acid). These suspensions, containing a mixture of ceramic powder and additives, are milled for durations ranging from 0.17 to 48 hours, followed by drying and calcining at 500 °C, which enhances crystallinity and stability [118]

In a sol-gel process, $(NH_4)_2\ Ce(NO_3)_6 \cdot 6H_2O$ is mixed with NaOH in a 1:6 mole ratio and subjected to high-energy ball milling with stainless-steel balls, leading to the formation of CeO_2 after drying in a vacuum. This method allows for precise control over particle size through thermal treatments at various temperatures (200 to 800 °C), improving crystallization and phase purity [119].

Additionally, techniques such as high-energy milling in a controlled atmosphere can yield metal-ion-free CeO_2, enhancing the purity of the final product [120]. This method involves careful milling of starting materials, including $CeCl_3 \cdot 6H_2O$, NaOH, and NaCl, under argon atmosphere, followed by calcination and ultrasonic dispersion to remove any residual salts [121]. Characterization techniques like X-ray diffraction (XRD) and transmission electron microscopy (TEM) are commonly employed to analyze the crystallographic structure, particle size, and morphology, providing critical insights into the properties of the synthesized nanoparticles [118, 119].

From the description of the ceria synthesis techniques, table 2 was created to summarize the synthesis methods, key features, and advantages associated with each technique as follows:

Synthesis Method	Key Features	Advantages
Precipitation method	Simultaneous precipitation	Simple, cost-effective
Hydrothermal and Solvothermal Methods	High temperature and pressure	Highly crystalline, scalable
Sol-gel method	Liquid-to-gel transition	High purity, control over size
Mechanochemical Synthesis Method	Mechanical energy-induced reactions	Solvent-free, environmentally friendly

Table 1: Summary of ceria synthesis techniques, key features, and their advantages.

2.3 Characterization techniques of polishing powders

Accurate characterization of powders, especially in particle size analysis, requires individual particles to be well dispersed. When powders are agglomerated, the measured particle size distribution can be skewed, leading to erroneous interpretations of their physical properties.

2.3.1 Dispersing and Deagglomeration

Ultrasound is a well-established method for particle size reduction in dispersions and emulsions. Ultrasonic processors are used in the generation of nano-size material slurries. Dispersion by ultrasound is a consequence of microturbulence caused by fluctuation of pressure and cavitation. Investigations of different materials, such as aqueous solutions of nanoparticulate silicium dioxid powder and spray frozen agglomerates with a variable solid content has demonstrated the considerable advantage of ultrasound when compared with other technologies, such as rotor-stator mixers (e.g. turrax) or colloid mills. For small matter from several nanometers to a couple of microns, ultrasonic cavitation is very effective in breaking agglomerates, aggregates, and even primaries. When ultrasound is being used for the milling of high-concentration batches, the liquid jets streaming resulting from ultrasonic cavitation make the particles collide with each other at velocities of up to 1000km/h. These breaks van der Waals forces in agglomerates and even primary particles. Large particles are subject to surface erosion (via

cavitation collapse in the surrounding liquid) or particle size reduction (due to fission through interparticle collision or the collapse of cavitation bubbles formed on the surface). [122]

2.3.2 Particles size distribution

Knowledge of particle sizes and the size distribution of a powder system is a prerequisite for most production and processing operations. Particle size and size distribution have a significant effect on the mechanical strength, density, electrical and thermal properties of the finished object. Significant production losses can be incurred due to high rejection rates if the size and size distribution of powders being used in a process are not adequately controlled. In most instances powder suppliers provide size and size distribution information, but that information needs to be checked for quality control purposes. In addition, the validity of the supplied size information needs to be evaluated if the powder batch has been divided into smaller batches based upon the user's requirements. In certain processing operations, powder size and size distribution may have to be monitored at different stages of a processing operation for suitable process control [123]. Centrifugation, ultrasonic spectroscopy, turbidimetry, image analysis, light extinction, dynamic and static light scattering are typically employed to measure these properties. All different techniques are relevant because of the large variety of both products and particle size range. [124] Since there are always some deviations during their generation or production. Sometimes, these deviations are small, and all particles are nearly the same size: the PSD is narrow. According to NIST (National Institute of Standards and Technology), the particles are called monodisperse if at least 90% lies within 5% of the median size (See Table 2). Often, however, PSDs are broad [125].

Particle dispersion	**PSD width (D90/D10 ratio)**
Monosized	< 1.02 (ideally = 1.00)
Ultra narrow	1.02–1.05
Narrow	1.05–1.5
Medium	1.5–4
Broad	4–10
Very broad	> 10

Table 2: particle dispersion according to the D90/D10 ratio [125].

The D50, the median, is defined as the particle size where half the population lies below this value. Similarly, 90 percent of the population lies below the D90 point, and 10 percent of the population lies below the D10 [126] as shown in Figure 23

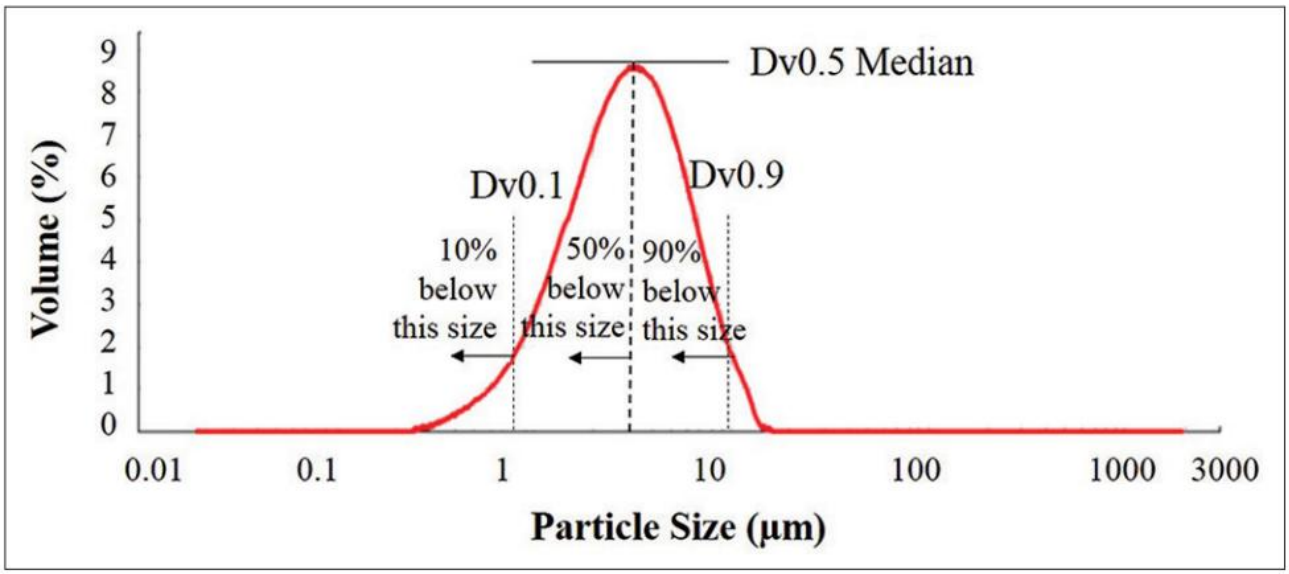


Figure 23: How D-values are measured according to the three-axis values [127].

Particle size distribution (PSD) measurements are crucial in the polishing process, significantly influencing both material removal rates and the frictional forces between slurry abrasives and the polished surface. Larger abrasive particles generally enhance material removal due to their increased contact area, while smaller or irregularly shaped particles can elevate friction levels. However, a broad PSD characterized by substantial variation in particle sizes can lead to interference among abrasives during polishing, reducing the efficiency of abrasive contact and ultimately resulting in lower removal rates [128]. Additionally, PSD measurements are essential for detecting particle aggregation that exceeds critical sizes (ex. see Figure 24), which can adversely affect surface quality and increase the risk of damaging the substrate. Through this analysis, researchers gain insights into how particle size and distribution influence polishing performance, leading to improved control over slurry behavior [129, 130].

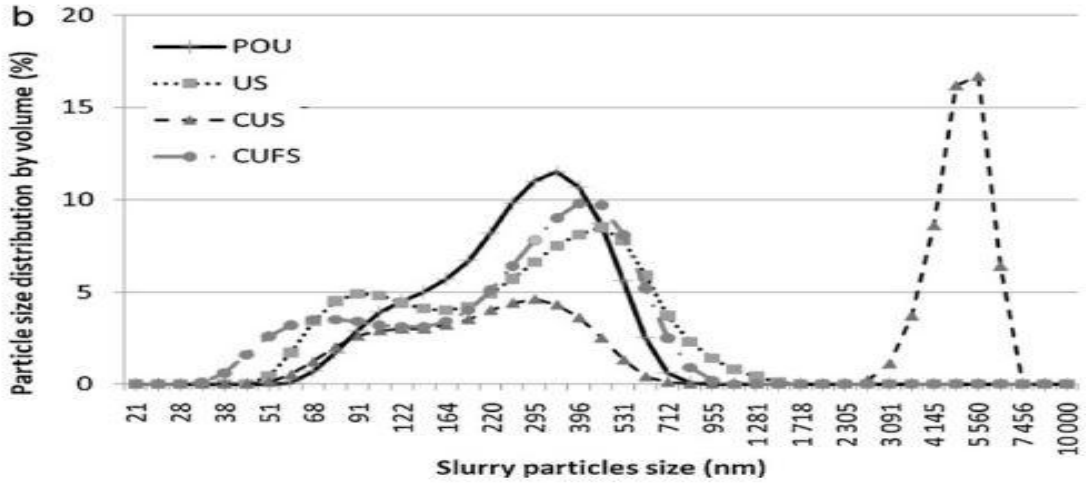


Figure 24: Slurry particle size distribution in number and volume percentages with the observation of some agglomerates (CUS slurry). [130].

Monitoring PSD allows for tracking abrasive grain size changes over time, providing valuable information on slurry behavior and identifying colloidal effects that can cause agglomeration, negatively affecting polishing performance. Understanding the evolution of particle size ensures consistent removal rates and maintains surface quality, as varying particle sizes influence polishing effectiveness [131]. Analyzing the size distribution of particles also aids in assessing their potential for consistent performance during polishing. A stable PSD helps prevent significant morphological changes in abrasive particles, which is vital for effective material removal and desired surface quality. Well-characterized PSD enables better control over interactions between different particle types within a slurry, enhancing the overall polishing process. By monitoring shifts in mean particle size and distribution curves as slurries are mixed with coarser particles, researchers can establish critical detection limits for larger particles, facilitating the identification of concentrations that indicate significant changes. This ultimately aids in assessing slurry stability and effectiveness, allowing for optimized formulations for improved polishing efficiency and surface quality while maintaining desired particle characteristics throughout the process [132, 133].

2.3.3 Large particle count

Large Particle Count (LPC) plays a crucial role in characterizing CMP slurries because it significantly affects both surface quality and overall process performance. Monitoring LPC is

essential as large particles in the slurry are directly linked to the formation of surface defects, such as scratches, which are particularly detrimental in industries requiring ultra-smooth surfaces, such as semiconductor manufacturing and optical wafer polishing. Owing to the limited optical resolution of the LPC, the original slurry sample is first diluted a few ten times using deionized water. Moreover, the diluted slurry flows into the detection module of the LPC at a specific flow rate (see Figure 25), about tens of milliliters per minute, wherein the number of large particles is counted for a given period, typically a few minutes. Finally, the concentration of large particles, i.e., the particle number per 1 ml, is calculated from the measured experimental data. Consequently, the net volume of the slurry used is typically about tens of microliters for a single measurement [134].

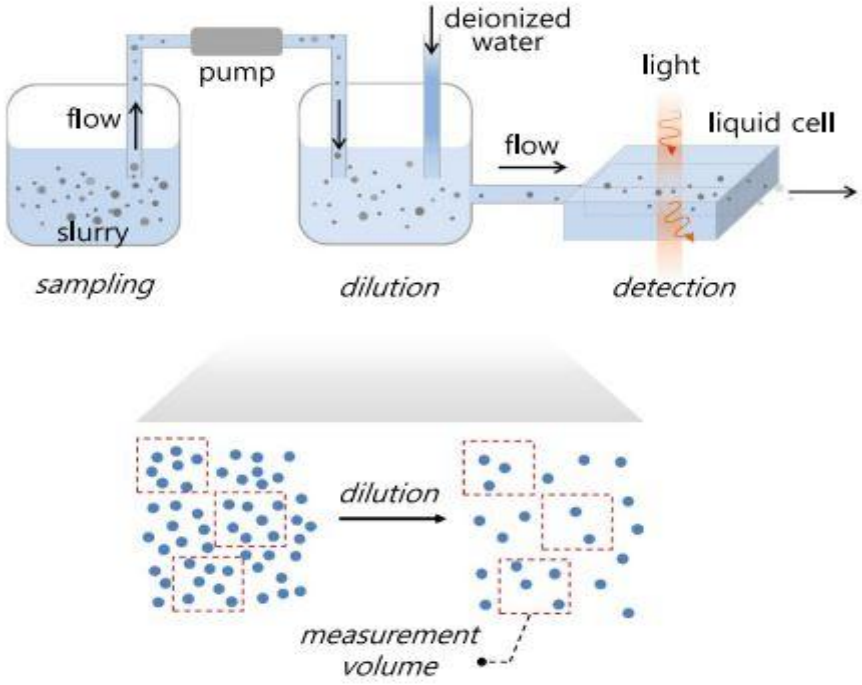


Figure 25: Procedure for Determining Large Particle Count in Slurry Samples [134].

A higher LPC often correlates with an increased risk of scratches, which can compromise the quality and yield of polished substrates. Furthermore, LPC serves as a key indicator of slurry stability over time. In stable slurries, particles remain uniformly distributed, but an increase in LPC suggests that particle aggregation or contamination may be occurring, which makes them valuable for tracking slurry ageing, as an elevated LPC indicates that the slurry may be approaching the end of its effective lifespan. [135]

Additionally, understanding LPC trends can help optimize slurry storage and handling conditions to prolong stability and prevent unwanted aggregation. LPC measurements are also critical for maintaining process control, ensuring that material removal rates remain uniform, and minimizing surface roughness or defects. When combined with particle size distribution (PSD) data, LPC provides a more complete picture of the slurry's performance. While PSD offers detailed information on the overall distribution of particle sizes, LPC specifically focuses on larger particles, which are more likely to cause mechanical damage during polishing. This complementary relationship between LPC and PSD allows manufacturers to gain a deeper understanding of slurry behavior, enabling more precise control over the chemical mechanical polishing process and ultimately improving the quality and yield of polished surfaces. [136]

2.3.4 Zeta potential measurements

Zeta potential is a measure of the magnitude of the repulsion or attraction between particles. Its measurement brings detailed insight into the dispersion mechanism and is the key to electrostatic dispersion control. Measurement of zeta potential is an extremely important parameter across a wide range of industries including brewing, ceramics, pharmaceuticals, medicine, mineral processing, and water treatment [137]

2.3.4.1 Theory

Surface charge and zeta potential (ZP) are distinct properties. While surface charge refers to the density of charges present on the particle's surface, zeta potential reflects the strength of the shear plane of the particle during electrophoresis—where charged particles (ions) move under the influence of an electric field. Although ZP is not a direct measurement, it serves as an important parameter for understanding colloidal stability, without directly addressing the charge density of the particles [138, 139].

The movement of particles (mobility) in this context depends on factors like the dielectric constant, the viscosity of the liquid, and the electrical potential at the slipping plane [140]. The slipping plane marks the boundary between the particle and the liquid where the Stern layer (Figure 26), which is tightly bound to the particle, meets the diffuse layer. The zeta potential is the electrical potential at this junction, influencing particle mobility.

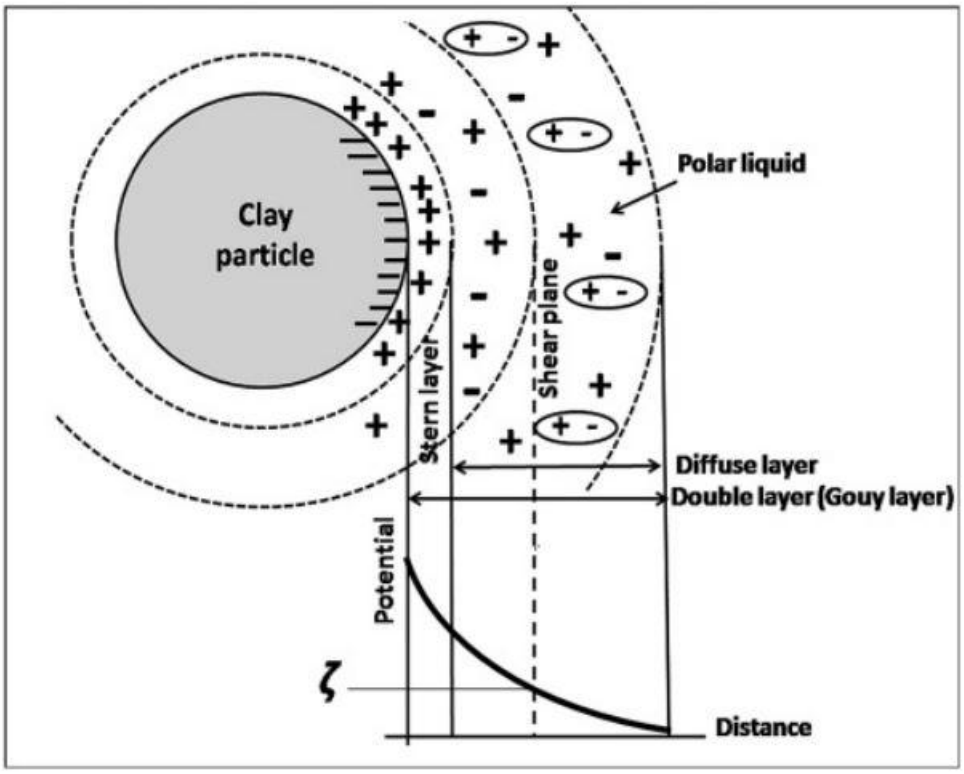


Figure 26: Potential distribution around a clay particle suspended in a polar liquid (water). The thickness of the Gouy electrical double layer is the sum of the Stern and the diffuse layers. ζ is the zeta potential. [141]

The stability of colloidal systems, based on the DLVO (Derjaguin, Landau, Verwey, Overbeek) theory, is governed by the balance between two opposing forces: van der Waals attractions and electrical double-layer repulsion [142, 143].

When a suspension has a high absolute zeta potential (either strongly positive or negative), particles tend to repel each other more strongly, reducing the likelihood of aggregation. This results in a more stable suspension, with less tendency for particles to settle or form clusters. Conversely, when the zeta potential is close to zero, repulsive forces between particles are weaker, and attractive forces, such as van der Waals interactions, may dominate, leading to flocculation or sedimentation.

The significance of zeta potential extends beyond just stability. It also influences the rheological properties of a suspension. The reduction of zeta potential with decreasing pH leads to

the formation of a network structure in the suspension. This change is associated with an increase in viscosity and the emergence of a yield stress, which reflects the suspension's resistance to flow. A higher yield stress, observed at lower pH values with reduced zeta potential, indicates a stronger network that can resist sedimentation under certain conditions. [144]

2.3.4.2 Application of zeta potential measurements

The zeta potential plays a critical role in various industrial applications, particularly in stabilizing emulsions, dispersions, and slurries. It measures the electric charge at the particle-liquid interface, influencing stability by preventing aggregation. In processes such as Chemical Mechanical Polishing (CMP), zeta potential monitoring ensures the slurry remains stable, avoiding large particles that could scratch delicate surfaces. Additionally, it aids in controlling the long-term stability of emulsions, such as bitumen used for road repairs, where high zeta potential ensures the emulsion remains fluid and stable during storage [145].

2.3.4.3 Effect of pH.

The relationship between pH and zeta potential is primarily influenced by the protonation and deprotonation of surface sites. At low pH, surfaces become more protonated, leading to a positive zeta potential, while at higher pH, deprotonation occurs, resulting in a more negative zeta potential. The zeta potential tends to decrease and approach zero at a specific pH, known as the isoelectric point. Around this point, the repulsive forces between particles are minimal, leading to aggregation and sedimentation. Beyond the isoelectric point, as pH increases, the zeta potential becomes increasingly negative, creating stronger electrostatic repulsion between particles and enhancing suspension stability. Factors such as ion type, concentration, and surface kinetics can cause variability in zeta potential, but the general trend is that higher pH leads to greater stability due to increased repulsion from deprotonated sites. Surfactants can further alter the zeta potential, either stabilizing or destabilizing the suspension depending on their interaction with particle surfaces. [146, 147].

Zeta potential measurements of ceria particles reveal their surface charge and stability in dispersions. High positive or negative zeta potential indicates strong repulsion between particles, preventing aggregation and promoting stability. In aqueous dispersions, pH influences zeta

potential, with acidic conditions generally resulting in positive values and basic conditions leading to negative values (see Figure 27). [148, 16]

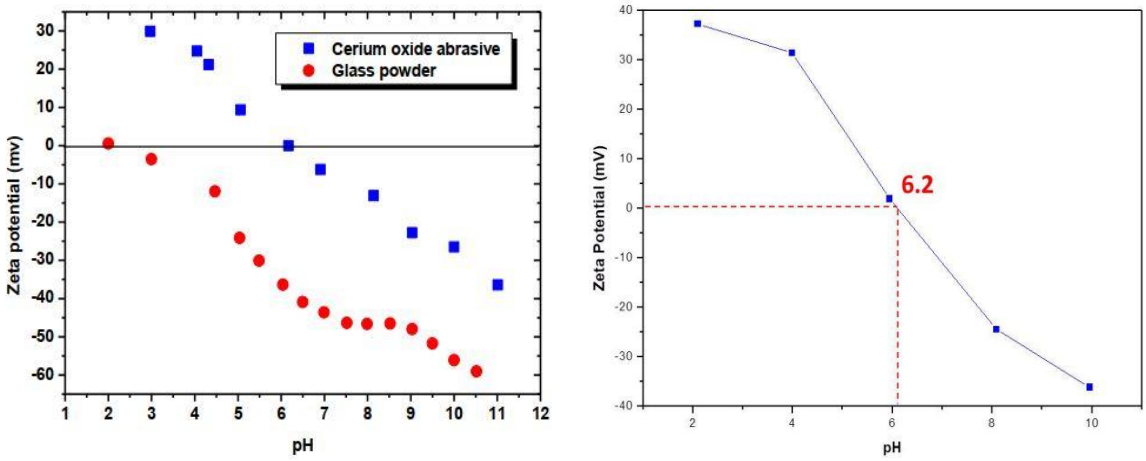


Figure 27: zeta potential of cerium particles (left) [149] and cerium nanoparticles (right) [150] in function of pH.

2.3.4.4 Effect of Conductivity

The thickness of the double layer depends upon the concentration of ions in the solution and can be calculated from the ionic strength of the medium. The higher the ionic strength, the more compressed the double layer becomes. The valency of the ions will also influence double-layer thickness. A trivalent ion such as Al_3^+ will compress the double layer to a greater extent in comparison with a monovalent ion such as Na^+. Inorganic ions can interact with charged surfaces in one of two distinct ways (i) nonspecific ion adsorption where they do not affect the isoelectric point. (ii) Specific ion adsorption, which will lead to a change in the value of the isoelectric point. The specific adsorption of ions onto a particle surface, even at low concentrations, can have a dramatic effect on the zeta potential of the particle dispersion. In some cases, specific ion adsorption can lead to charge reversal of the surface. [151]

2.3.5 Sedimentation method

Sedimentation techniques are widely used for particle size analysis due to their straightforward nature and the ability to provide mass-weighted size distributions. In these methods, particles in a liquid suspension settle at different rates depending on their size, with larger

particles settling faster than smaller ones. The settling process is typically measured using tools such as Andreasen pipettes, sedimentation balances, or sediment graphs. These techniques rely on Stokes' law, which calculates particle size based on settling velocity. However, the methods require careful sample preparation and are sensitive to particle interactions and suspension conditions, offering insights into the dispersion and stability of particles in slurries [152].

Moreover, sedimentation techniques are employed to evaluate the colloidal stability and particle size distribution in mixed abrasive slurries. Settling experiments often involve visual observation or systematic sampling from suspensions to track the settling behavior over time (Figure 28); researchers can assess the stability of slurries, which is influenced by factors such as particle concentration, surface charge, and the weight ratios of different components. This analysis, when combined with other measurements like zeta potential, allows for a deeper understanding of slurry behavior. These insights are crucial in applications like chemical mechanical polishing (CMP), where the interaction of chemical and mechanical forces directly affects material removal rates [153]

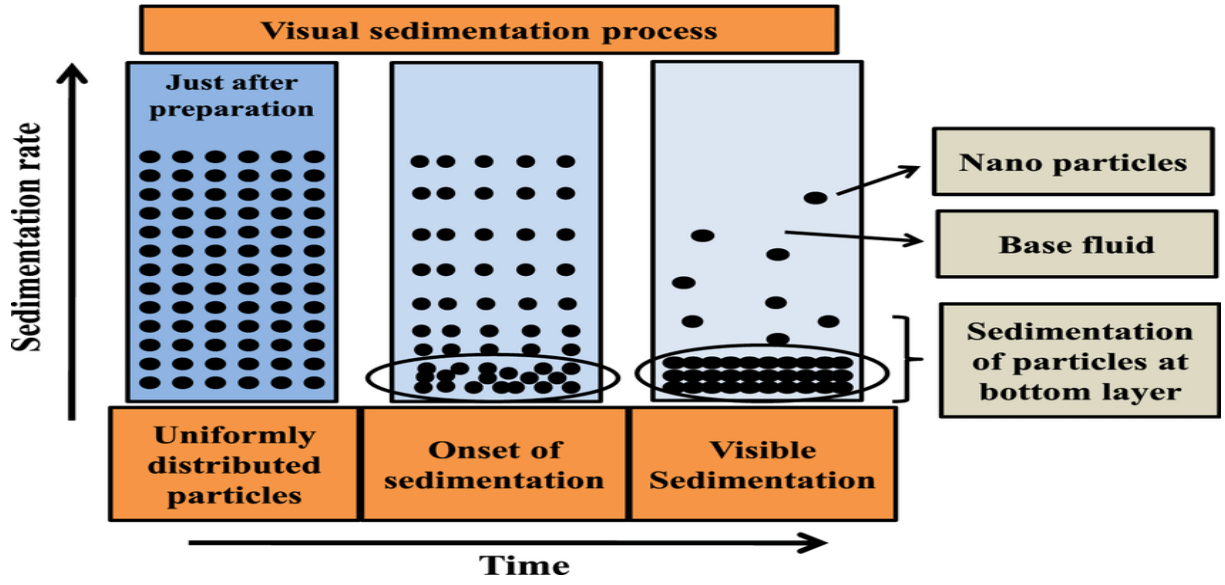


Figure 28: Schematic diagram of sedimentation test [154].

2.4 Conclusion

This chapter provided an overview of the most used polishing powders in CMP, including colloidal silica, diamond-based, alumina-based, and cerium oxide slurries, showing their different properties and applications. A variety of characterization techniques were also discussed, such as particle size distribution, zeta potential, sedimentation, and large particle count, as well as methods for dispersing and deagglomerating powders. These tools are essential for understanding and optimizing slurry performance, ensuring stable dispersion, and minimizing defects during the polishing process.

Chapter3. Investigation of the Impact of Optical Glass composition on Ceria Slurry Stability during Chemical Mechanical Polishing process.

3.1 Introduction

Cerium oxide (CeO_2) is one of the most effective glass polishing agents, providing high-quality polished surfaces [155-157]. it provides superior polishing performance compared to other materials, citing typical abrasive materials such as SiO_2 and Al_2O_3. The mechanical strength of CeO_2 is less than that of glass materials. Nevertheless, it achieves higher MRR combined with excellent surface quality of material [158]. The high polishing efficiency of cerium oxide stems from its chemical properties because the polishing of glass and certain other surfaces is not only a purely mechanical process but also involves a complex set of chemical interactions between the polishing agent, the polished surface and the polishing medium [159,160].

Difficulties associated with improving abrasive performance center around an understanding of how the chemistry and physical properties of the abrasive slurry affect polishing [161]. In recent years, scholarly attention has been directed toward investigating the influence of slurry parameters on the polishing outcomes of optical glass, particularly with regard to material removal rate and surface roughness. Pal et al. [162] observed that increasing concentrations of abrasive particles in the slurry allow more particles to come in direct contact with the workpiece surface, resulting in higher material removal rates. The study also found that changing the abrasive concentration from 5 wt.% to 6.25 wt.% increased the material removal rate by approximately 56%. Zhang et al. [163] showed that the MRR linearly increases with increasing abrasive concentration, reaching its maximum at 20 wt.% and then stabilizing while the observations of Wang et al. [39] contradict the conventional belief that the MRR would decrease with decreasing concentration, especially at very low concentrations, this abnormal increase of MRR was attributed to the good dispersion of slurry particles and the change from Ce^{4+} to Ce^{3+} as the ceria concentration decreased.

Particle size distribution (PSD) has a significant impact on the removal rate and surface roughness during CMP polishing [164]; it affects the load per particle and the fraction of particles removing material by plastic removal. A wider PSD leads to a greater difference in removal rates between different glasses [165]. According to Sampurno et al. [166], the particle size of cerium oxide directly affects the coefficient of friction (COF) and removal rate in the polishing process. The larger the particle size, the higher the COF and removal rate. In Kim's et al. study, the particle

size distribution of the slurry begins to increase in the temperature range of 50-60 °C in all experiments. This increase in PSD is attributed to an increase in the kinetic energy, leading to a higher probability of collisions between dispersed particles. This suggests that in addition to the mechanical energy resulting from slurry flow, higher temperatures can result in particle aggregation, leading to higher material removal rates [167].

In addition to the previously mentioned parameters, it is important to consider the pH value during the glass polishing process to achieve the desired surface quality [168] [169]. The pH value of the slurry used for polishing affects the MRR and surface roughness of the glass. Both acidic and alkaline conditions can lead to higher MRRs, while higher pH values can result in rougher surface textures [170]. Modifying the slurry's pH will make particles aggregate or disaggregate, which modifies the particle size distribution [171]. Good suspension stability can ensure a steady stream of slurry delivery and supply. It also influences the formation of surface scratches and pitting during the polishing process [172] [173]. Wakamatsu et al. showed in their study that colloidal ceria particles could be aggregated by adding potassium hydroxide (KOH) to the colloidal ceria slurry. The concentration of KOH has a strong correlation with the extent of particle aggregation. By actively aggregating colloidal ceria particles, it is possible to achieve a higher removal rate during glass substrate chemical mechanical polishing [174]. Surtwala et al. added glass components (K_3PO_4 for phosphate glass and $Si(OH)_4$ for fused silica) to the slurry to simulate the real chemical reactions that might occur between glass and the slurry at the polishing interface. However, it is important to note that the study does not provide conclusive evidence for the occurrence of these chemical reactions during glass polishing [87].

All previously cited works make it evident that slurry aggregation behavior affects the particle size distribution and particle concentration which are the main factors affecting material removal and surface roughness. Recently the work has focused on the optimization of slurry stability to have more efficient and precise polishing results. Controlling the zeta potential by introducing electrolytes such as sodium citrate ($Na_3C_6H_5O_7 \cdot 2H_2O$) can improve suspension stability by reducing particle agglomeration. It has been observed that the slurry with $Na_3C_6H_5O_7 \cdot 2H_2O$ exhibits the highest stability compared to slurries without electrolytes or containing NaCl and $BaCl_2$ [175]. The addition of different organic acids as additives in the slurry can significantly affect the dispersion stability. Acetic acid shows the best dispersion performance, resulting in a stable slurry with a smaller particle size and higher zeta potential compared to lactic

acid and oxalic acid [19]. The addition of APS (g-Aminopropyltriethoxysilane) to ceria nanoparticles helps to eliminate agglomeration and improve their stability in aqueous fluids. The modified particles exhibit better dispersibility in aqueous media and eliminate agglomeration compared to unmodified particles [176].

Most studies on slurry behavior focused on assessing the stability of ceria abrasives before the polishing process. However, there are a few works investigating the impact of certain factors on particle stability during the actual polishing process. In this paper, the impact of glass chemical composition on the stability of ceria particles during the polishing process is studied. Specifically, three glass types, fused silica glass, borosilicate glass, and soda-lime-silicate glass were investigated in detail. Our approach involved measuring the slurry pH, zeta potential, and particle size distribution. Additionally, we employed real-time imaging to capture the sedimentation and stability state of particles at various time intervals. To complement this, scanning electron microscopy (SEM) was employed to visualize the aggregation and dispersion of particles. The combined analyses aim to provide a comprehensive understanding of how the chemical composition of glass influences the stability of ceria particles throughout the polishing process.

3.2 Materials and Methods

In this study, three different glass samples: soda-lime glass (SL), borosilicate glass (BS), and fused silica (FS) of 7×7 cm^2 area were selected and polished based on their chemical compositions representing high, medium, and zero alkali content, respectively. The borosilicate glass was produced in our laboratory using the melt-quench technique.

3.2.1 Borosilicate glass production

The glass was specifically produced to achieve a desired composition, with a focus on the concentration of alkali elements. The composition of the glass, including the alkali elements, is detailed as follows:

Chemical element	Concentration (mol)	Concentration(g)
SiO_2	75	180.83
B_2O_3	14	43,032
NaO_2	8	34.03
CaO	2	8.03
Al_2O_3	1	4.09

Table 3: Concentration of the chemical elements in borosilicate glass.

To produce glass with a specific composition, raw materials such as SiO_2, B_2O_3, Al_2O_3, Na_2O, and CaO are weighed according to the desired proportions, with B_2O_3 typically added in slightly higher weight (× 1.1) to compensate for evaporation during melting (Figure 29).



Figure 29: Raw materials preparation before mixing (left) and after mixing (right).

The materials are ground into fine powders, thoroughly mixed, and placed into a high-purity crucible. The batch is melted in a furnace at temperatures between 1580°C and 1600°C, held for about 2 hours and 20 minutes to ensure homogeneity, and refined to remove bubbles and impurities (Figure 30). The molten glass is poured into a mold and allowed to cool. The mold is then placed in an annealing furnace, where the glass undergoes controlled cooling from its annealing temperature of 570°C, to room temperature to relieve internal stress.



Figure 30: Fabrication process of molten glass: (left) A crucible containing molten glass at high temperature, showing its bright orange glow due to thermal radiation. (right) The molten glass is poured and shaped using a metal mold, highlighting its transition from a liquid to a solid state.

The chemical compositions of the glasses are given in Table 4. Two types of slurries were used as abrasives: Nano-cerium oxide (CeO_2) particles with an average particle diameter around 80 nm from (supplier Pieplow&Brandt GmbH), as well as ceria (CeO_2) powder with an average particle diameter around 400 nm from (supplier Treibacher Industry AG)

	SiO_2	**Na_2O**	**MgO**	**Al_2O_3**	**B_2O_3**	**K_2O**	**CaO**	**TiO_2**	**Fe_2O_3**
Soda-lime wt.%	72.80	13.07	4.21	0.48	-	0.28	8.80	0.03	0.08
Borosilicate wt.%	75.00	8.00	-	1.00	14.00	-	2.00	-	-
Fused silica wt.%	99.99	-	-	-	-	-	-	-	-

Table 4: Chemical composition of the used glass samples.

3.2.2 The polishing process

Before the polishing process, the samples were ground using a consistent grinding sequence with grinding disks of different grain sizes (see Figure 31).

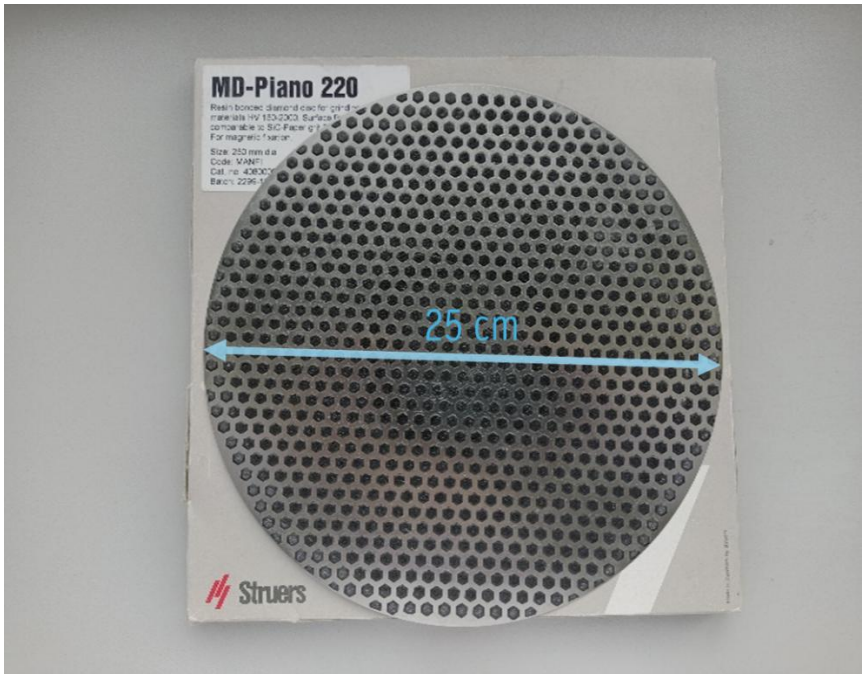


Figure 31: Example of one of the grinding disks used before the polishing process.

The polishing was performed using a semi-automatic Struers polishing machine (figure 32), characterized by adjustable rotation speeds and controlled pressure application. However, slight vibrations were observed in the rotating tool as illustrated in Figure 33, which may influence the uniformity of the polished surface. To address the issue of vibrations in the rotating tool, a series of tests were conducted (Figure 34). The final solution involved polishing a single sample with a 7 × 7 cm square area at a time. The region with uniform surface roughness was a circular area within the polished glass. To ensure consistency, each glass sample was positioned identically, resulting in the same uniform polished circle across all glass types. This approach allowed for accurate comparisons in terms of material removal and surface roughness measurements.



Figure 32: the-polishing machine used for the experiment.

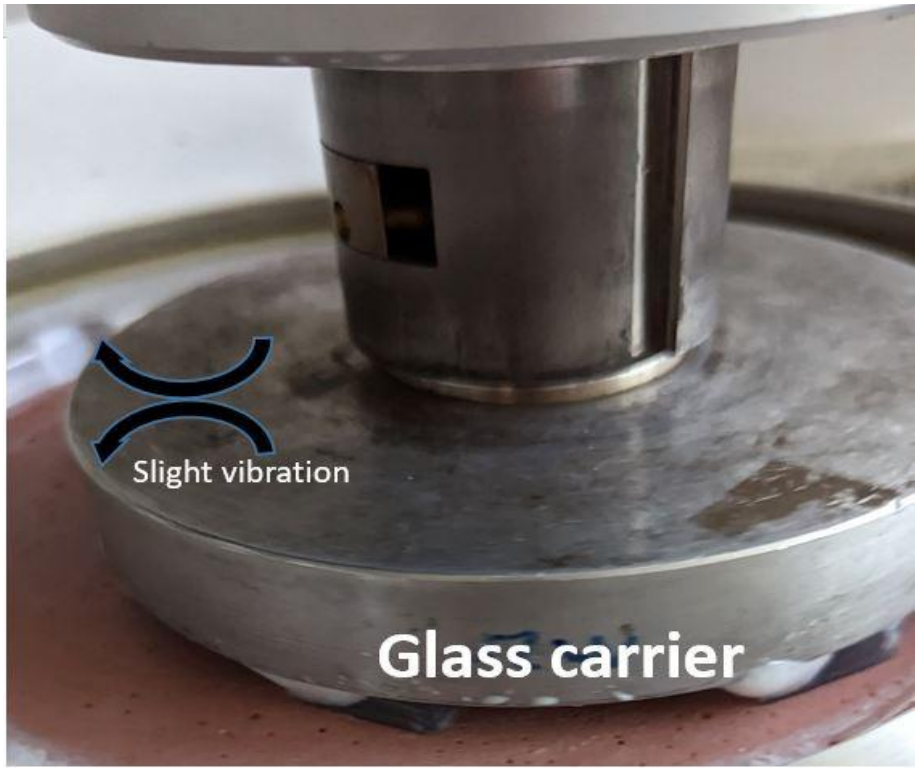


Figure 33: Illustration of the slight vibration within the glass carrier (⌀= 15 cm) .

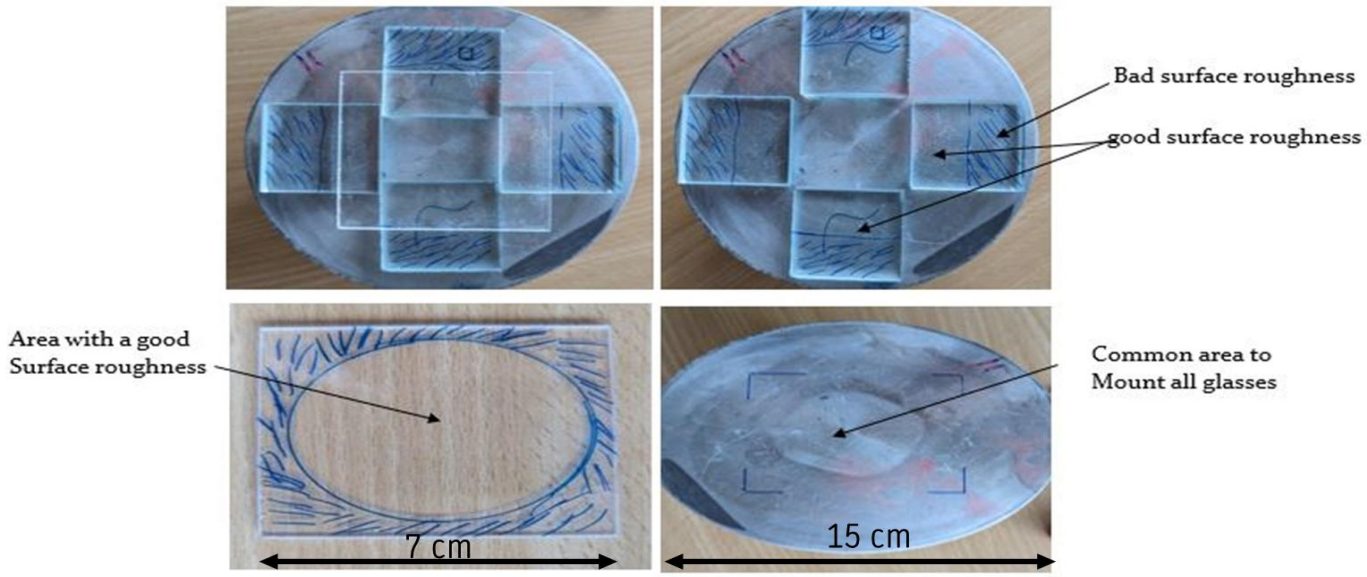


Figure 34: Illustration of the Polished Glass Sample: Circular Uniform Area, Mounting Region, and Surface Quality Zones (Good and Bad Polished Areas).

A customized polishing plate shown in Figure 35 was designed and produced to effectively collect the abrasives during the polishing process, as illustrated in Figure 36.

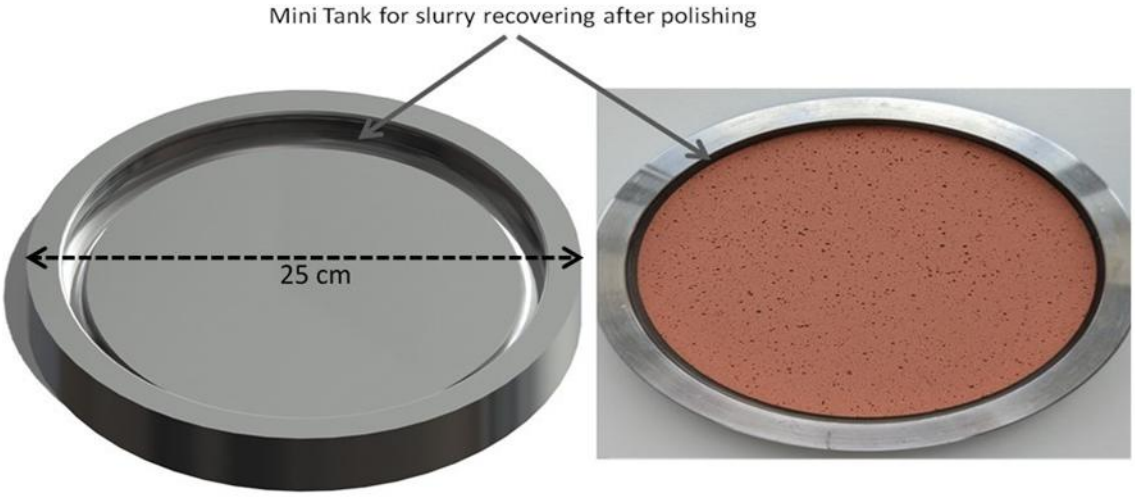


Figure 35: CAD image (left) and photograph (right) of the polishing plate (polishing pad included) made for the experiments.

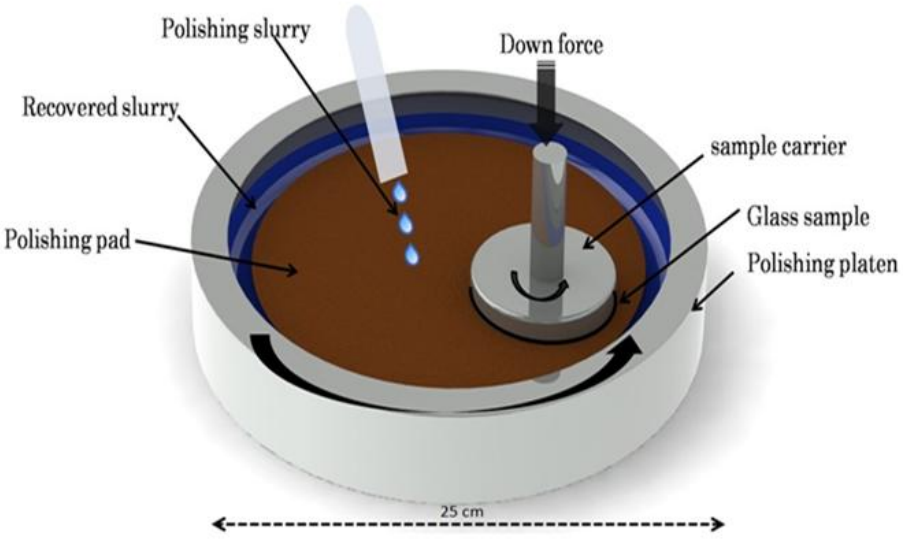


Figure 36: Schematic illustration of the polishing process and slurry recovery.

The polishing process consisted of an 8-minute cycle for each glass substrate using only 100 ml of each slurry type with the same concentration to maximize any potential interaction between the glass chemicals and ceria particles. The polishing time was selected to be 8 minutes to have enough data to study the pH variation over time. pH measurements of the slurry were conducted at 2-minute intervals to monitor potential changes. Polyurethane P-66 polishing pads and consumables were systematically replaced following each successive polishing operation as a preventive measure against potential contamination. This rigorous protocol aimed to maintain the integrity of the polishing process by ensuring that any potential residues or impurities from prior operations did not interfere with subsequent polishing procedures. The regular replacement of pads and consumables adhered to established standards of cleanliness and quality control, contributing to the reliability and reproducibility of the experimental results. The material removal (MR) was determined by measuring the mass difference of the glass substrate before and after the polishing, using a digital weighing scale (AUW220D, Shimadzu Corp.), with considerations for substrate density and area.

Surface roughness (Ra) was measured using a specialized profilometer (Alpha-Step IQ surface profiler), which provided insights into the roughness changes on the glass substrates. The dispersion or aggregation of abrasive particles was visualized using SEM (Auriga 60 Crossbeam Carl Zeiss AG). The particle size distribution and zeta potential of the slurries were measured using a Zetasizer Nano (Malvern Panalytical GmbH). Before each measurement, the slurries were

sonicated for 5 minutes to ensure uniform dispersion of particles. Fresh consumables were used to transfer a fraction of the slurry into the measuring cells to avoid cross-contamination. Different measuring cells were used depending on the particle size, with separate cells for samples containing 80 nm particles and those containing 400 nm particles. Between repeated tests, the cells were cleaned using Deionized (DI) water under pressure, followed by gentle wiping with a thin cotton cloth, and then rinsed again with DI water; the cells were dried to prevent the addition of water droplets that could cause unintentional dilution of the slurry during subsequent measurements.

Detailed polishing parameters and conditions are presented in Table 5.

Work pieces	Soda-lime, fused silica, and borosilicate glasses (7x7 cm)
Slurry	• ceria powder of average ⌀≈400 nm diluted in DI water "Large" • Nano ceria type PB from Pieplow& Brandt ⌀≈80 nm "Small"
Polishing pad	LP-66 polyurethane pad
Polishing pressure	12.2 kPa
Plate rotation speed	150 min^{-1}
Slurry flow rate	12 ml/min
Slurry concentration wt%	3 %
Polishing machine	Struers Rotopol polishing machine

Table 5: Experimental conditions of polishing.

3.3 Material removal and surface roughness

In this investigation, material removal (MR) and surface roughness are crucial parameters used to evaluate the impact of removed material on pH variations. Notably, in this study, MR and surface roughness are independent of slurry aggregation, as the polishing particles were collected immediately after rubbing the glass surface and not reused, unlike traditional CMP processes where the slurry is reused for multiple polishing cycles.

3.3.1 *Effect of Particle Size on Material Removal*

The polishing using 400 nm particles resulted in higher material removal for all glass types compared to 80 nm particles (see Figure 37), with soda-lime glass exhibiting the highest MR, followed by borosilicate and fused silica showing minor removal. The higher MR using 400 nm abrasives is attributed to their ability to produce higher contact pressures at the surface and their capacity to remove more significant fractions of glass material during polishing. The differences in MR are also influenced by glass hardness and chemical composition [177]. Harder materials

tend to resist mechanical abrasion more effectively, leading to lower MR. Fused silica, being the hardest of the three, exhibits the least MR due to its high resistance to both mechanical abrasion and chemical attack. Its high purity and stable structure, which are composed of around 99.9% silicon dioxide, make it highly resistant to dissolution in CMP slurries. Borosilicate glass, which contains additional components like boron oxide and alumina, shows intermediate MR. While more chemically resistant than soda-lime glass, it is still more soluble than fused silica in CMP environments, contributing to its moderate MR. Soda-lime glass, being the softest and most chemically reactive, showed the highest MR. Its composition, which includes sodium and calcium oxides, makes it more prone to reacting with CMP slurries, and consequently, more significant material removal during polishing. The material removal results observed in this study closely match those reported by Suratwala et al. [178], with the difference that phosphate glass was polished instead of soda-lime glass. Both studies show a similar trend: phosphate and soda-lime glasses are softer than fused silica and borosilicate glasses and register higher material removal rates.

Furthermore, it is important to acknowledge that the material removal pattern across the three glasses varied when 80 nm abrasives were used. This change was largely due to the small amount of material removed, which is close to the polishing machine's error, making it difficult to distinguish significant differences in material removal.

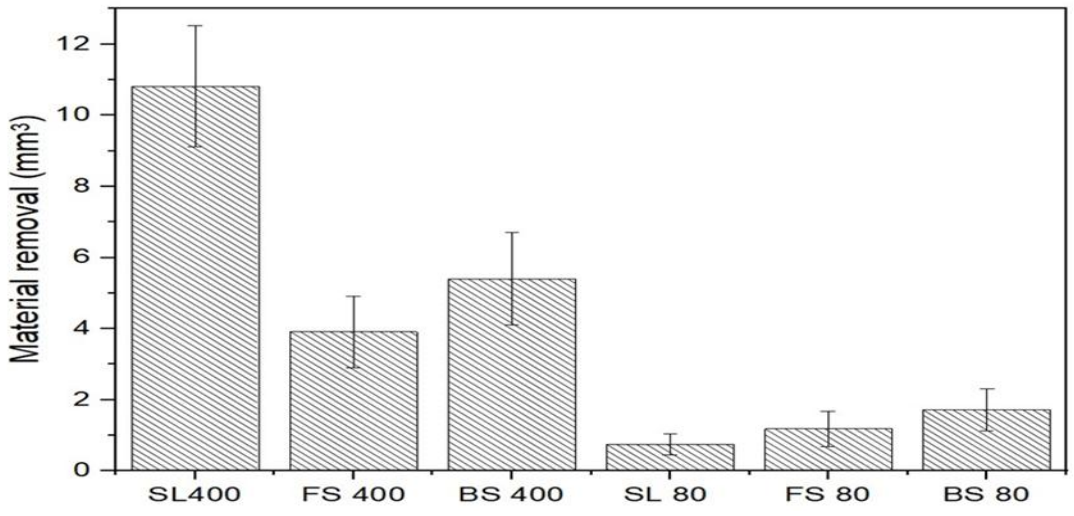


Figure 37: Material removal after 8 min of polishing using 400 nm ceria particles (SL400, FS400, BS400) and 80 nm particles (SL80, FS80, BS80) for all glass types (soda-lime, fused silica, borosilicate).

3.3.2 *Effect of Abrasive Size on Surface Roughness*

Using 80 nm ceria abrasives for polishing resulted in reduced material removal but improved surface roughness (see Figure 38). This decrease in MR is attributed to the lower contact pressure and smaller interaction volume of the finer abrasives. Although the 80 nm abrasives remove less material, they achieve a finer polish, leading to enhanced surface roughness. Typically, smaller abrasives contribute to superior surface quality. Additionally, the smoother surface observed with 80 nm particles compared to 400 nm particles is attributed to the fact that the 80 nm abrasives are used as a final polishing step, following initial polishing with larger particles. This sequence ensures that the finer abrasives refine the surface left by the bigger abrasives, resulting in a smoother final surface.

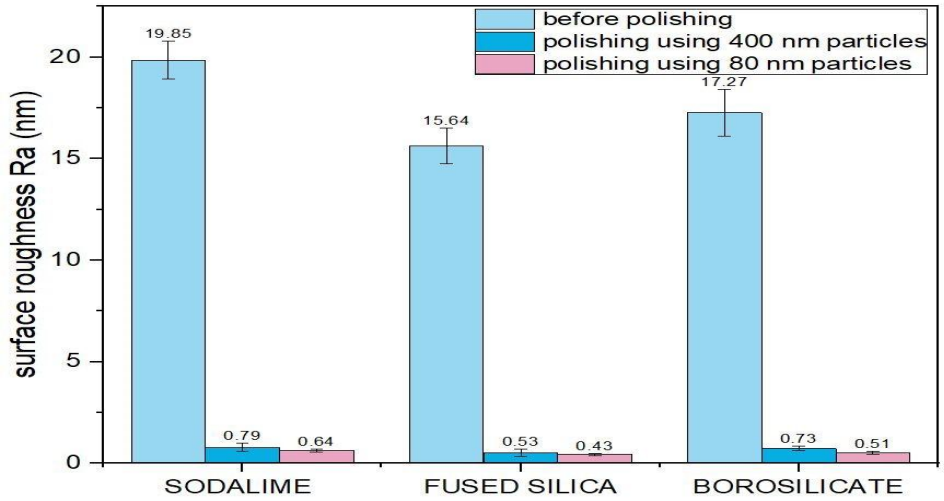


Figure 38: Surface roughness of glasses before and after polishing using 400 nm and 80 nm ceria particles.

3.4 pH MEASUREMENTS

The pH of the slurry is a pivotal parameter that has a direct influence on the zeta potential, particle size distribution, and overall chemical-mechanical polishing (CMP) performance [179]. Figure 39 shows the pH measurements of different slurries during the polishing of different glass samples.

3.4.1 *pH Stability using 80 nm ceria abrasives.*

The results reveal that the pH of slurries containing 80 nm ceria particles (SL80, BS80, and FS80) stays constant during the polishing of all glass types. This consistent pH is likely due to several factors, cited as follows:

Low Material Removal: The 80 nm ceria particles remove less material compared to larger particles. The small amount of glass removed during polishing leads to the minimal release of glass compounds into the slurry. Since these materials, such as alkali or alkaline earth oxides, have a limited impact on the overall pH, the slurry pH remains stable.

Limited Dissolution**:** With lower material removal, fewer chemical compounds from the glass dissolve into the slurry. This reduced dissolution means that fewer ions are introduced into the slurry, minimizing potential shifts in pH.

Buffering Capacity**:** Commercial slurries often contain stabilization agents or additives designed to buffer the pH [180, 181]. These agents play a crucial role in maintaining a stable pH by neutralizing minor fluctuations. For instance, if a small amount of solute species from the removed material is introduced due to the polishing process, these buffering agents can effectively neutralize these changes, thereby ensuring the stability of the slurry pH.

3.4.2 *pH modification using 400nm ceria abrasives.*

The findings indicate a noticeable increase in pH after the polishing of soda lime and borosilicate glass using 400 nm abrasive particles, registering values of 9.86 and 8.43, respectively. In contrast, the pH of fused silica glass remains stable after the polishing process using same-sized abrasives. This notable pH disparity is assumed to correlate with the variations in material removal and the alkaline element content within each glass composition. Specifically, glasses exhibiting higher material removal and elevated alkaline element concentrations, such as soda-lime glass. Studies of Suratwala et al. [87] and (E). Becker et al. [182] have discussed the potential dissolution of glass compounds into the slurry during CMP and its effect on pH. Becker et al. utilized HSC Chemistry software to simulate this process and found that the dissolution of glass compounds can alter slurry pH. Overall, the potential reasons for pH variations in this study can be discussed as follows:

Soda-lime and borosilicate glasses exhibit higher material removal rates compared to fused

silica. This increased removal leads to a greater amount of glass material dissolving into the slurry. For soda-lime glass, which contains significant amounts of alkali oxides (e.g., 13.07 wt.% Na_2O and 4.21 wt.% MgO), and borosilicate glass with moderate alkali content (e.g., 8 wt.% Na_2O), the dissolution introduces more alkaline ions (e.g., Na^+) into the slurry.

The presence of alkali elements in soda-lime and borosilicate glasses contributes to a higher pH in the slurry. Alkali oxides such as sodium oxide (Na_2O) react with water to form basic hydroxides as follows:

$$Na_2O + H_2O \rightarrow 2Na^+ + 2OH^- \quad (1)$$

The increase in hydroxide ions (OH^-) due to the dissolution of these alkaline oxides raises the slurry pH, making it more alkaline.

Furthermore, unlike soda-lime and borosilicate glasses, fused silica does not contain significant amounts of alkali oxides. SiO_2 does not readily react with water to form basic ions. Thus, the pH of the slurry remains stable since there are no significant sources of hydroxide ions from the glass itself.

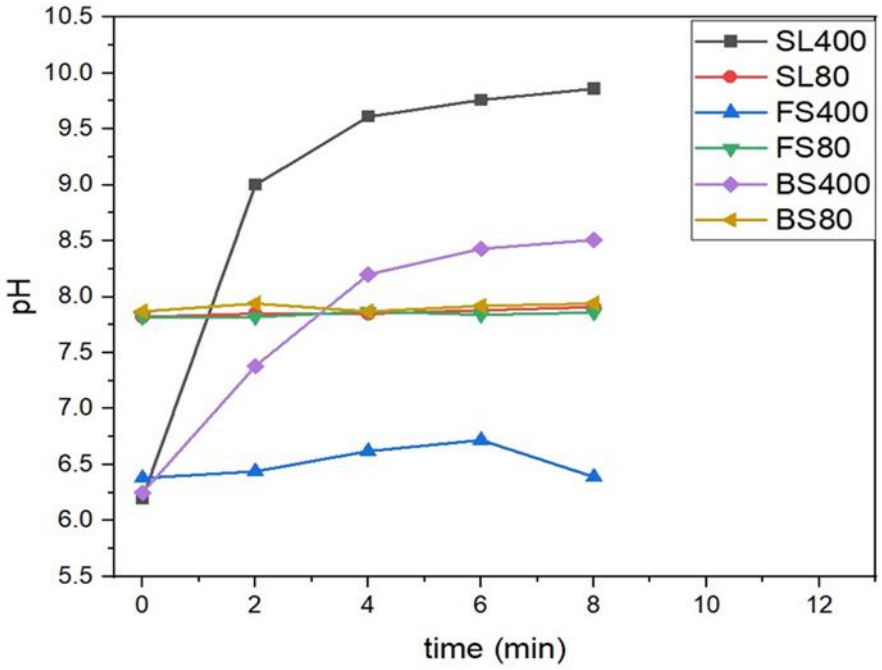


Figure 39: pH measurements of slurries over time.

3.4.3 *pH calculation.*

Understanding the complex chemical reactions occurring between glass substrates and polishing slurries is challenging, given the complexity of interactions among all chemical elements present during polishing. To gain an approximate perspective, it was focused on the impact of Na2O rates within the removed material of soda lime and borosilicate glasses, employing equation (2) to assess its effect on slurry pH. The calculated pH values after the polishing were found to be 11.09 for soda lime glass and 10.66 for borosilicate glass. While these values slightly surpass the experimental results, it is essential to recognize that other chemical elements interact concurrently, and not all elements from the removed glass are presumed to dissolve in the slurry.

$$pH = 14 - pOH = 14 - (-\log [OH^-]) \quad (2)$$

$$[OH^-] = 2(W_{mr} \times C_{Na2O}) / (M_{Na2O} \times V_s) \quad (3)$$

Where W_{mr} is the material removed from the polished glass, C_{Na2O} is the concentration of Na_2O in the selected glass, M_{Na2O} is the molar mass of Na_2O, and Vs is the volume of the slurry. It's important to clarify that the aim of this calculation is not to precisely determine the pH, but rather to evaluate whether the concentration of alkaline elements, specifically Na_2O in the removed material post-polishing of borosilicate and soda lime glasses, is significant enough to cause the observed pH increase in the experimental data.

3.5 Zeta potential measurements

The zeta potential is very significant for the polishing process since it is closely related to dispersion stability. In general, higher zeta potential (positive or negative) leads to higher slurry stability; otherwise, lower potential results in an increased tendency to agglomerate [132].

3.5.1 *Zeta potential of 400 nm particles.*

In aqueous solutions, ceria particles often have hydroxyl groups (-OH) attached to their surface. When the pH is high, an abundance of hydroxide ions (OH^-) leads these surface hydroxyl groups to deprotonate [183], resulting in the formation of negatively charged oxide ions ($Ce–O^-$) on the surface. This reaction can be represented by the following equation [184]:

$$Ce–OH + OH^- \rightarrow Ce–O^- + H_2O \quad (4)$$

As a result, the surface of ceria particles becomes negatively charged, increasing the overall negative surface charge density and making the zeta potential more negative. This effect is demonstrated in Figure 40, where the increase in the slurry pH after the polishing of borosilicate and soda-lime glass using 400 nm abrasives altered the ceria particles' surface charge from -9 mV to -37 mV and -32 mV, respectively. This shift significantly improves the stability of particles in the slurry, moving them from the low stability region to the good stability region by promoting repulsive forces between them. On the other hand, at average pH levels, where the concentration of hydrogen ions (H_3O^+) and hydroxide ions (OH^-) is more balanced, the surface hydroxyl groups of ceria particles undergo partial deprotonation or protonation. This leads to the zeta potential being closer to zero, particularly near the isoelectric point (IEP), where the overall charge on the particle surface is minimal. Within this pH range, the zeta potential value is low, indicating weaker electrostatic forces between particles. This is observed in both slurries before (OS400) and after the polishing of fused silica glass (FS400). This weaker repulsion reduces particle stability, leading to a greater tendency for particle aggregation compared to situations where the zeta potential is more negative.

3.5.2 *Zeta potential of 80 nm particles*

As expected, post-polishing using commercial slurries containing 80 nm ceria abrasives, characterized by minimal material removal and stable pH, resulted in nearly identical zeta potential values to those measured before polishing (Figure 40). Specifically, the zeta potential was -53.5 mV for the slurry before polishing and -54.4 mV, -51.7 mV, and -55.9 mV for the slurries after polishing soda-lime glass, fused silica, and borosilicate glass, respectively. A small change in the zeta potential of the slurry was observed, with a peak value of 2.4 mV. This slight deviation is unlikely to affect the stability of the slurry significantly and may be due to experimental factors such as the introduction of small volumes of slurry into the measurement cells, which could affect particle concentration. Zeta potential is known to be sensitive to changes in particle concentration [185, 186]. However, while it is uncertain whether the variations in concentration within the tested slurry, in the range of 3 wt.%, have a significant impact, Gregory et al. [187] reported that zeta potential measurements have a reliability of approximately ±10% of the measured value. Importantly, our measured results fall within this ±10% deviation range, indicating the reliability

of our results despite the minor variation observed. This reliability confirms that the stable pH values observed after the polishing of all glasses using 80 nm slurries did not modify the surface charge density of those particles, therefore conserving the stability of the pristine slurry.

3.5.3 *Zeta potential of 400 nm ceria particles after fused silica glass polishing*

The 400 nm ceria particles showed reduced stability after polishing fused silica glass, with a zeta potential value of -0.65 mV, compared to -9 mV before polishing, even though the pH remained constant. This reduction in stability can be attributed to the mechanical interaction between the abrasives and the glass substrate during polishing. The friction and wear of abrasives caused by the polishing process [58] could modify the surface morphology of ceria particles and reveal different crystallographic orientations, exposing fresh sites with new chemical characteristics [188, 189]. These newly exposed sites, such as additional oxygen vacancies or modified hydroxyl groups, are more reactive and can interact differently with ions present in the slurry. As a result, acidic sites may attract hydroxide ions (OH^-), while basic sites may attract hydrogen ions (H_3O^+). This shift in ion adsorption modifies the surface charge density, resulting in changes to the zeta potential without any pH modification, unlike the slurries after the polishing of borosilicate (BS400) and soda-lime glass (SL400), where the pH of the slurry increases because of the glass compounds dissolution (8.43 and 9.86, respectively). In these alkaline conditions, the increased hydroxide ions (OH^-) concentration causes the newly exposed acidic sites on the ceria particle surfaces to accept hydroxide ions, resulting in deprotonation and the formation of negatively charged conjugate bases, such as $Ce–O^-$, as shown in equation (5). For instance, hydroxyl groups (-OH) on the ceria surface become deprotonated, enhancing the negative surface charge and zeta potential.

Conversely, basic sites that can accept protons are less affected because the already high concentration of hydroxide ions reduces their opportunity to become protonated. This shift enhances the negative surface charge density of the ceria particles, resulting in increased stability. Conversely, a low surface charge density will promote particle aggregation, as seen for FS400 and OS400 slurries.

3.5.4 *Effect of electrolytes nature on zeta potential*

This study suggests a complex interaction between pH, electrolyte nature, ionic strength, and glass composition. Interestingly, slurries used for polishing borosilicate glass exhibited significantly higher stability (-37 mV) compared to those used for polishing soda-lime glass (-32 mV) despite the higher pH observed after soda-lime glass polishing. Although an increase in pH generally leads to an increase in negative surface charge and a more negative zeta potential, the results of this study indicate a more complex interaction. While many studies evaluate zeta potential in relation to pH using the same chemical agent to adjust the pH [190-192], it is essential to recognize that the nature of the electrolytes present in the slurry and the ionic strength of additives can also influence zeta potential. For example, different additives and ionic environments, even at the same pH, can yield varying zeta potential values, affecting particle stability [179, 193].

In this study, the slurry used after polishing borosilicate glass demonstrated greater stability, as indicated by higher negative zeta potential values; even though its pH was lower than that of the slurry used after polishing soda-lime glass. This behavior likely results from differences in the chemical composition of the glasses. The distinct elemental compositions of the two glasses are assumed to interact differently with the abrasives in the slurry, further highlighting the complex interplay between pH, electrolyte nature, ionic strength, and glass composition in determining zeta potential and particle stability.

This observation reinforces the understanding of the different interactions between ceria abrasives and various glass substrates; while polishing fused silica glass decreases slurry stability, polishing borosilicate glass improves it, surpassing even the stability achieved when polishing soda lime glass. This complexity in ceria abrasive behavior shows the significant influence of glass composition on slurry characteristics during the polishing processes.

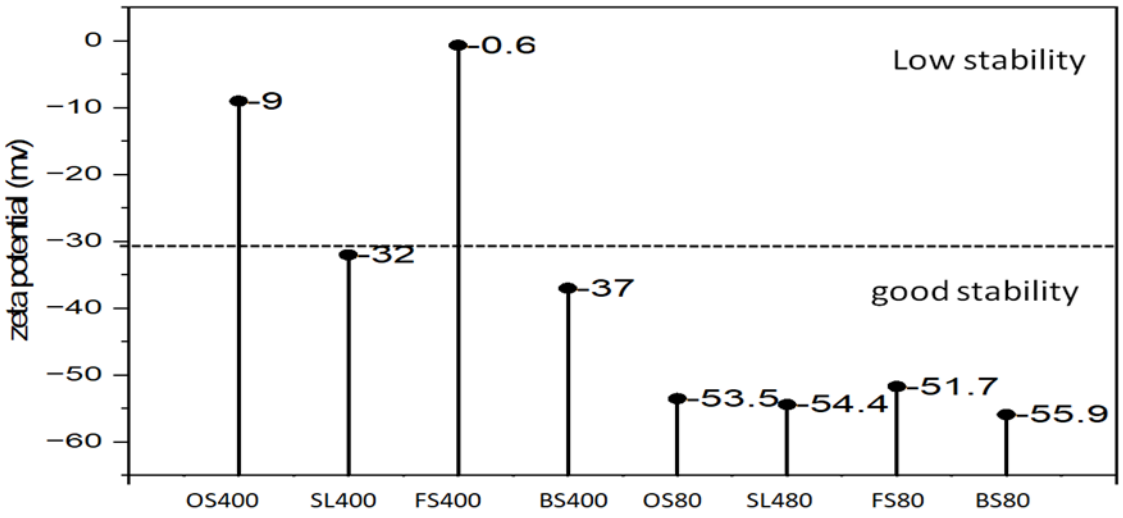


Figure 40: Zeta potential measurements of different ceria slurries: with 400 nm ceria particles (SL400, FS400, BS400, OS400) and 80 nm ceria particles (SL80, FS80, BS80, OS80), for all glass types (soda lime, fused silica, borosilicate).

3.6 Particles size distribution measurements

3.6.1 *Particles size distribution measurements of the 80 nm particles*

Figure 41 shows the particle size distribution (PSD) of 80 nm ceria particles in two conditions: before polishing (OS80) and after 8 minutes of polishing of the three glasses. Additionally, the PSD of the slurry before polishing with a reduced concentration is included to check the real size of those abrasives. Notably, the reported particle sizes exceeded the manufacturer's specified D50 size of 80 nm.

Acknowledging the Brownian motion phenomenon of nanoparticles, particularly those below 100 nm, is important [194]. To address this, the concentration was reduced to minimize its impact on the accuracy of particle size measurement. Higher concentrations can lead to multiple scattering during laser scanning. Multiple scattering occurs when light interacts with several particles before detection, causing deviations from the expected scattering patterns and resulting in inaccurate size measurements. By lowering the concentration, multiple scattering effects are minimized, improving the precision of the particle size measurements.

The results presented after reducing the concentration provide a more accurate representation of the actual particle sizes. Moreover, the comparison of particle size distribution curves of 80 nm particle slurries before and after the polishing of all glasses revealed no significant

differences (D50 size between 170 and 220 nm), which aligns with earlier pH and zeta potential measurements. A constant pH ensures the stability of surface charges on particles, as it directly influences their electrostatic interactions. At the same time, a stable zeta potential ensures sustained electrostatic repulsion between particles, preventing aggregation. The synergy of stable pH and zeta potential contributes to the overall electrokinetic and chemical stability of the system, preserving the initial PSD and minimizing the particle size variations.

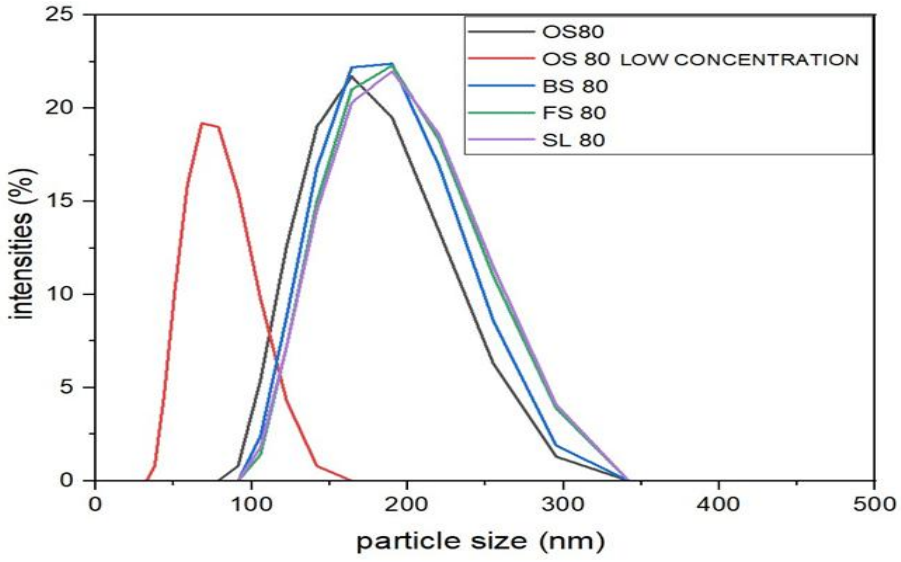


Figure 41: Particle size distribution of 80 nm ceria slurries before (OS80) and after polishing soda lime, fused silica, borosilicate glasses (BS80, FS80, SL80, respectively), and of the OS80 slurry after decreasing the concentration of particles.

3.6.2 *Particles size distribution measurements of 400 nm particles*

Figure 42 illustrates the particle size distribution of slurries containing 400 nm particles before and after the polishing of three different glasses at various time intervals following ultrasonic dispersion (6 min, 8 min, 12 min, and 60 min). In Figure 41a, ceria particle dispersion before polishing is shown, and initial observations reveal slight aggregation, with an average D50 size of approximately 700 nm after 6 minutes of ultrasonic dispersion. Subsequently, a significant portion of particles starts to sediment after 8 minutes, forming larger aggregates after 12 minutes. The global D50 size increases to around 2300 nm after one hour.

Moving to Figure 41b, which illustrates the aggregation behavior of ceria particles after

polishing fused silica glass over time, two distinct peaks emerge. The first peak indicates a slight aggregation of particles around 650 nm after 6 minutes, with a larger peak around 1900 nm. This behavior persists at 8 minutes and 12 minutes, with a continuous increase in average particle size from approximately 2000 nm to 4000 nm, ultimately reaching an average diameter of 5000 nm after 60 minutes. Despite the constant pH, the results align with zeta potential measurements, highlighting that slurry at the zero-zeta potential point (isoelectric point) exhibits higher aggregation compared to particles without polishing characterized by a zeta potential value of -9 mV, slightly below the isoelectric point.

Figure 41c shows particle sizes after polishing soda-lime glass, with aggregation observed after 8 and 12 minutes, reaching an average diameter of around 1300 nm. After 60 minutes, the particle size distribution stabilizes around an average diameter of 600 nm, suggesting a more stable state. Additionally, a small portion of the particles is sedimenting. Figure 41d (borosilicate glass) shows a completely different behaviour, with the particle size distribution remaining stable throughout all periods. A small aggregation appears after 8 minutes, possibly due to a small sedimentation over time; however, most particles maintain good dispersion, even after 1 hour of ultrasonic dispersion, with a D50 size of around 450 nm.

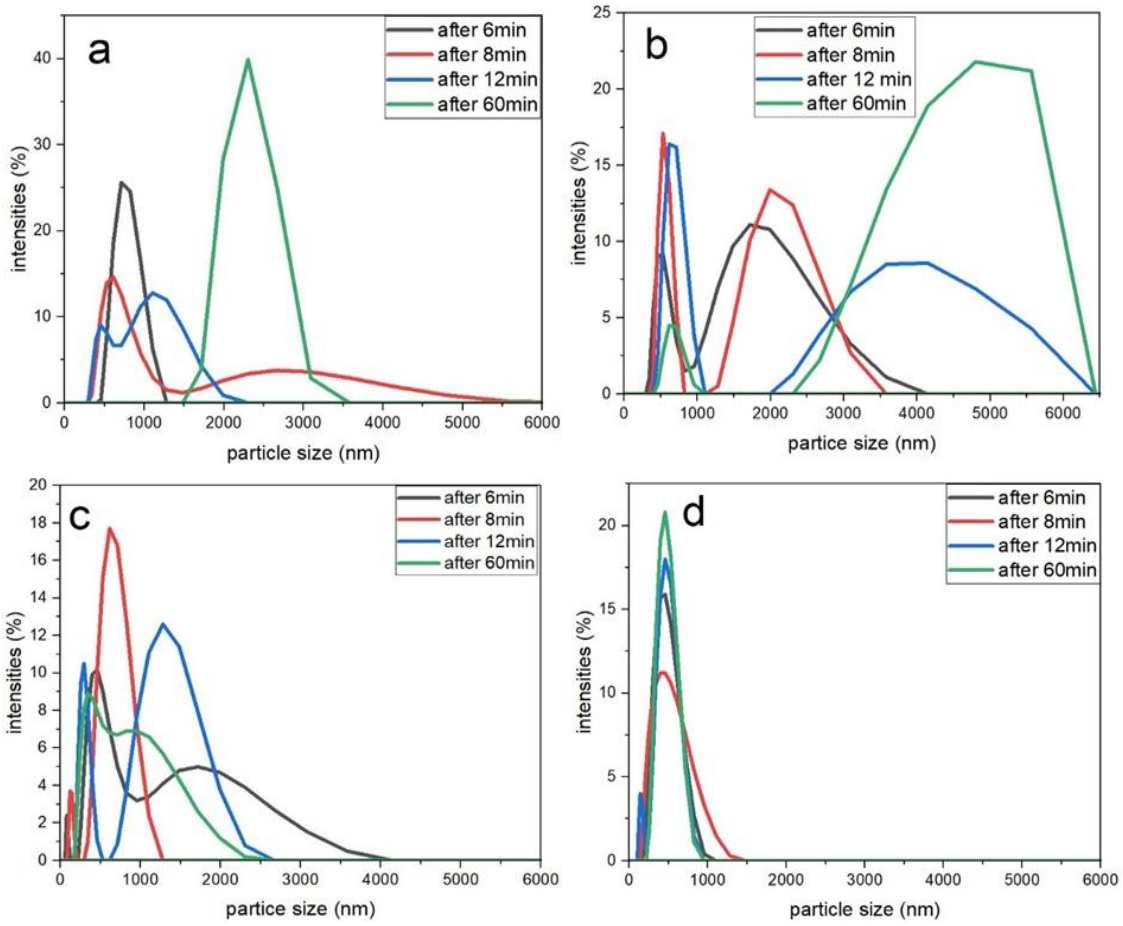


Figure 41: Particle size distribution of 400 nm ceria particles before polishing (a). and after the polishing process for 8 minutes of fused silica glass (b), soda-lime glass (c) and borosilicate glass (d) following 6 min, 8 min, 12 min and 60 min after ultrasonic dispersion.

3.7 Correlation between the sedimentation, particle size distribution (PSD), and SEM images.

The correlation between sedimentation, particle size distribution (PSD), and SEM images offers a comprehensive understanding of slurry stability and behavior. In the sedimentation tests (Figure 42), slurries using commercial ceria powder (BS80, SL80, FS80, and OS80) with high zeta potential values and consistent particle size distribution showed no visible color change over the 270-minute observation period. This indicates their excellent dispersion, as confirmed by the SEM images (Figure 43), which show well-dispersed particles with minimal aggregate formation. The particle size distribution (Figure 41) further supports this, with the particle sizes remaining stable

over time, demonstrating the stability of these slurries.

Similarly, BS400 and SL400 slurries, which had relatively high zeta potential values (-37 mV and -32 mV, respectively), exhibit minimal sedimentation, as observed in the sedimentation tests where no significant color change over time was observed. The SEM images confirm this by mainly showing dispersed particles with only minor aggregation. The PSD data (Figure 41) also aligns with these findings, showing that while some aggregation occurred, the particle size remained relatively stable over time. For instance, in the case of SL400, the particle size distribution after polishing soda-lime glass showed some aggregation initially. Eventually, it stabilized around a 600 nm average diameter, reflecting the relatively stable state indicated by the zeta potential.

In contrast, the FS400 and OS400 slurries exhibited noticeable sedimentation after 60 minutes, which became more pronounced after 270 minutes. This sedimentation behavior is consistent with their low zeta potential values (-0.65 mV and -9 mV, respectively), placing them in the non-stable region. The SEM images (Figure 43) of these slurries reveal significant aggregate formation, confirming that the low zeta potential values led to poor dispersion and increased particle aggregation, which was previously shown by the PSD data (Figure 41), where a significant increase in particle size was observed over time. For instance, after polishing fused silica glass (Figure 41b), the particle size distribution revealed two distinct peaks, indicating the presence of both small and large particle aggregates. This bimodal distribution suggests that the slurry experienced a significant particle aggregation, where smaller particles coalesced into larger clusters. The presence of these large aggregates points to significant instability within the slurry, leading to sedimentation over time. This behavior correlates with the very low zeta potential values measured, indicating that the electrostatic repulsion between particles was insufficient to prevent aggregation, resulting in poor colloidal stability and accelerated sedimentation.

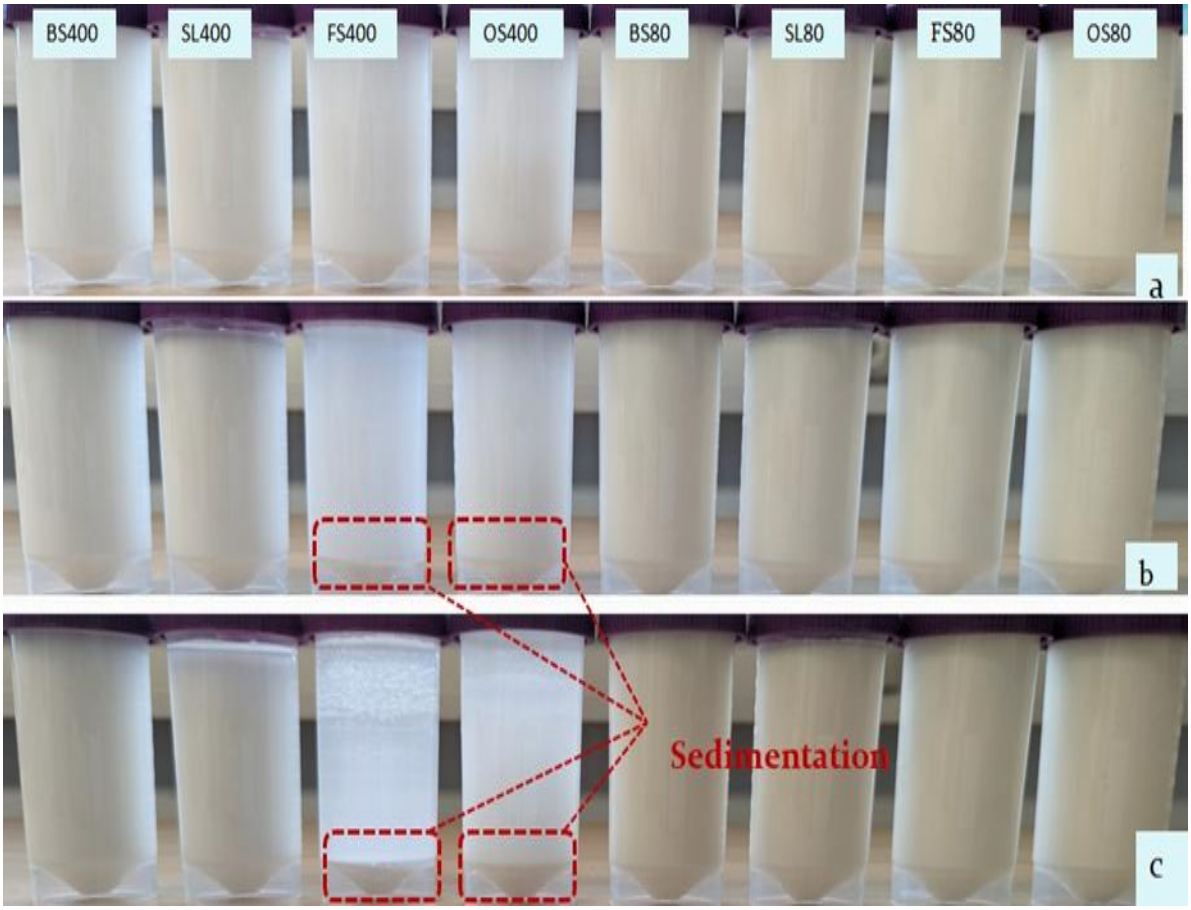
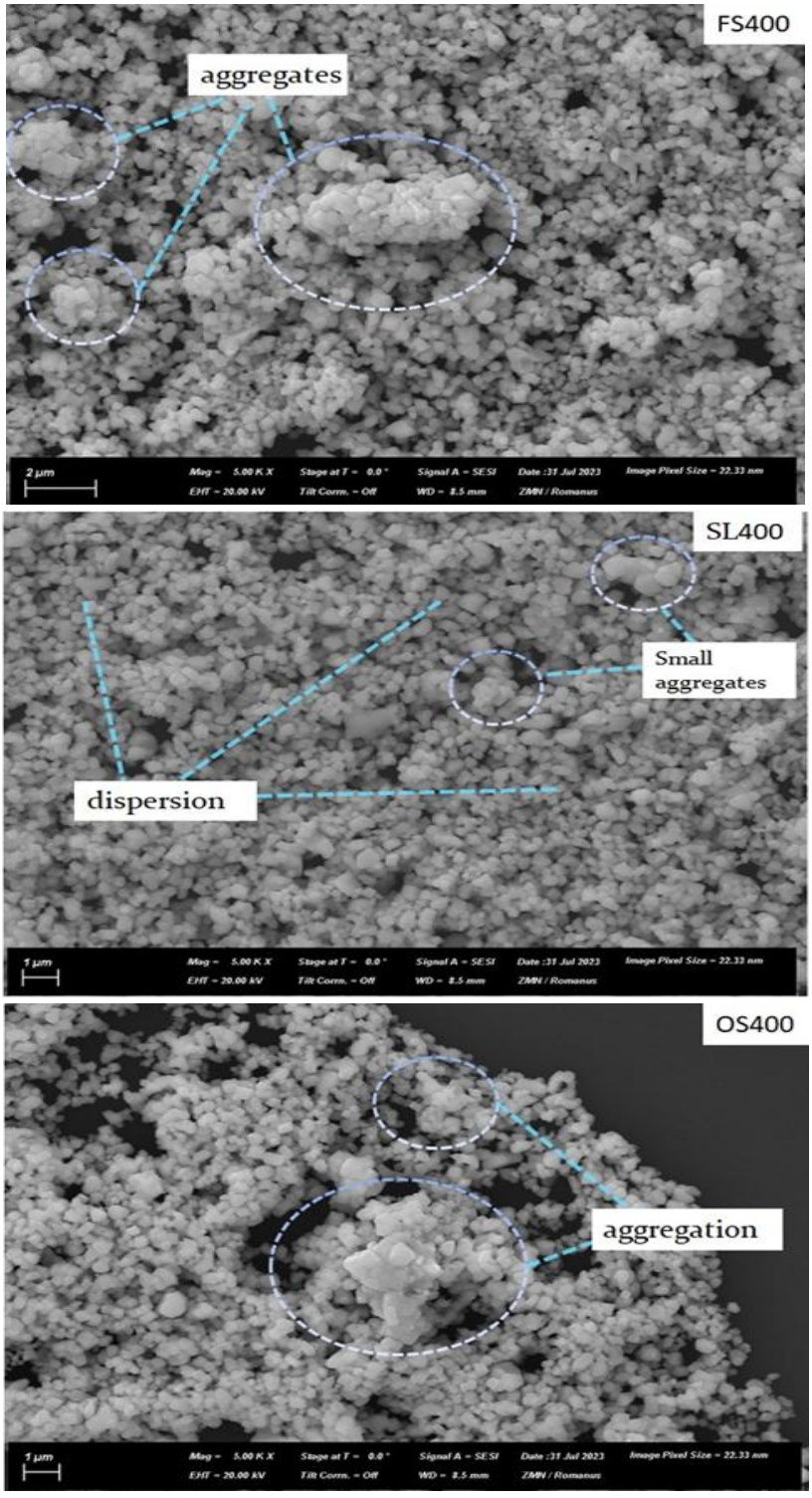
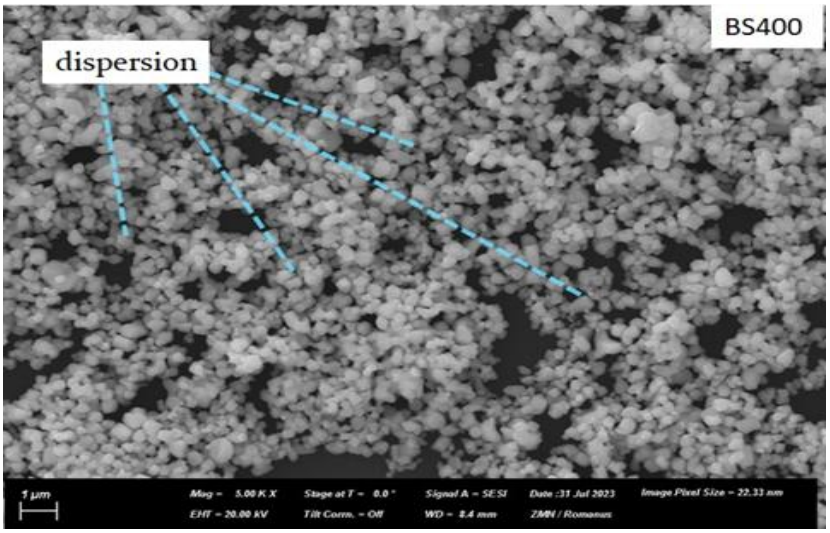
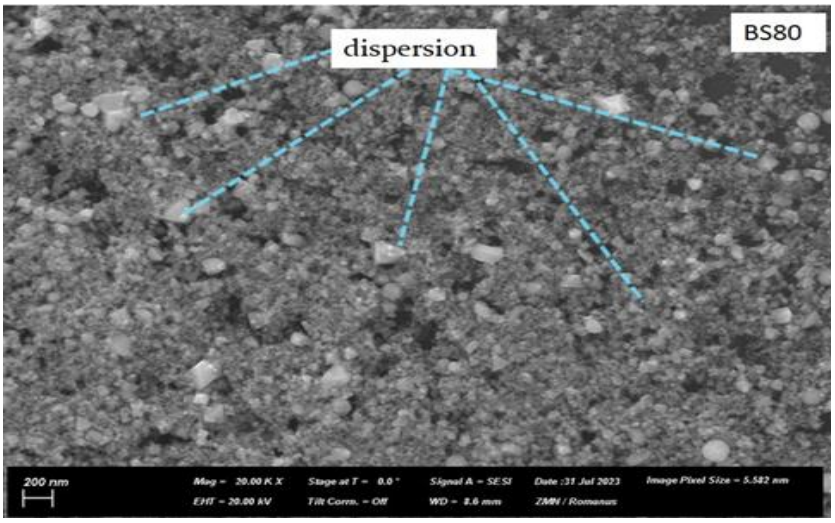


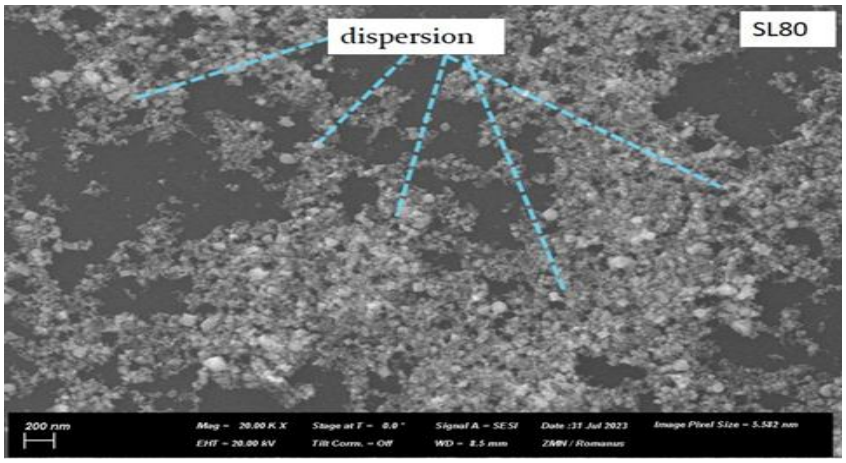
Figure 42: Sedimentation and aggregation states of 400 nm ceria abrasives BS400, SL400, FS400, OS 400 and 80 nm ceria abrasives BS80, SL80, FS80 and OS80 after a: 5 min, b: 60 min and c: 270 min from ultrasonic dispersion of all samples.

These observations highlight the strong correlation between zeta potential, particle size distribution, and the degree of dispersion or aggregation seen in both the sedimentation tests and SEM results. Slurries with high negative zeta potential values show more stable dispersion with minimal aggregation, as reflected in both PSD and SEM images. Conversely, slurries with zeta potential values near the isoelectric point show larger particle size distributions and significant aggregation, corresponding to the visual sedimentation and aggregate formation observed in SEM images.


FS400
aggregates
SL400
Small aggregates
dispersion
OS400
aggregation


BS400
dispersion
1 µm


BS80
dispersion
200 nm


SL80
dispersion
200 nm

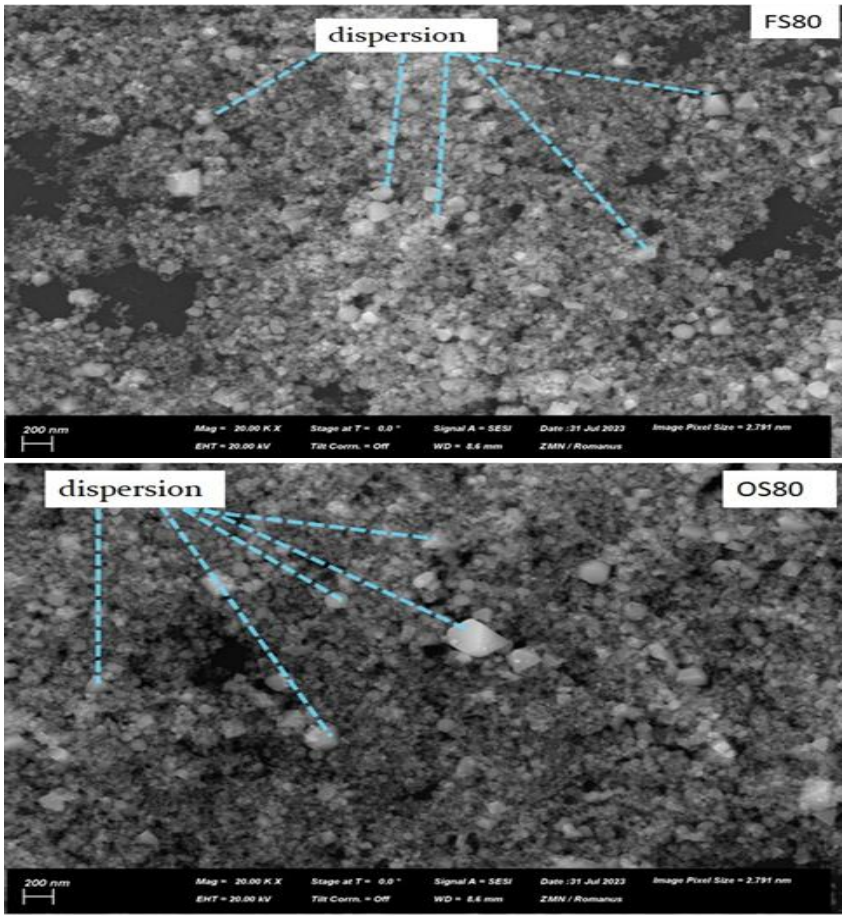


Figure 43: SEM pictures of 400 nm and 80 nm ceria slurries before polishing (OS) and after the polishing of soda lime, fused silica, borosilicate glasses after ultrasonic dispersion for 5 min. Scale bar: 1µm for (BS400, SL400, OS400), 2 µm for FS400 and 200 nm for all 80 nm ceria slurries.

3.8 Conclusion

A customized polishing setup was designed with a dedicated system to recover the slurry after each polishing cycle, minimizing external contamination. Consumables such as polishing pads and measurement cells were replaced between experiments to prevent carryover and maintain chemical integrity. The results suggest that in industrial contexts where slurry is reused, the progressive dissolution of glass compounds can modify abrasive stability if not adequately managed, especially in the absence of sufficient stabilizing agents.

Chapter4. Effect of slurry parameters on the polishing results

Chapter 4. Effect of slurry parameters on the polishing results

4.1 Introduction

Polishing results are influenced by various parameters, including tool velocity, pad type, polishing pressure, and slurry properties. Among these, slurry parameters are particularly difficult to control due to the complex behavior of millions or billions of abrasive particles within the polishing gap. These particles exhibit random motion and trajectories, leading to variations in slurry concentration and non-uniform participation of particles in material removal. Additionally, the initial particle size distribution tends to change during polishing due to two primary factors: changes in the slurry's chemical properties, which can induce particle aggregation, and abrasive wear during prolonged polishing, which alters particle size. These changes make the polishing process unpredictable.

To address these challenges, the influence of slurry aggregation on polishing results was investigated. Three types of slurries were prepared, representing different aggregation states: low, medium, and high. These slurries were used to polish N-BK7 (a standard optical glass) and fused silica (FS). The effects of the aggregation state on surface roughness and material removal rate (MRR) for each glass were analyzed. Additionally, an integrated sensor in the polishing machine measured the electrical active power during the polishing process. This data provided insights into changes in electrical power consumption due to the addition of chemicals affecting the slurry’s aggregation behavior.

The impact of prolonged polishing on particle size and its subsequent effect on MRR and surface roughness was also examined. Fused silica samples were polished over different time durations, to determine whether continuous polishing alters particle size due to abrasive wear and whether these changes influence polishing results. This investigation aims to provide a comprehensive understanding of how slurry behavior, influenced by aggregation and particle wear, affects the polishing process and its outcomes.

4.2 Investigation of Slurry Aggregation Effects on CMP Process with Electrical Power Sensor Utilization.

4.2.1 Preparation of slurries with different aggregation states

Three ceria-based slurries with different aggregation states (small, medium, and high) were prepared for the experiments, each having distinct pH values of (5.6), (6.7), and (12.6), respectively. The slurries consisted of ceria powder (PZ 500 Treibacher) diluted in deionized water (DIW) at a concentration of 4 wt.%. For the low aggregation state, 0.05 gL^{-1} of Tamol® NN 9104 was added to the slurry. Tamol, a BASF Group stabilization agent, is the sodium salt of a condensation product of naphthalene-sulfonic acid with formaldehyde.

The medium aggregation state slurry comprised only ceria particles and DIW, leading to automatic aggregation due to the known instability of ceria particles in the pH region between 6 and 7 [150, 191, 195, 196]. For the high aggregation state, 0.1 mol of KOH was added to the slurry. A SEM (micrograph) of the used ceria abrasives is shown in Figure 1 and the particles size distribution of the slurries (PSD) using the Zetasizer Nano (Malvern Panalytical GmbH) is shown in Figure 45.

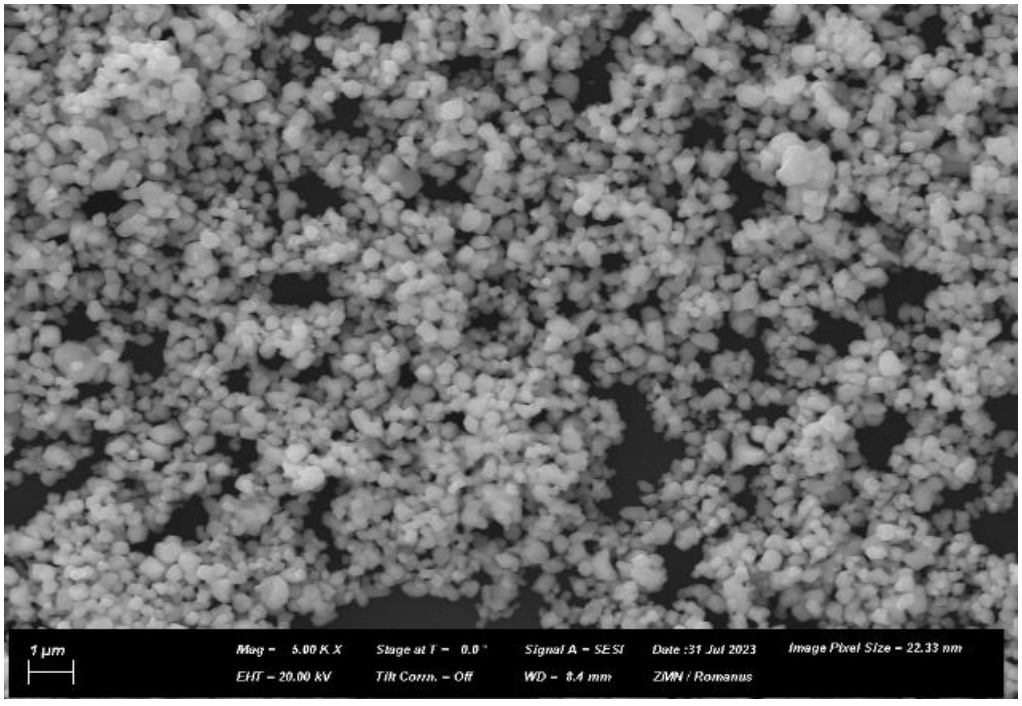


Figure 44: SEM image of the used ceria abrasives.

4.2.1.1 Particle size evolution

The particle size distribution measurements (PSD) in Figure 45 reveal that the addition of Tamol led to an average particle size of around 500 nm, while the slurry without any additives exhibited a D50 average of approximately 1400 nm. Remarkably, the D50 size increased to around 2500 nm after adding 0.1 mol of KOH.

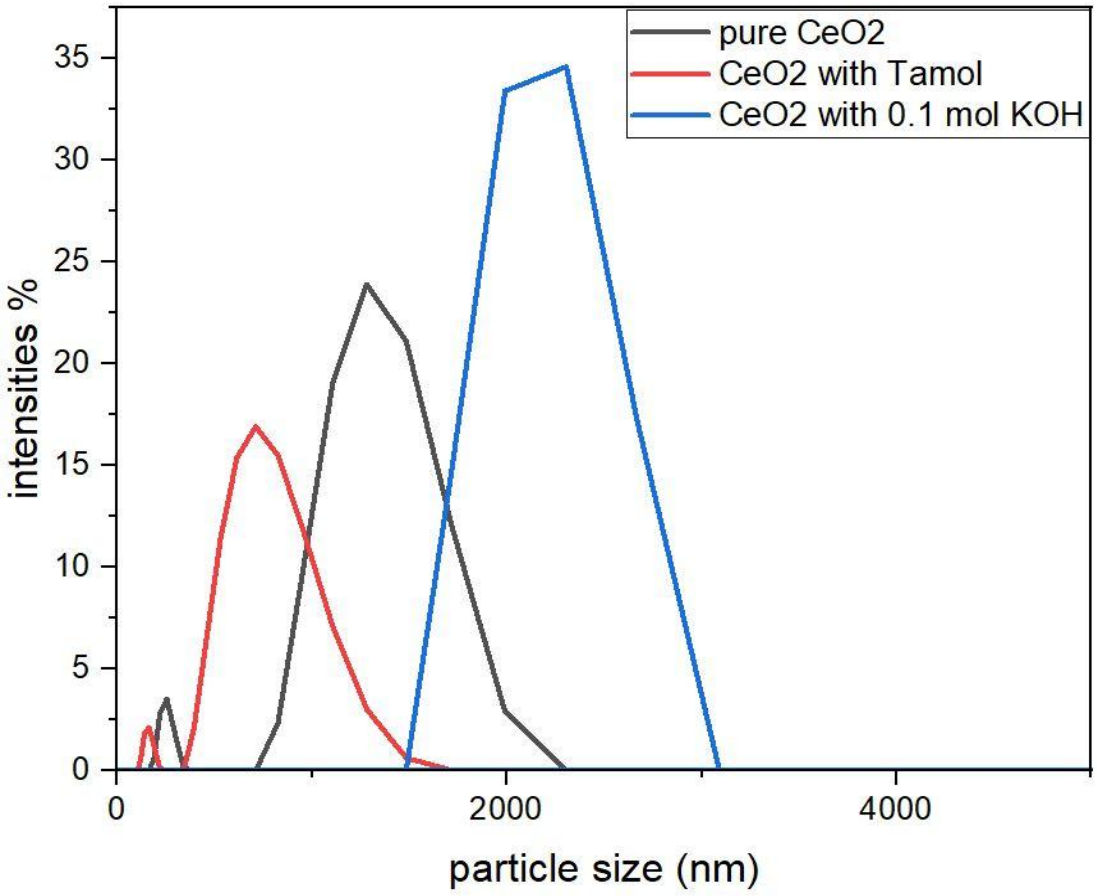


Figure 45: Particle size distribution (PSD) of the slurries in different stability states.

Figure 46 illustrates the increase in average particle size over time. The slurry with Tamol showed a low aggregation rate, reaching around 730 nm in 12 minutes. In contrast, the slurry without additives shows a higher aggregation rate, reaching approximately 1600 nm in the same period. The slurry with KOH experienced a rapid increase from 500 nm to 3200 nm in 9 min, followed by a slowed aggregation rate.

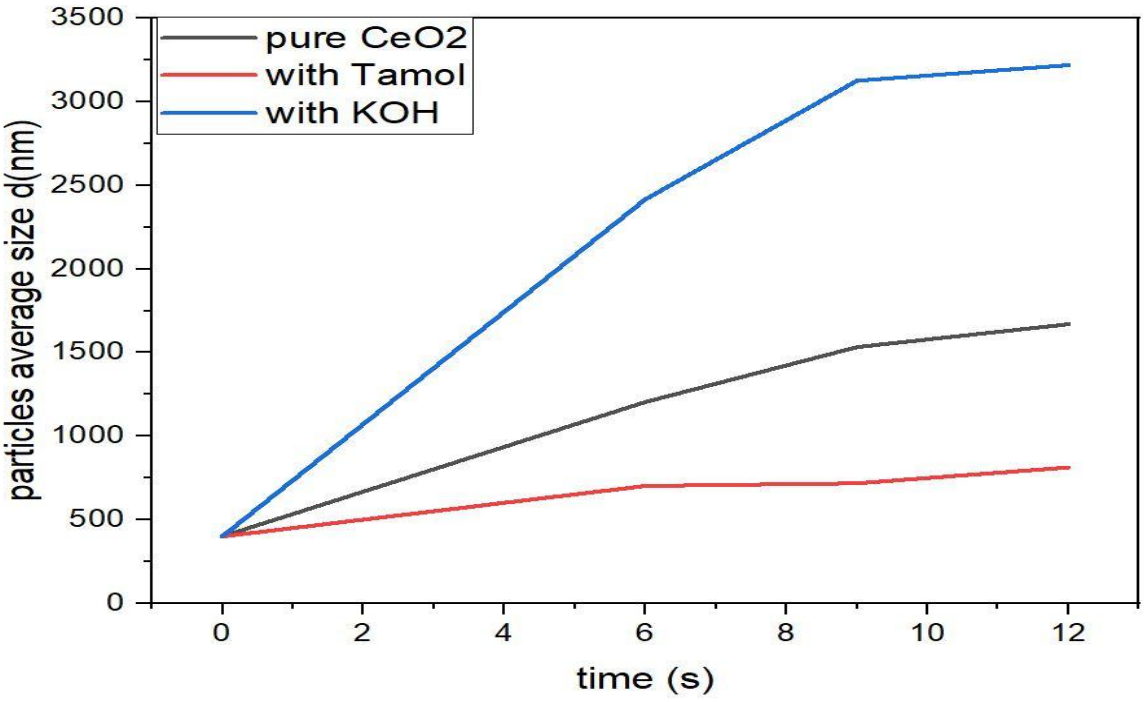


Figure 46: Particle average size variation after 12 min of ultrasonic dispersion.

4.2.1.2 Sedimentation behavior of the slurry

Figure 47 shows the sedimentation behavior of the three slurries. The slurry with Tamol demonstrated the lowest sedimentation rate, with a significant portion sedimenting after 60 min. The slurry without additives exhibited higher sedimentation rates, and the slurry containing KOH showed the highest sedimentation rates aligning with the particle size distribution results. In summary, the suspension containing Tamol stabilization agent exhibited lower particle size distribution, a slower increase in size over time, and lower sedimentation rates while the suspension without additives had relatively high PSD (170 % more than slurry with Tamol), faster aggregate formation, and higher sedimentation rates. The slurry containing KOH showed the highest PSD (500 % more than the slurry with Tamol), the fastest aggregation, and the highest sedimentation rates.

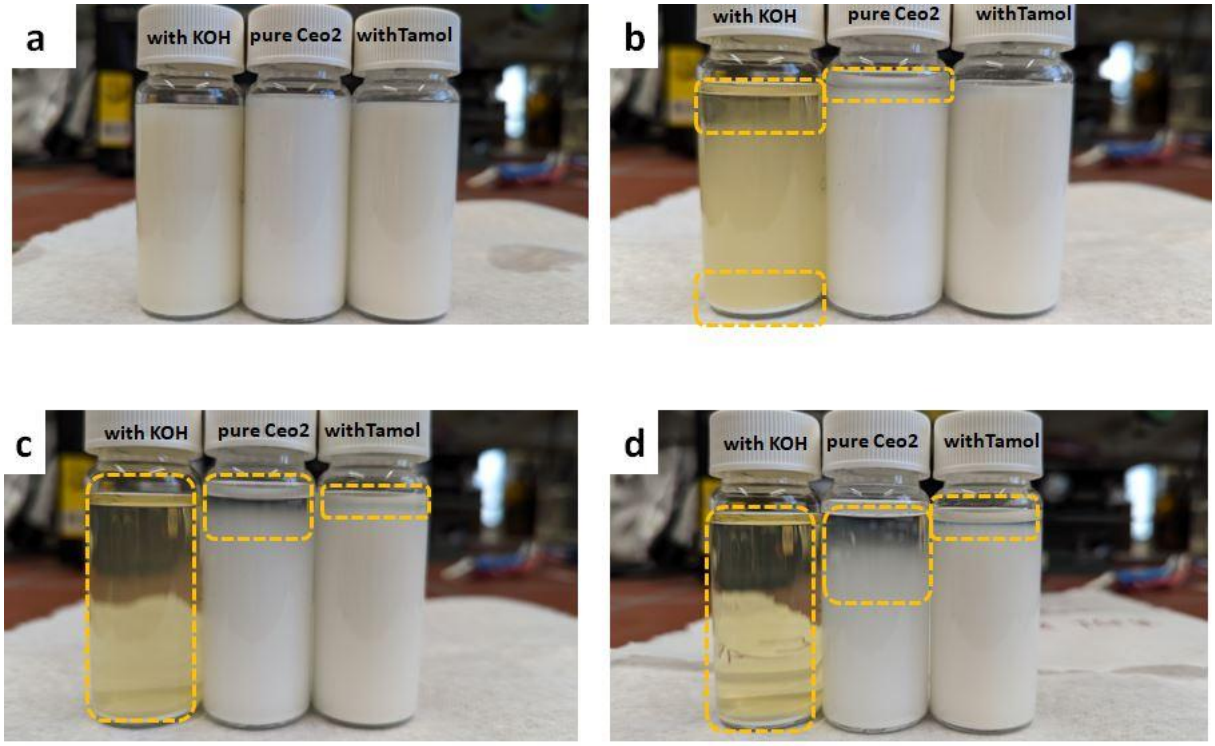


Figure 47: Different precipitation states of slurries; without additives, after adding 0.1 mol of KOH, and after adding Tamol in different periods after a) 1 min, b) 20 min, c) 60 min, and d) 240 min of ultrasonic dispersion.

4.2.2 Machine and Polishing Process

The polishing experiments were conducted using a conventional polishing machine (Stock RSP40), as shown in Figure 48. This machine allows for a polishing pressure of 300 N and a rotational speed range from 0 to 2500 rpm. Moreover, the process employed was a standard synchro speed polishing method. During polishing, the glass samples were held in place on a carrier via vacuum while the polishing slurry was dispersed onto the polishing pad. Both the lens and the polishing carrier rotated independently in the same direction. A full schematic representation of the polishing process is shown in Figure 59.



Figure 48: image of the synchro-speed polishing machine used for the experiments.

The sample carrier consisted of an aluminum body equipped with an LP66 polishing pad (Pieplow & Brandt), which has a Shore D hardness of approximately 25. Two types of glass were used as polishing samples: FS (Corning 7980 5F) and N-BK7 (SCHOTT). FS was selected for its excellent chemical resistance, while N-BK7, a standard optical glass, has lower chemical resistance compared to FS. The samples were cylindrical, with diameters of 40 mm and heights ranging from 1.5 cm to 2 cm. Prior to polishing, the surface of each sample was roughened through a defined grinding process. The weight of the samples was measured before and after polishing to calculate the material removal rate.

Surface roughness was measured using a white light interferometer (WLI. Zygo NewView 7200). To ensure accuracy and account for variations across the surface, roughness was measured at nine different points on each sample. These points were distributed to provide a representative average roughness value.

The polishing machine was equipped with power sensors that measured the electrical power of both the workpiece and platen spindles. The spindle for the workpiece operated at lower power than the tool spindle and the combined power signals were processed using dedicated software. The overall polishing process parameters are shown in Table 6.

POLISHING MACHINE	Stock RSP40
glass samples	FS (Corning 7980 5F) and N-BK7 (SCHOTT).
glass diameter	40 mm
polishing pad	Polyurethane LP66
polishing slurry	ceria powder (PZ 500 Treibacher)
glass carrier speed	1250 rpm
platen speed	1250 rpm
pressure	0.7 bar
slurry concentration	4 % wt.

Table 6: Polishing parameters used for the experiments.

The polishing processes were repeated several times for statistical validation. After three tests with both types of glass (six tests in total) and a new polishing suspension.

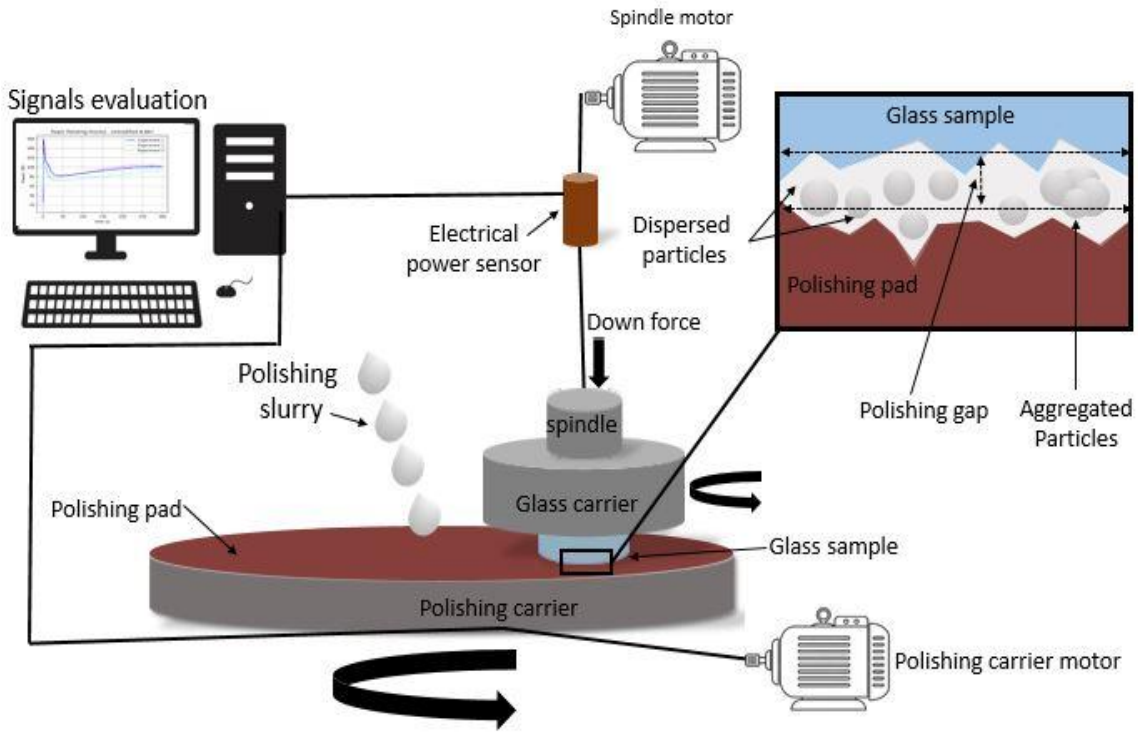


Figure 49: Schematic representation of the polishing process.

4.2.3 Material Removal Rate

Figure 50 presents the material removal rates (MRR) for N-BK7 and FS glasses polished using ceria-based slurries under three conditions: without additives, with Tamol®, and with KOH. The results indicate that the MRR for FS glass is consistently lower than that for N-BK7 after using all slurries for polishing. This difference in material removal is primarily attributed to differences in glass hardness and chemical composition [177]. Numerous studies, including that of Suratwala et al. [165], have reported that the high hardness and purity of FS result in a lower material removal rate compared to other glass types, such as soda-lime glass, borosilicate glass and phosphate glasses.

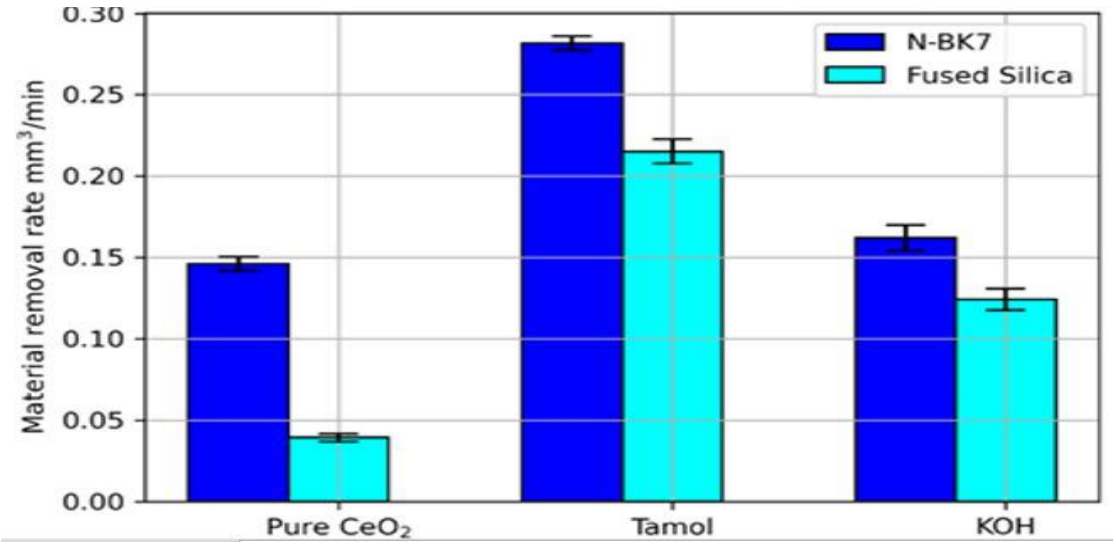


Figure 50: MRR of polished glasses N-BK7 and FS with cerium oxide particles without additives, with Tamol, and with KOH.

4.2.3.1 Material removal rates using slurry without additives.

In this experiment, the slurry without additives showed high particle aggregation and resulted in the lowest material removal rates for both N-BK7 and FS glasses. It is assumed that the aggregation of particles leads to a reduction in the number of active abrasives in the slurry, lowering the abrasive concentration, which is a critical factor for effective polishing. Without additives, the slurry lacks stability, causing particles to form larger clusters, which reduces the availability of abrasives that actively contribute to material removal, diminishing the overall efficiency of the polishing process. The same behavior was documented in the study of Bakier et

al. [173], where particle aggregation led to a decrease in slurry concentration and, consequently, a decrease in the material removal rates.

4.2.3.2 Material removal rates using a slurry containing Tamol agent

The slurry containing Tamol®, a dispersing agent, produces the highest material removal rates. This is attributed to the enhanced dispersion of ceria particles, which leads to a more controlled and uniform particle size distribution and ensures that the slurry maintains its initial concentration. The greater dispersion of particles increases the number of active abrasives, improving the efficiency of the polishing process. As a result, both N-BK7 and FS glasses exhibit higher material removal rates compared to slurries with higher particle aggregation. The increased number of well-dispersed particles ensures that more abrasives interact with the glass surface during the process, making the slurry with Tamol® the most effective in terms of material removal.

4.2.3.3 Material Removal Rates Using Slurry Containing KOH

The slurry containing KOH at a pH of 12.6 exhibits a higher material removal rate than the unmodified slurry despite increased particle aggregation. This can be attributed to the additional chemical etching provided by KOH, which enhances material removal alongside mechanical abrasion. However, the material removal rate remains lower than that achieved with the Tamol®-containing slurry, where the more dispersed particles lead to improved abrasive efficiency and greater material removal. Wang et al. [197] noted in their study that for BK7 glass, the alkali ions would accelerate the glass network dissolution and surface hydroxylation, which we believe will be boosted even more in the presence of high alkali medium. Furthermore, the study of Oey et al. [198] showed that the solution's pH significantly influences silicate dissolution in silicate glass. At higher pH levels, dissolution rates increase due to the nucleophilic attack of hydroxide ions (OH^-) on the silicate network. The alkaline environment promotes the breakdown of the silicate network to tetrahedral $[SiO_4]^{4-}$ units, leading to faster dissolution. This effect is more pronounced in silicates with lower network rigidity, as these structures have fewer atomic constraints, making them more susceptible to dissolution. Overall, higher pH conditions accelerate silicate dissolution by enhancing chemical reactions that break the silicate network. Overall, using slurry with a high alkali concentration, such as the one containing KOH, resulted in increased dissolution rates for both BK7 glass and FS, leading to higher material removal rates (MRR) compared to the less

aggregated slurry without additives. The high pH environment enhances the chemical etching process, compensating for the reduced abrasives number in the slurry due to particle aggregation. However, the slurry with more dispersed particles, such as the one containing Tamol®, achieved the highest MRR. This is because the good dispersion of particles in the slurry enhances abrasive efficiency, maximizing the overall material removal.

4.2.4 Surface Roughness

Figure 51 presents the surface roughness of polished N-BK7 and FS glasses using ceria particles with different additives: without additives, with Tamol, and with KOH. The surface roughness of N-BK7 and FS glasses is slightly influenced by the stability and dispersion of ceria particles in the polishing slurry. When using a slurry without additives, medium particle aggregation leads to a higher surface roughness, particularly for N-BK7. This aggregation reduces the abrasive concentration and widens the grain size distribution, resulting in less effective material removal and more mechanical streaks, consistent with the findings of Yan et al. [199], who noted that changes in slurry pH affect particle size distribution and post-CMP surface roughness.

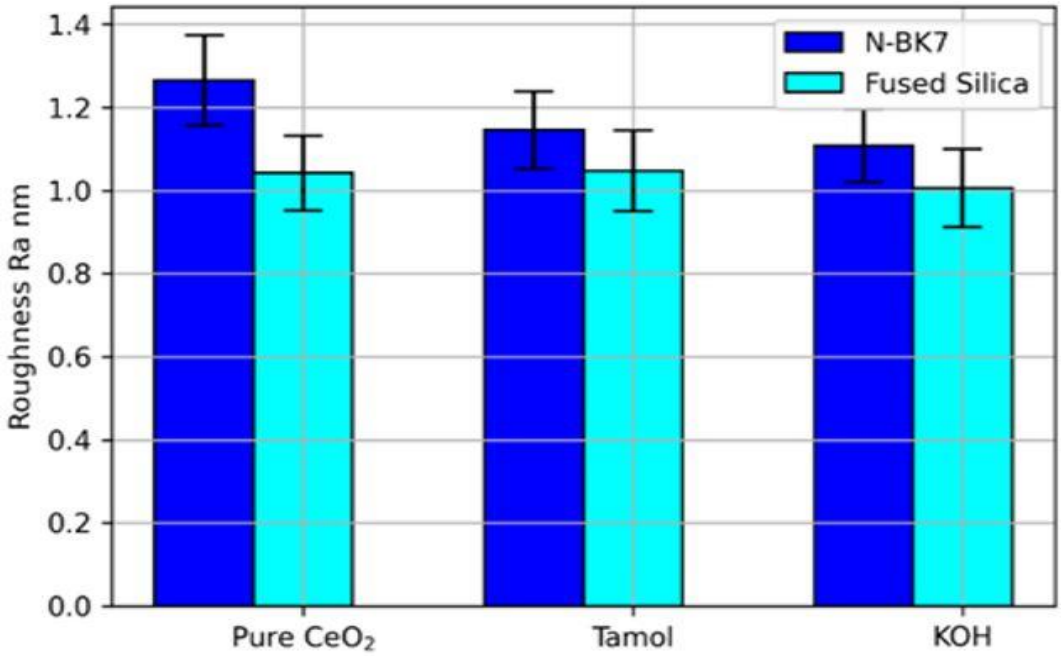


Figure 51: Surface roughness of polished glasses N-BK7 and FS with Ce particles without additives, with Tamol and with KOH.

Zhang et al. [200] showed that slurries with larger particle size distributions tend to produce rougher surfaces, whereas better-dispersed slurries with narrower distributions lead to smoother finishes. While Zhang et al. reported substantial differences in surface quality with different slurry stability; our study observed minimal differences in surface roughness among the three slurries tested. However, an important factor that needs to be considered is the optimal polishing time, during which the balance between material removal rate (MRR) and surface quality is achieved without over or under-polishing. The initial roughness of the samples was not measured directly. However, it is known that they are produced with a good reproducible grinding process and are in the range of approximately 2 µm.

In the case of the slurry containing Tamol®, better particle dispersion led to an improved surface quality in a shorter polishing time. As seen in Figure 51, despite all samples being polished for 5 minutes, the more stable slurry containing Tamol® removed more material than the others did. This suggests that the Tamol slurry may have reached the optimal polishing time faster than the other slurries. Extending the polishing beyond this point could lead to over-polishing, where the surface becomes smoother initially but then roughens again. Therefore, the dispersed Tamol slurry appears to be the most efficient, achieving an optimal surface finish within a shorter time.

On the other hand, the slurry containing KOH produced the smoothest surface finish due to strong chemical etching, which effectively removed fine scratches. However, the KOH slurry did not enhance the MRR as much as the Tamol® slurry, indicating that while surface roughness was optimized, a longer polishing time may be required to achieve the best finish. In summary, the Tamol®-stabilized slurry provided the best balance between MRR and surface quality, offering greater efficiency in achieving optimal roughness in less time.

4.2.5 Power measurement

Both the MRR and the roughness are determined after the process. However, it is necessary to measure values not only after the process but also to gain a live insight into the effective gap of the polishing partners. Live measurement of the active electrical power offers the opportunity to do this. It provides an in-situ insight into the process and shows the changes within the polishing gap. The polishing gap is the area between the polishing layer and the workpiece surface where mechanical and chemical interactions occur (see Figure 49). The polishing machine sets this gap

using a manual process that depends to a certain extent on the operating personnel's expertise. It is set using a distance gauge, which can result in (small) deviations. The signals obtained from the machine are processed mathematically. Specifically, the individual signals from the spindle and the quill are combined, and mean values are calculated to provide a comprehensive understanding of the power dynamics in the system. The shape of the curves stays uniform within one polishing experiment with the same slurry state, as shown in Figure 52. At the beginning, a short peak appears due to the initial current of the polishing machine. This is followed by a minimum, after which the power increases and reaches a plateau. This plateau suggests a stable polishing process.

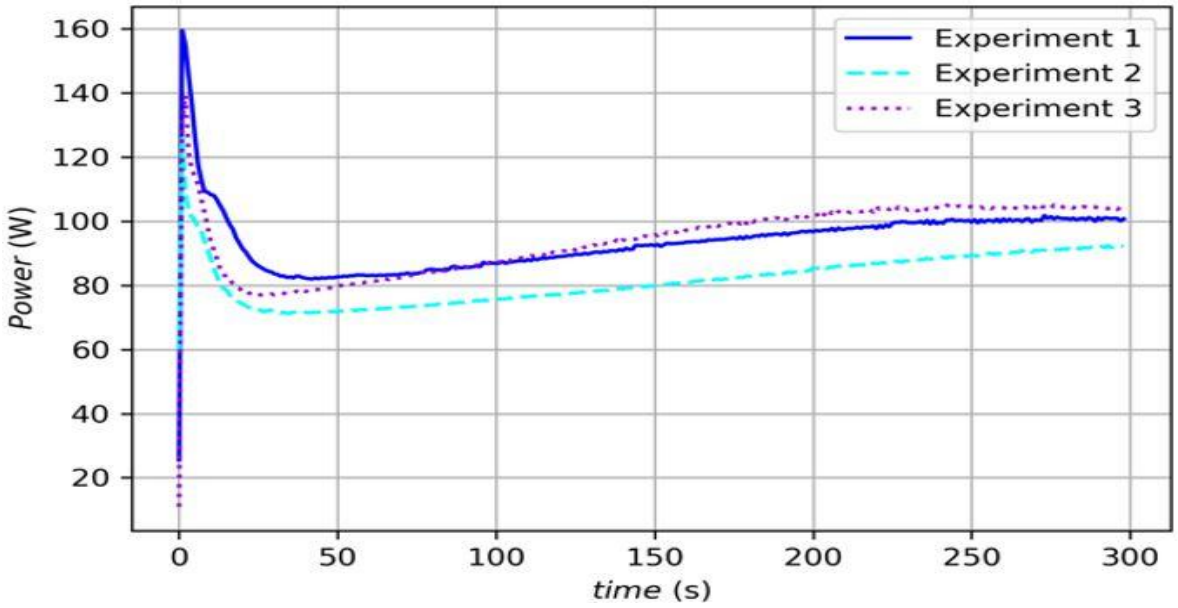


Figure 52: Power diagram for polishing N-BK7 and FS with unmodified polishing slurry.

To demonstrate the effect of the process setup on this behavior, power curves comparing results from three repetitions of each polishing condition are shown in Figure 52. Notable variations in the curves can be observed, primarily due to differences in the polishing setup, particularly the size of the polishing gap, which significantly affects the shape and magnitude of the power curves. Additionally, minor differences in the initial glass quality and the condition of the polishing pad may also contribute to these variations.

However, as the polishing grains are modified, it remains meaningful to compare the curves across all three polishing slurry conditions. This comparison is detailed in Figures 53 and 54, which display the power signals for FS and N-BK7 glasses.

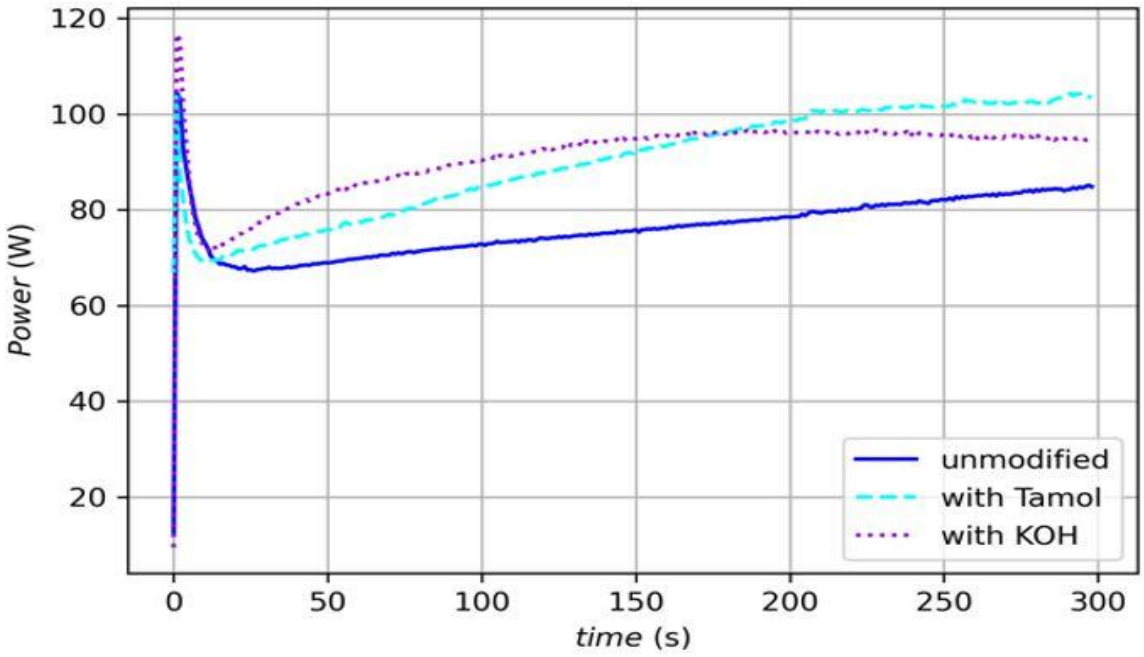


Figure 53: Power diagram for polishing FS glass in the different suspension states.

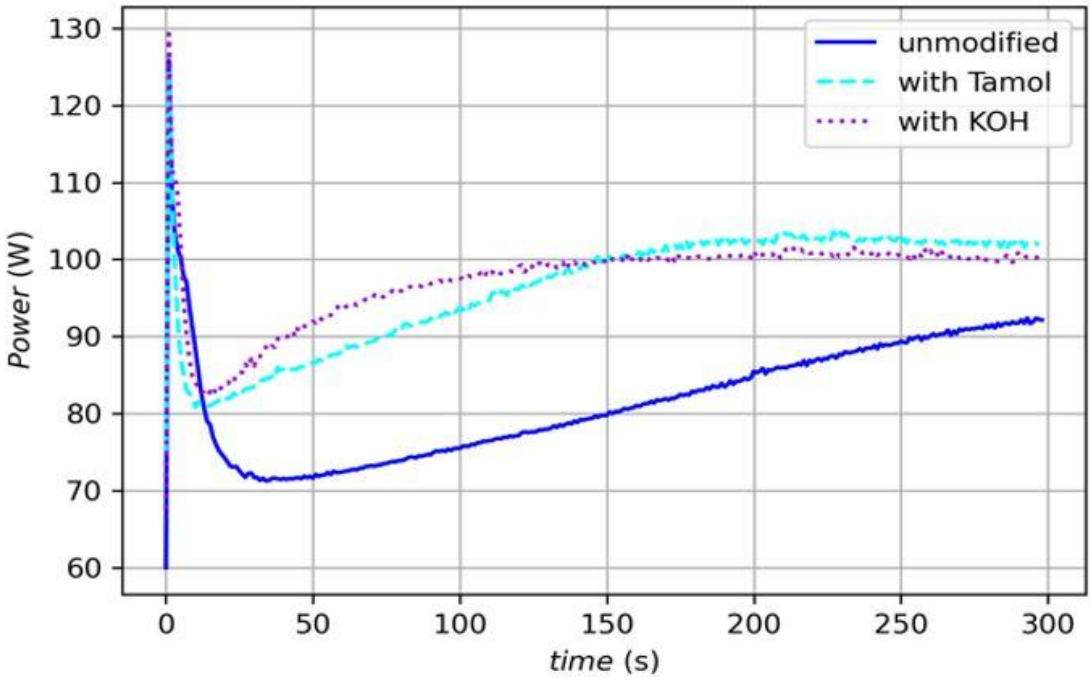


Figure 54: Power diagram for polishing N-BK7 in the different suspension states.

Although the power curves correspond to different glasses, they demonstrate certain similarities. The power curve for the unmodified slurry stands apart from the other two, displaying consistently higher values. Unlike the modified slurries, the unmodified slurry shows a continuously increasing power curve throughout the entire 300-second measurement period, without reaching a steady state. In contrast, the slurry modified with KOH achieves a constant power value after a specific period (approximately 100 to 200 seconds), a behavior similarly observed with the slurry containing Tamol.

It can be assumed that a constant value indicates a stable polishing condition. The effective electrical power (indirectly) reflects the mechanical conditions in the polishing gap. If there is more friction there, more energy is required to keep the spindle in motion. The process energy is increased by the addition of Tamol. This might be due to the fact, that agglomeration is hindered and more polishing grains take place in the process, resulting in a higher friction in the polishing gap and a higher MRR as observed in Figure 50.

The addition of potassium hydroxide solution significantly alters the polishing suspension, rendering it soapy and greasy compared to the suspension without potassium hydroxide. This greasy film is also observed on the glass surface after polishing. Cleaning with ultrasonic treatment and acetone effectively removes the film. This soapy film likely modifies the frictional conditions during polishing, leading to a noticeable reduction in friction, which occurs earlier than with other slurries, as shown in Figures 53 and 54.

To further explore the relationship between power measurements and the effect of slurry properties on the efficiency of material removal rate, the mean power of the process for both glasses and the corresponding state of the slurry (unmodified, with Tamol®, and with KOH) are shown in Table 7. The overall required power to polish the two glasses using the most dispersed slurry (95,66±8,52 W for N-BK7 and 91,36±1,00 W for FS) is higher compared to the aggregated slurries. As explained previously, a more dispersed slurry means more involved particles in the material removal process, which leads to both high material removal rates, as shown in Figure 50, and more friction in the polishing gap, as indicated by the higher power consumption in Figures 52 and 53.

	Mean power in W	
Slurry	N-BK7	FS
Without additives	81,31±8,96	82,33±8,10
With Tamol®	95,66±8,52	91,36±1,00
With KOH	84,24±7,00	85,73±8,29

Table 7: Mean power of the process and the corresponding slurry state. It is visible that the slurry with Tamol® seems to have the highest mean power, while the mean powers of the other states are very close to each other.

Lower mean power was observed during the polishing of both glasses when using aggregated slurries, indicating lower friction within the polishing gap. This is because particle clustering reduces the number of particles available for abrasion. Fewer particles in contact with the glass surface result in lower friction and, consequently, lower power consumption.

4.2.6 Correlation between power measurements and polishing results measurements

The surface roughness and material removal rates observed under different slurry conditions correlate with the active power measurements recorded during polishing. Changes in slurry composition affect friction and material removal dynamics within the polishing gap, resulting in distinct power curves that provide insights into the stability and efficiency of each slurry.

For the slurry without additives, the power curve showed a continuously increasing trend during the polishing process, indicating unstable polishing conditions. This increasing friction is likely due to the medium aggregation of ceria particles, leading to inefficient material removal and rougher surface finishes, particularly for N-BK7 glass. Aggregated particles resulted in a wider grain size distribution and reduced effective contact between the abrasives and the glass surface. This led to non-uniform material removal, as some particles clustered together rather than uniformly covering the glass surface. Consequently, more areas required continuous polishing, increasing friction within the polishing gap and progressively raising power values. This instability was reflected in the rough surface quality observed and a lower material removal rate.

In contrast, the slurry with Tamol, which showed better particle dispersion and higher MRR, displayed a plateau-like power curve after approximately 100–150 seconds. It is important to note that the initial high-power peak was due to the starting current and is not relevant for further interpretation. The plateau indicates stable polishing conditions with consistent friction between the glass and the polishing carrier. The early rise in power corresponds to the presence of well-dispersed particles in the polishing gap, leading to higher material removal and faster achievement of optimal surface roughness. The stability reflected by the plateau aligns with the observed smoother surfaces achieved with the Tamol slurry, effectively balancing MRR and surface quality. In an alkaline environment, glass dissolution is accelerated as OH^- ions attack and break the Si–O–Si bonds in the glass network, which can lead to the formation of a thin gel layer on the surface [201, 202]. For the slurry containing KOH, this dissolution mechanism contributed to the formation of a soapy film on the glass, which, while reducing friction in the polishing gap, particularly after 150 seconds for N-BK7 and 170 seconds for FS, also contributes to a decrease in the overall material removal rate (MRR). This lower MRR, compared to the Tamol® slurry, can be attributed to the reduced friction conditions, as fewer abrasive particles were actively engaged

in material removal. Although the KOH-modified slurry produced the smoothest surface finish due to its enhanced ability to remove scratches by chemical etching, the soapy nature of the slurry limited the effective removal of material. Over time, continuous exposure to alkaline conditions could lead to changes in the gel layer's composition and structure, reducing its protective function [203]. Thus, the combination of reduced friction, lower particle engagement, and evolving gel layer characteristics explains the lower MRR in the KOH slurry despite its good surface roughness.

In summary, the active power measurements provide a valuable understanding of the mechanical conditions in the polishing gap for each slurry condition. The slurry without additives, with its steadily increasing power, indicates an unstable polishing process that leads to higher roughness. The Tamol®-stabilized slurry, with its plateau-like power curve, correlates with higher MRR and smoother surfaces in less time. The KOH-modified slurry, with lower friction and a later plateau-like power curve, produced the smoothest surface but required longer polishing to achieve this due to the reduced MRR. These results show the importance of slurry stability and additive selection in optimizing both surface roughness and polishing efficiency. They also show that both glasses behave very differently under identical polishing conditions, this can be explained by the difference in their mechanical and chemical properties, which is reflected in their response to mechanical abrasion and chemical etching.

4.3 Effect of the long-time polishing on particle size

4.3.1 Experimental procedure

A slurry made of ceria powder (PZ 500 Treibacher) diluted in Deionized water (DIW) at a concentration of 4 wt.%, was used for the polishing of N-BK7 glass samples in a conventional polishing machine (see Figure 48), Tamol®, a BASF Group stabilization agent, is the sodium salt of a condensation product of naphthalene-sulfonic acid with formaldehyde was added to the slurry for the goal to prevent any possible aggregation that can affect the analysis of the particles size evolution over time. The pH of the suspension was measured using a calibrated METTLER TOLEDO pH meter (Figure 55) and the particle size distribution of the slurries (PSD) using the Zetasizer Nano (Malvern Panalytical GmbH) (Figure 56)



Figure 55: image of Mettler Toledo pH meter.



Figure 56: image of the Malvern Zetasizer.

The polishing process was conducted in six separate operations with durations of 5 minutes, 10 minutes, 15 minutes, 30 minutes, 60 minutes, and 120 minutes. After each operation, the pH of the suspension, surface roughness, material removal rate (MRR), and particle size distribution were measured. These measurements were used to investigate correlations between

the parameters and to examine the relationship between abrasive wear, surface roughness, and MRR.

The polishing conditions used for the experiment are presented in Table 8 as follows:

Polishing abrasives	**CeO_2 (450- 500 nm)**
Polishing time	5, 10, 15, 30, 60, 120 min
Polishing pad	LP-66 polyurethane pad
Glass carrier speed	1250 rpm
Platen speed	1250 rpm
Pressure	0.7 bar
Glass sample	40 mm N-BK 7

Table 8: polishing conditions for the experiment.

4.3.2 PH measurement of the slurry

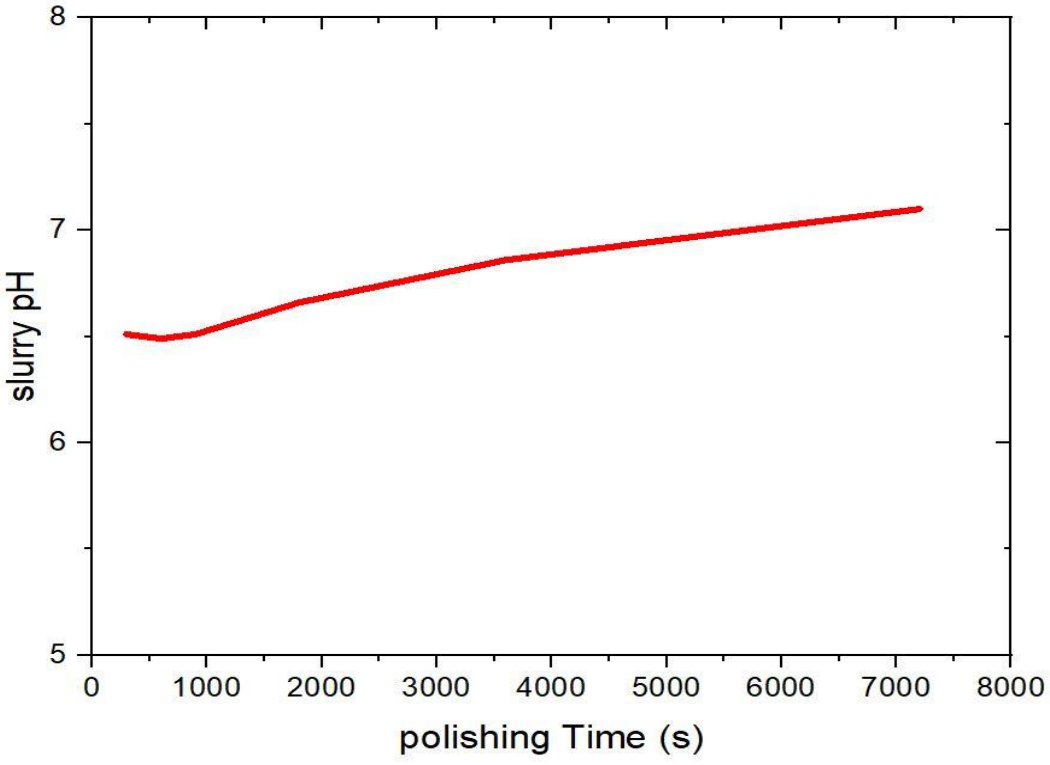


Figure 57: pH measurements of the slurries during different polishing periods.

Figure 57 illustrates the pH evolution of slurry over the polishing time. The results indicate a stable pH value during the initial 15 minutes, measuring 6.51, 6.49, and 6.51 at 5, 10, and 15 minutes, respectively. After 30 minutes, the pH begins to increase slightly, reaching a value of 7.1 after 2 hours of polishing. This behavior is likely attributed to the wear of the polyurethane polishing pad, which may release certain chemicals into the slurry, or to minor contamination from the polished glass. However, any chemical elements released from the glass are presumed to be either neutralized by the Tamol stabilization agent or diluted in the slurry, considering the high volume of the polishing agent (2 L).

The sedimentation test results, shown in Figure 58, reveal a noticeable color change in the slurries during polishing. Initially, after 30 minutes, the slurry appears light yellowish-white. After one hour of polishing, it transitions to a light brown color. At the end of two hours, the slurry adopts a brown tint, closely matching the color of the polishing pad.

The gradual darkening of the slurry color, in accordance with the slight increase in pH over time, supports the assumption that the wear of the polishing pad could be contributing to this pH rise.

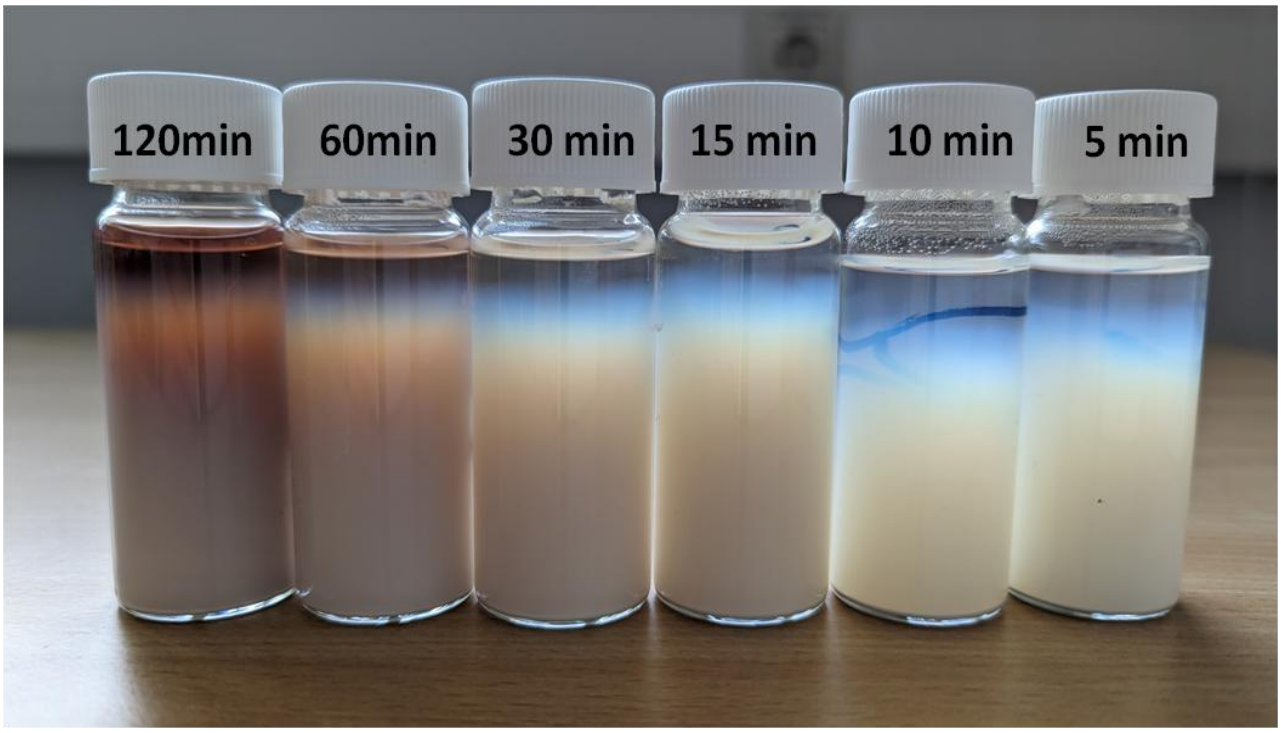


Figure 58: The sedimentation test of the slurries over time, after around 20 hours after ultrasonic dispersion for 5 minutes.

In addition to the color change that Figure 58 shows, the sedimentation tests reveal the dispersion and stability of the slurry. After more than 20 hours of particle rest, the visual analyses of the slurries didn't show any significant difference in their dispersion state, suggesting that the slight difference in the pH didn't modify the chemical parameters of the slurry, thereby preserving the equilibrium of the inter particles charges throughout the polishing process, this equilibrium is assumed to be maintained for two main reasons:

- The presence of the stabilization agent and its role in neutralizing surface charges of particles and any minor chemicals released from the polished glass
- The small amount of chemicals released in the slurry compared to the high volume of the slurry used for polishing

4.3.3 Surface roughness and material removal measurements throughout the polishing process

The analysis of both material removal and surface roughness results can give valuable insight into the abrasion behavior of the glass using ceria particles, The measurements are presented in Figures 59 and 60 as follows:

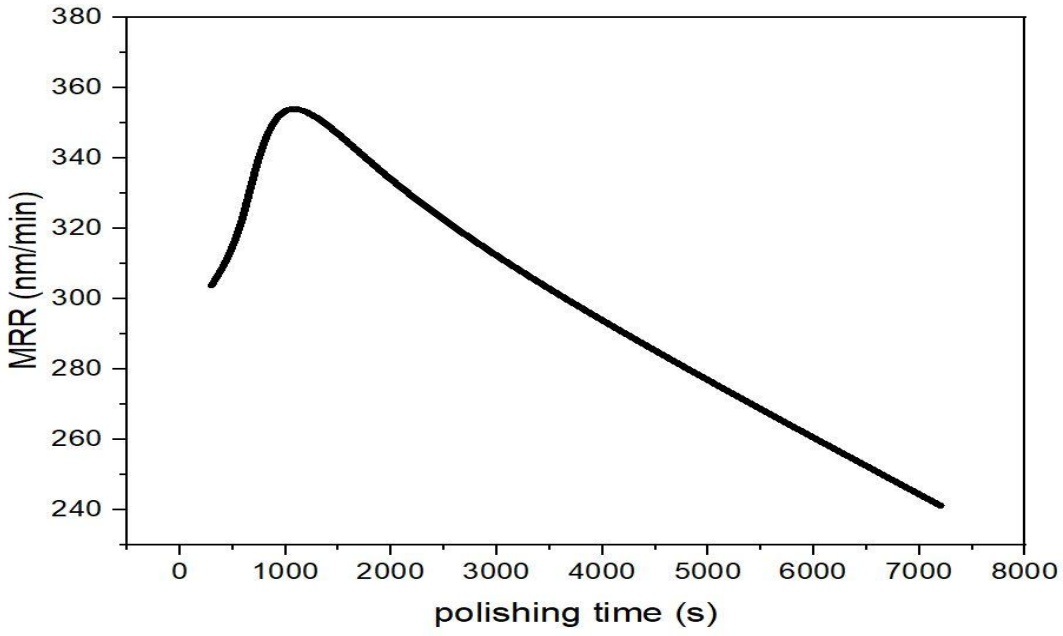


Figure 59: Material removal rates result in function of polishing time of N-BK7 glass using ceria abrasives.

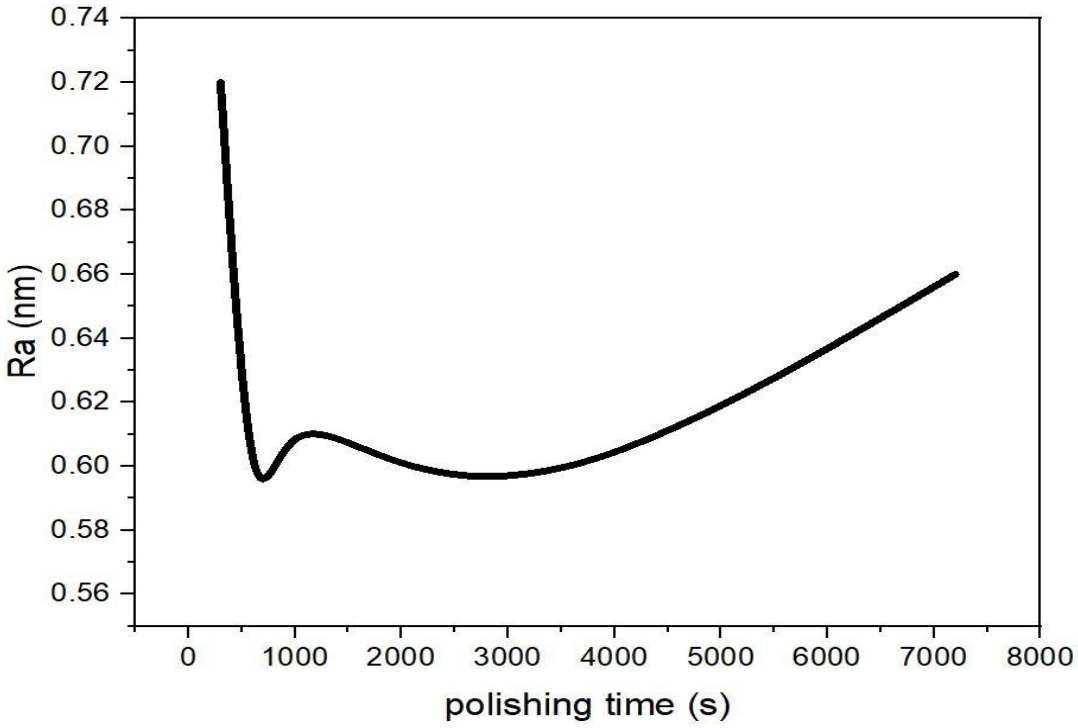


Figure 60: Surface roughness results in function of polishing time of N-BK7 glass using ceria abrasives.

Figure 59 and 60 show the evolution of material removal and surface roughness in function of time, The results can be classified into four phases as follows:

In the Initial phase (0 – 1000 s), the MRR increases rapidly during the initial phase due to the freshness of the abrasives, indicating efficient mechanical abrasion of the glass. This process leads to a gradual improvement in surface roughness, which initially starts with relatively high Ra, likely due to insufficient polishing time to achieve optimal surface finishing. As MRR keeps increasing, the surface reaches its optimal Ra after approximately 10 minutes of polishing. Beyond this point, with the consistent increase in material removal, Ra begins to deteriorate again. This phenomenon, commonly referred to as over-polishing [204–206], results in the formation of new streaks on the surface, leading to a rougher surface.

In the Second phase (1000 – 3000 s), it is observable that the MRR starts to decrease gradually; it can be attributed to the potential wear of ceria particles that start to become rounded, and the Ra decreases slowly as the mechanical abrasion is less aggressive.

In the final phase (3000 – 7200 s), the abrasives are assumed to be significantly rounded, which reduces their abrasiveness. The process enters a regime where the surface is being polished and roughened multiple times. As a result, the surface roughness slowly and progressively deteriorates with continued polishing, indicating that the process is less effective due to the wear of abrasives

4.3.4 Particle size distribution measurements

Figure 60 represents the particle size distribution of slurry over time; the results show the evolution of particles due to their wear and aggregation.

At the beginning of the process, the PSD is relatively narrow with most particles distributed in a smaller size; this distribution consisted after 600 s of polishing. Those results are in agreement with the MRR results, where the abrasion was aggressive, leading to a higher material removal rate, which indicates that the particles maintained their size and sharpness throughout this period

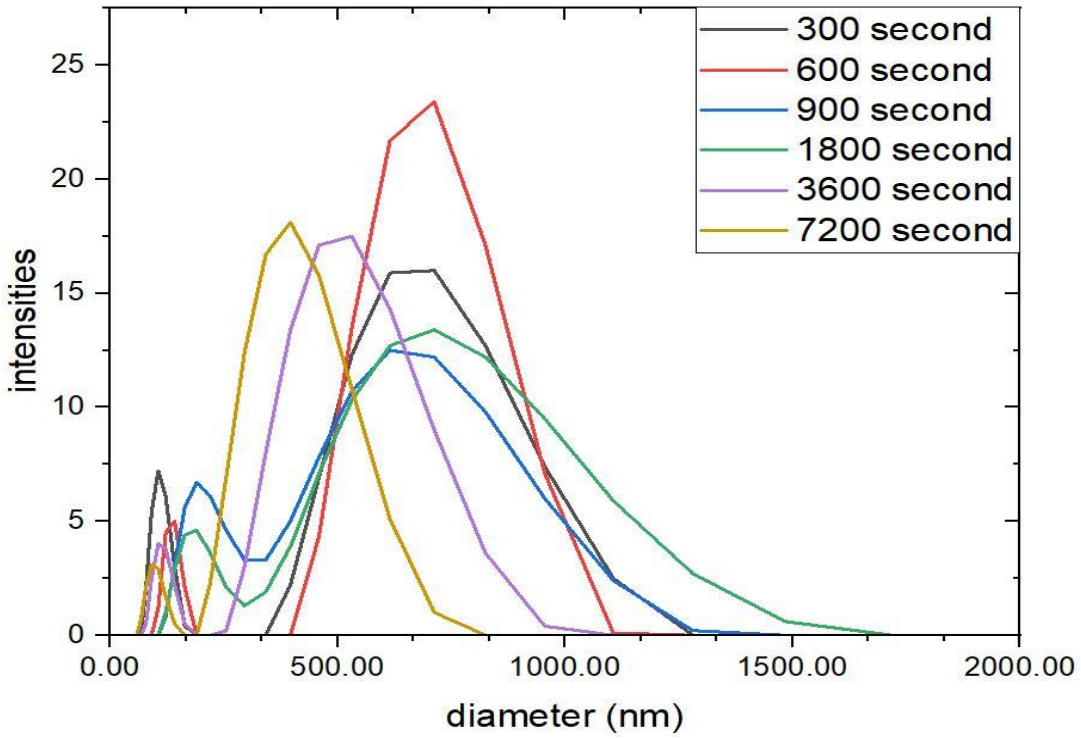


Figure 60: particle size distribution of abrasives in function of polishing time.

After 1800 seconds, the size of abrasives increased relatively, indicating the formation of small aggregates, which is probably due to the clustering of particles with other particle fragments.

After 3600 s until 7200 s the size of particles starts to decrease due to the continuous friction between the particles and the glass surface, the smaller size of particles is assumed to be the result of the wear of abrasives, those results correlate with the loss of polishing efficiency shown by the decrease in MRR and the deterioration of surface roughness.

4.4 Conclusion

This chapter highlights the importance of slurry composition, particle dispersion, and abrasive durability in achieving effective and stable chemical mechanical polishing. Well dispersed slurries were shown to improve both material removal efficiency and surface quality, while long polishing time led to a decline in performance due to abrasive wear. The results reveal the need for careful control of slurry stability and particle behavior to optimize polishing results across different glass types and conditions.

General conclusion

This thesis investigated the influence of slurry parameters on the efficiency of the polishing process, focusing on glass chemistry, ceria abrasive aggregation, and long-term slurry behavior. The results show the important role of slurry composition and stability in achieving optimal material removal rates (MRR) and surface quality.

To investigate the influence of glass chemistry on ceria slurry behavior during the polishing process, three glass types with high, medium, and zero alkaline concentrations were used as polishing samples. The Polishing process was conducted using ceria abrasives of two different sizes (80 and 400 nm) for 8 minutes. Based on the obtained results, several conclusions can be drawn. Alkaline elements present in glass composition increased the slurry pH during the polishing process using 400 nm ceria abrasives, confirming the hypotheses from the literature, whereas fused silicate had no impact on pH. The 80 nm-sized slurry characterized by the presence of stabilization agents and low material removal showed no pH change post-polishing for all glass types. pH modifications during the polishing affected the slurry's zeta potential, influencing the aggregation or disaggregation tendencies and, therefore, leading to the modification of particle size distributions. In industrial polishing systems, the slurry is typically reused over many cycles to polish numerous glass samples. In these systems, it is believed, according to this study, that the continuous abrasion of the optical glass, specifically glass containing high concentrations of chemicals during the polishing, may lead to a progressive accumulation of chemical compounds from the glass within the polishing suspension, which can impact the properties of the slurry leading to uncontrolled stability of abrasives during all the process especially when no stabilization agent is used or is not enough.

The role of particle aggregation was further analyzed through different slurry formulations, each with a different level of aggregation: low, medium, and high. The results demonstrated that slurries without additives, characterized by higher particle aggregation, resulted in the lowest MRR for both glass types. However, the slurry containing Tamol, with highly dispersed particles, achieved the highest MRR, showing the importance of particle dispersion. The slurry with KOH, despite higher aggregation, showed good MRR due to additional chemical etching effects, particularly in FS. Surface roughness analysis indicated that slurry with Tamol balanced high MRR and good surface quality, while KOH-induced chemical etching improved surface smoothness by

removing abrasion streaks.

Additionally, the wear of ceria particles during long polishing times and its effect on the polishing results were studied. N-BK7 glass was polished for different durations, and the results showed that the pH of the slurry remained relatively stable. The sedimentation test didn't indicate any significant aggregation even when the PSD measurements showed a slight aggregate after 900 and 1800 sec from polishing, but the clustering of particles was likely limited and stabilized, preventing the formation of sediments. On the other hand, the particle size after 3600 and 7200 seconds of polishing appears to decrease, indicating significant wear due to the long polishing duration. The wear of particles affects the efficiency of MRR as it starts to decrease after 1500 sec of polishing while surface roughness starts to deteriorate after around 1800 sec.

Overall, this thesis revealed the importance of slurry parameters in polishing efficiency. Well-dispersed slurries achieved the best MRR and surface quality, while long polishing led to abrasive wear, reducing MRR and deteriorating surface roughness. Controlling the dispersion and wear of particles is crucial for optimizing the polishing process. Additionally, continuous control of slurry chemistry is essential for achieving consistent and high-quality polishing results, as it enhances reproducibility and minimizes the risk of defects. For industrial operations, investing in automated monitoring and control systems can lead to significant improvements in process efficiency and product quality by allowing for more precise adjustments and optimizations, contributing to the overall consistency, reliability, and prediction of polishing results. Furthermore, the Ceria abrasive polishing process can be optimized by tailoring the slurry composition to match specific glass chemical compositions. This optimization promises more precise polishing outcomes, efficient utilization of stabilization agents, and the development of eco-friendly slurries.

References

[1] Sudarsan, V. (2012). Optical materials: fundamentals and applications. *Functional Materials: Preparation, Processing and Applications*, 285-322.

[2] Xie, M., Pan, Y., An, Z., Huang, S., & Dong, M. (2022). Review on surface polishing methods of optical parts. *Advances in Materials Science and Engineering*, *2022*(1), 8723269.

[3] Lee, K., Seo, J., & Paik, U. (2022). Preparation and characterization of slurry for CMP. In Advances in Chemical Mechanical Planarization (CMP) (pp. 323-354). Woodhead Publishing.

[4] CHEN, Chuandong, CUI, Yanying, LI, Xiaopei, *et al.* Novel ceria/graphene oxide composite abrasives for chemical mechanical polishing. *Ceramics International*, 2024, vol. 50, no 15, p. 26325-26333.

[5] JHA, Asu Ram. *Rare earth materials: properties and applications*. CRC Press, 2014.

[6] LEE, Yen-Chun, JOSHI, Vishwanath, ORLOV, Alexei O., et al. Si single electron transistor fabricated by chemical mechanical polishing. Journal of Vacuum Science & Technology B, 2010, vol. 28, no 6, p. C6L9-C6L13.

[7] PRAVEEN, B. V. S., CHO, Byoung-Jun, PARK, Jin-Goo, et al.Effect of lanthanum doping in ceria abrasives on chemical mechanical polishing selectivity for shallow trench isolation. Materials Science in Semiconductor Processing, 2015, vol. 33, p. 161-168.

[8] HAN, Xinyu, LIU, Renhao, TAN, Baimei, et al. Research progress on the application of ceria nanoparticles as abrasives in dielectric layer CMP and post cleaning structure, morphology, doping, and mechanism. Colloids and Surfaces A: Physicochemical and Engineering Aspects, 2023, p. 132551.

[9] WANG, Li, REN, Gaoyuan, XIE, Wenxiang, et al. Simple and facile synthesis of single-crystal CeO_2 abrasives and its highly efficient removal mechanism on SiO_2 film. Applied Surface Science, 2024, vol. 654, p. 159510.

[10] CADIEN, Kenneth C. et NOLAN, Lucy. Chemical mechanical polishing method and practice. In: Handbook of Thin Film Deposition. William Andrew Publishing, 2018. p. 317-357.

[11] DATTA, Debottam, RAI, Himanshu, SINGH, Swarnima, et al. Nanoscale tribological aspects of chemical mechanical polishing: A review. Applied Surface Science Advances, 2022, vol. 11, p. 100286.

[12] ZHONG, Zhao-Wei. Recent developments and applications of chemical mechanical polishing. The International Journal of Advanced Manufacturing Technology, 2020, vol. 109, no 5, p. 1419- 1430.

[13] Murata, J., &Goda, K. (2019). Abrasive-free surface finishing of glass using a Ce film. Journal of Materials Processing Technology, 265, 56-62.

[14] ZHENG, Yuanyuan, WANG, Ning, FENG, Zongyu, et al. The effects of precursors on the morphology and chemical mechanical polishing performance of ceria-based abrasives. Materials, 2022, vol. 15, no 21, p. 7525.

[15] JANO, Pavel, EDERER, Jakub, PILAOV, Vra, et al. Chemical mechanical glass polishing with cerium oxide: Effect of selected physico- chemical characteristics on polishing efficiency. Wear, 2016, vol. 362, p. 114-120.

[16] COOK, Lee M. Chemical processes in glass polishing. Journal of Non-crystalline solids, 1990, vol. 120, no 1-3, p. 152-171.

[17] Abbas, F., Belkhir, N., Herrmann, A., & Rädlein, E. (2024). Investigation of the impact of optical glass composition on ceria slurry stability during chemical mechanical polishing process. Powder Technology, 448, 120290.

[18] CHENG, Jie, HUANG, Shuo, et LU, Xinchun. Preparation of surface modified ceria nanoparticles as abrasives for the application of chemical mechanical polishing (CMP). ECS Journal of Solid State Science and Technology, 2020, vol. 9, no 2, p. 024015.

[19] WANG, Ye, ZHANG, Baoguo, WU, Pengfei, et al. Study on Preparation and Polishing Performance of Ceria Slurry. In: 2022 China Semiconductor Technology International Conference (CSTIC). IEEE, 2022. p. 1-3.

[20] BARANY, S., BOHACS, K., CHEPURNA, I., et al. Electrokinetic properties and stability of cerium dioxide suspensions. RSC advances, 2016, vol. 6, no 73, p. 69343-69351.

[21] BUETTNER, Katherine M., RINCIOG, Claudia I., et MYLON, Steven E. Aggregation kinetics of cerium oxide nanoparticles in monovalent and divalent electrolytes. Colloids and Surfaces A: Physicochemical and Engineering Aspects, 2010, vol. 366, no 1-3, p. 74-79.

[22] DANDU, Veera PR et BABU, S. V. The role of Ce^{3+} vs. Ce^{4+} during the polishing of silicon dioxide and silicon nitride films using ceria abrasives. In: Optical Fabrication and Testing. Optica Publishing Group, 2012. p. OM2D. 1.

[23] WEI, Qilong, LUO, Zixin, YANG, Qiang, et al. Dispersion and agglomeration behaviors of submicron ceria particles in concentrated slurries. Colloid and Polymer Science, 2021, vol. 299, p. 1683-1694.

[24] SUN, Congtinget XUE, Dongfeng. Size- dependent oxygen storage ability of nano-sized ceria. Physical Chemistry Chemical Physics, 2013, vol. 15, no 34, p. 14414-14419.

[25] GHOSALYA, Manoj Kumar, LI, Xiansheng, BECK, Arik, et al. Size of ceria particles influences surface hydroxylation and hydroxyl stability. The Journal of Physical Chemistry C, 2021, vol. 125, no 17, p. 9303-9309.

[26] LIU, Min, ZHANG, Baoguo, LIU, Shitong, et al. Research on the Dispersion Stability and Polishing Performance of Ceria Slurry. In : 2023 China Semiconductor Technology International Conference (CSTIC). IEEE, 2023. p. 1-3.

[27] Cao, J., Wei, C., Liu, S., Dun, A., Yang, M., Xu, X., & Shao, J. (2015, October). Polishing performances of different optics with different size powder and different pH value slurries during CMP polishing. In *Optifab 2015* (Vol. 9633, pp. 670-679). SPIE.

[28] Venkataronappa, A., Bankaitis, J., & Seo, J. (2024). Enhancing dispersion stability and recyclability of ceria slurry with polyacrylic acid for improved glass polishing performance. *Journal of Industrial and Engineering Chemistry*.

[29] HE, Hanwei. Preparation and dispersion of nanosize ceria in high electrolyte slurry by ball-milling. *Integrated Ferroelectrics*, 2015, vol. 161, no 1, p. 36-44.

[30] PETTERSSON, Alf, MARINO, Gonzalo, PURSIHEIMO, Antti, *et al.* Electrosteric stabilization of Al_2O_3, ZrO2, and 3Y–ZrO2 suspensions: effect of dissociation and type of polyelectrolyte. *Journal of colloid and interface science*, 2000, vol. 228, no 1, p. 73-81.

[31] CHEN, Yang, LI, Zhina, et MIAO, Naiming. Polymethylmethacrylate (PMMA)/CeO2 hybrid particles for enhanced chemical mechanical polishing performance. *Tribology International*, 2015, vol. 82, p. 211-217.

[32] Yadav, H. N. S., Kumar, M., Kumar, A., & Das, M. (2023). Plasma polishing processes applied on optical materials: A review. *Journal of Micromanufacturing*, *6*(1), 27-39.

[33] Dietz, R. W., & Bennett, J. M. (1966). Bowl feed technique for producing supersmooth optical surfaces. *Applied Optics*, *5*(5), 881-882.

[34] Bingham, R. G., Walker, D. D., Kim, D. H., Brooks, D., Freeman, R., & Riley, D. (2000, October). Novel automated process for aspheric surfaces. In *Current developments in lens design and optical systems engineering* (Vol. 4093, pp. 445-450). SPIE.

[35] Pan, R., Zhong, B., Wang, Z., Ji, S., Chen, D., & Fan, J. (2018). Influencing mechanism of the key parameters during bonnet polishing process. *The International Journal of Advanced Manufacturing Technology*, *94*, 643-653.

[36] Feng, Z. H. A. O., Zhang, Z., Jianjun, Y. A. N. G., Jiaxin, Y. U., Junyuan, F. E. N. G., Hongxiu, Z. H. O. U., ... & Fanning, M. E. N. G. (2024). Advanced nonlinear rheology magnetorheological finishing: A review. *Chinese Journal of Aeronautics*, *37*(4), 54-92.

[37] Lu, M. M., Yang, Y. K., Lin, J. Q., Du, Y. S., & Zhou, X. Q. (2024). Research progress of magnetorheological polishing technology: a review. *Advances in Manufacturing*, 1-37.

[38] Pattanaik, L. N., & Agarwal, H. (2014). Development of magnetorheological finishing (MRF) process for freeform surfaces. *Int. J. Adv. Mech. Eng.*, *4*, 611-618.

[39] Wang, L., Zhang, K., Song, Z., & Feng, S. (2007). Ceria concentration effect on chemical mechanical polishing of optical glass. *Applied surface science*, *253*(11), 4951-4954.

[40] Sivanandini, M., Dhami, S. S., & Pabla, B. S. (2013). Chemical mechanical polishing by colloidal silica slurry. International Journal of Engineering Research and Applications, 3(3), 1337-1345.

[41] Chiu, W. L., & Huang, C. I. (2023). Polymer Nanoparticles Applied in the CMP (Chemical Mechanical Polishing) Process of Chip Wafers for Defect Improvement and Polishing Removal Rate Response. *Polymers*, *15*(15), 3198.

[42] Hang, W., Song, C., Yin, Z., Liu, Y., Wang, Q., Wang, Y., ... & Zeng, Q. (2023). Research on chemical mechanical polishing technology for zirconium-based amorphous alloys. *Micromachines*, *14*(3), 584.

[43] Qian, Y., Yang, W., Chen, C., & Yu, X. (2022). Fixed abrasive polishing in an anhydrous environment: a material removal model for fused silica. *Machines*, *10*(2), 147.

[44] BOUZID, D. et BELKHIR, N. Investigation of alumina pellets for optical glass grinding. Arch Mater Sci Eng, 2014, vol. 67, p. 14-17.

[45] Vega, F., Cebrian, J. A., Lupon, N. B., & Laguarta, F. (1999, September). Surface Dynamics during laser polishing of glass. In *Computer-Controlled Microshaping* (Vol. 3822, pp. 92-102). SPIE.

[46] HECHT, Kerstin. Entwicklung eines Laserstrahlpolierverfahrens für Quarzglasoberflächen. 2012.

[47] Gerhard, C., Weihs, T., Tasche, D., Brückner, S., Wieneke, S., & Viöl, W. (2013). Atmospheric pressure plasma treatment of fused silica, related surface and near-surface effects and applications. *Plasma Chemistry and Plasma Processing*, *33*, 895-905.

[48] Singh Yadav, H. N., Krishna, E., Kombath, S., Dev, D. S. D., & Das, M. (2023). Investigation of MRR and surface characterization using plasma process. Materials and Manufacturing Processes, 38(13), 1716-1728.

[49] Li, Z., Wang, J., Peng, X., Li, S., & Yin, Z. (2010). Abrasive jet polishing and its applications in surface finishing. Current Research in Nanotechnology, 1(1), 86-93.

[50] Annoni, M. P. G., Monno, M., & Ravasio, C. (2007). Water jet, a flexible technology (pp. 1-250). Polipress.

[51] Liu, H. (2004). A study of the cutting performance in abrasive waterjet contouring of alumina ceramics and associated jet dynamic characteristics (Doctoral dissertation, Queensland university of technology).

[52] Seshan, K. (Ed.). (2012). *Handbook of thin film deposition*. William Andrew.

[53] Aida, H., Kim, S. W., Ikejiri, K., Doi, T., Yamazaki, T., Seshimo, K., ... & Aota, N. (2015). Precise mechanical polishing of brittle materials with free diamond abrasives dispersed in micro–nano-bubble water. *Precision Engineering*, *40*, 81-86.

[54] Stavreva, Z., Zeidler, D., Plötner, M., & Drescher, K. (1997). Influence of process parameters on chemical-mechanical polishing of copper. *Microelectronic engineering*, *37*, 143-149.

[55] Xu, W., Cheng, Y., & Zhong, M. (2019). Effects of process parameters on chemical-mechanical interactions during sapphire polishing. *Microelectronic Engineering*, *216*, 111029.

[56] Zhao, Y., & Chang, L. (2002). A micro-contact and wear model for chemical–mechanical polishing of silicon wafers. *Wear*, *252*(3-4), 220-226.

[57] Liu, D., Chen, G., & Hu, Q. (2017). Material removal model of chemical mechanical polishing for fused silica using soft nanoparticles. *The International Journal of Advanced Manufacturing Technology*, *88*, 3515-3525.

[58] Wan, L. L., Deng, Z. H., Wang, C. D., Liu, W., & Liu, Z. J. (2016). Process parameters optimisation for Si3N4 in chemical-mechanical polishing via Taguchi technique. *International Journal of Nanomanufacturing*, *12*(2), 143-153.

[59] Park, K. H., Kim, H. J., Chang, O. M., & Jeong, H. D. (2007). Effects of pad properties on material removal in chemical mechanical polishing. *Journal of Materials Processing Technology*, *187*, 73-76.

[60] Ramesh Kumar, C., & Omkumar, M. (2019). Optimisation of process parameters of chemical mechanical polishing of soda lime glass. *Silicon*, *11*(1), 407-414.

[61] Lee, H., & Sung, I.-H. (2019). Chemical mechanical polishing: a selective review of R&D trends in abrasive particle behaviors and wafer materials. Tribology and Lubricants, 35(5), 274–285

[62] Lee, H., Kim, H., & Jeong, H. (2022). Approaches to sustainability in chemical mechanical polishing (CMP): a review. International Journal of Precision Engineering and Manufacturing-Green Technology, 1-19.

[63] Basim, G. B., & Moudgil, B. M. (2003). Slurry design for chemical mechanical polishing. KONA Powder and Particle journal, 21, 178-184.

[64] Zhang, Z., Liu, W., & Song, Z. (2010). Effect of abrasive particle concentration on preliminary chemical mechanical polishing of glass substrate. Microelectronic Engineering, 87(11), 2168-2172.

[65] Cumbo, M. J., Fairhurst, D., Jacobs, S. D., & Puchebner, B. E. (1995). Slurry particle size evolution during the polishing of optical glass. Applied Optics, 34(19), 3743-3755.

[66] Armini, S., Burtovyy, R., Moinpour, M., Luzinov, I., De Messemaeker, J., Whelan, C. M., & Maex, K. (2008). Interaction forces between a glass surface and ceria-modified PMMA-based abrasives for CMP measured by colloidal probe AFM. Journal of the Electrochemical Society, 155(4), H218.

[67] Shao, Q., Duan, S., Fu, L., Lyu, B., Zhao, P., & Yuan, J. (2021). Shear thickening polishing of quartz glass. Micromachines, 12(8), 956.

[68] Danielis, M., Felli, A., Zampol, M., Fonda, N., Brüner, P., Grehl, T., ... & Trovarelli, A. (2024). Tuning Chemical and Morphological Properties of Ceria Nanopowders by Mechanochemistry. ACS omega, 9(10), 12046-12059.

[69] Ling, Y., Wang, X., Ma, Z., Wei, K., Wu, Y., Khan, M., ... & Wang, S. (2020). Review of experimental and modelling developments for ceria-based solid oxide fuel cells free from internal short circuits. Journal of Materials Science, 55, 1-23.

[70] Jasinski, P., Suzuki, T., & Anderson, H. U. (2003). Nanocrystalline undoped ceria oxygen sensor. Sensors and Actuators B: Chemical, 95(1-3), 73-77.

[71] Akil, J., Siffert, S., Pirault-Roy, L., Royer, S., Shen, F., Chen, W., ... & Poupin, C. (2021). Investigation of catalysts M/CeO 2 (M= Pt, Rh, or Pd) for purification of CO 2 derived from oxycombustion in the absence or presence of water. Environmental Science and Pollution Research, 28, 12521-12532.

[72] Álvarez-Asencio, R., Corkery, R. W., & Ahniyaz, A. (2020). Solventless synthesis of cerium oxide nanoparticles and their application in UV protective clear coatings. RSC advances, 10(25), 14818-14825.

[73] Brugnoli, L., Miyatani, K., Akaji, M., Urata, S., & Pedone, A. (2023). New atomistic insights on the chemical mechanical polishing of silica glass with ceria nanoparticles. Langmuir, 39(15), 5527-5541.

[74] Kim, S. D., Hwang, I. S., Park, H. M., Rhee, J. K., & Nam, C. W. (2002). Chemical mechanical polishing of shallow trench isolation using the ceria-based high selectivity slurry for sub-0.18 μm complementary metal–oxide–semiconductor fabrication. Journal of Vacuum Science & Technology B: Microelectronics and Nanometer Structures Processing, Measurement, and Phenomena, 20(3), 918-923.

[75] Andreescu, D., Bulbul, G., Özel, R. E., Hayat, A., Sardesai, N., & Andreescu, S. (2014). Applications and implications of nanoceria reactivity: measurement tools and environmental impact. Environmental Science: Nano, 1(5), 445-458.

[76] Kim, E., Hong, J., Seok, H., & Kim, T. (2022). Photo-oxidative degradation of polyacids derived ceria nanoparticle modulation for chemical mechanical polishing. Scientific Reports, 12(1), 1613.

[77] Myong, K. K., Byun, J., Choo, M. J., Kim, H., Kim, J. Y., Lim, T., & Kim, J. J. (2021). Direct and quantitative study of ceria–SiO2 interaction depending on Ce3+ concentration for chemical mechanical planarization (CMP) cleaning. Materials Science in Semiconductor Processing, 122, 105500.

[78] Netzband, C. M., & Dunn, K. (2019). Investigation into the effect of CMP slurry chemicals on ceria abrasive oxidation state using XPS. ECS Journal of Solid State Science and Technology, 8(10), P629.

[79] Mei, Y., Chen, W., & Chen, X. (2023). Synthesis, Characterization, and Polishing Properties of a Lanthanum Cerium Fluoride Abrasive. *Materials*, *16*(9), 3393.

[80] Liang, S., Jiao, X., Tan, X., & Zhu, J. (2018). Effect of solvent film and zeta potential on interfacial interactions during optical glass polishing. *Applied Optics*, *57*(20), 5657-5665.

[81] Kang, M. C., Kim, J. J., & Moon, D. K. (2005). Effect of organic additives on ceria slurry in shallow trench isolation chemical mechanical planarization. *Japanese journal of applied physics*, *44*(8R), 5949.

[82] Muskan, S. S., Hamada, S., Kim, Y. J., Kim, T. G., & Park, J. G. Investigation of Ceria-PAA interactions during STI CMP process leading to brush loading issues.

[83] Kim, H. M., Venkatesh, R. P., Kwon, T. Y., & Park, J. G. (2012). Influence of anionic polyelectrolyte addition on ceria dispersion behavior for quartz chemical mechanical polishing. *Colloids and Surfaces A: Physicochemical and Engineering Aspects*, *411*, 122-128.

[84] Vienna, J. D., Neeway, J. J., Ryan, J. V., & Kerisit, S. N. (2018). Impacts of glass composition, pH, and temperature on glass forward dissolution rate. npj Materials degradation, 2(1), 22.

[85] Jollivet, P., Gin, S., & Schumacher, S. (2012). Forward dissolution rate of silicate glasses of nuclear interest in clay-equilibrated groundwater. *Chemical Geology*, *330*, 207-217.

[86] Becker, E., Prange, A., & Conradt, R. (2009). Chemical-Mechanical polishing of optical glasses. *MRS Online Proceedings Library (OPL)*, *1157*, 1157-E03.

[87] Suratwala, T., Steele, W., Feit, M., Shen, N., Wong, L., Dylla-Spears, R., ... & Miller, P. (2017). Relationship between surface μ-roughness and interface slurry particle spatial distribution during glass polishing. *Journal of the American Ceramic Society*, *100*(7), 2790-2802.

[88] SEO, Jihoon. A review on chemical and mechanical phenomena at the wafer interface during chemical mechanical planarization. *Journal of MaterialsResearch*, 2021, vol. 36, p. 235-257.

[89] LI, Z., INA, K., LEFEVRE, P., *et al.* Determining the effects of slurry surfactant, abrasive size, and abrasive content on the tribology and kinetics of copper CMP. *Journal of The Electrochemical Society*, 2005, vol. 152, no 4, p. G299.

[90] ILIE, Filip et IPATE, George. Chemical-mechanical impact of nanoparticles and pH effect of the slurry on the CMP of the selective layer surfaces. *Lubricants*, 2017, vol. 5, no 2, p. 15.

[91] MA, Jiahui, XU, Ning, HU, Jinrong, *et al.* Doping strategy on properties and chemical mechanical polishing performance of CeO2 Abrasives: A DFT assisted experimental study. *Applied Surface Science*, 2023, vol. 623, p. 156997.

[92] SONG, Xiao-lan, XU, Da-yu, ZHANG, Xiao-wei, *et al.* Electrochemical behavior and polishing properties of silicon wafer in alkaline slurry with abrasive CeO2. *Transactions of Nonferrous Metals Society of China*, 2008, vol. 18, no 1, p. 178-182.

[93] OH, Myoung-Hwan, SINGH, Rajiv K., GUPTA, Sushant, *et al.* Polishing behaviors of single crystalline ceria abrasives on silicon dioxide and silicon nitride CMP. *Microelectronic engineering*, 2010, vol. 87, no 12, p. 2633-2637.

[94] LEE, Gi Sub, HWANG, HyunHee, SON, Chang Hyun, *et al.* The effect of slurry composition and flatness on sub-surface damage and removal in chemical mechanical polishing of 6H-SiC. In : *Materials Science Forum*. Trans Tech Publications Ltd, 2009. p. 605-608.

[95] KUNTZSCH, Timo, WITNIK, Ulrike, HOLLATZ, Mark, *et al.* Characterization of Slurries Used for Chemical-Mechanical Polishing (CMP) in the Semiconductor Industry. *Chemical Engineering & Technology: Industrial Chemistry-Plant Equipment-Process Engineering-Biotechnology*, 2003, vol. 26, no 12, p. 1235-1239.

[96] ILIESCU, Ciprian, POENAR, Daniel P., et SELVAN, Subramanian Tamil. Frequency dependence on the accuracy of electrical impedance spectroscopy measurements in microfluidic devices. *Journal of Micromechanics and Microengineering*, 2009, vol. 20, no 2, p. 022001.

[97] DOI, T., MARINESCU, I. D., et KUROKAWA, S. The current situation in ultra-precision technology–silicon single crystals as an example. In book: Advances in CMP Polishing Technologies. 2012.

[98] TSAI, Ming Yi et HOO, Zuan Tang. Polishing single-crystal silicon carbide with porous structure diamond and graphene-TiO 2 slurries. *The International Journal of Advanced Manufacturing Technology*, 2019, vol. 105, p. 1519-1530.

[99] JINDAL, A., HEGDE, S., et BABU, S. V. Chemical mechanical polishing using mixed abrasive slurries. *Electrochemical and Solid-State Letters*, 2002, vol. 5, no 7, p. G48.

[100] JIANXIU, S. U., JIAXI, D. U., HAINA, L. I. U., *et al.* Research on material removal rate of CMP 6H-SiC crystal substrate (0001) Si surface based on abrasive alumina (Al2O3). *Procedia Engineering*, 2011, vol. 24, p. 441-446.

[101] RUSSELL, Allen S. et LEWIS, John E. Abrasive characteristics of alumina particles. *Industrial& Engineering Chemistry*, 1954, vol. 46, no 6, p. 1305-1310.

[102] ZHANG, Zefang, LIU, Weili, SONG, Zhitang, *et al.* Two-step chemical mechanical polishing of sapphire substrate. *Journal of the Electrochemical Society*, 2010, vol. 157, no 6, p. H688.

[103] DHALL, Atulet SELF, William. Cerium oxide nanoparticles: a brief review of their synthesis methods and biomedical applications. *Antioxidants*, 2018, vol. 7, no 8, p. 97.

[104] ZHOU, Yunyun. *Nanostructured cerium oxide based catalysts: synthesis, physical properties, and catalytic performance*. The University of Nebraska-Lincoln, 2015.

[105] BORRA, Chenna Rao, VLUGT, Thijs JH, YANG, Yongxiang, *et al.* Recovery of cerium from glass polishing waste: a critical review. *Metals*, 2018, vol. 8, no 10, p. 801.

[106] MULLINS, David R. The surface chemistry of cerium oxide. *Surface Science Reports*, 2015, vol. 70, no 1, p. 42-85.

[107] DATTA, Sukanya et TORRENTE-MURCIANO, Laura. Nanostructured faceted ceria as oxidation catalyst. *Current opinion in chemical engineering*, 2018, vol. 20, p. 99-106.

[108] RENUKA, NeeroliKizhakayil. Structural characteristics of quantum-size ceria nano particles synthesized via simple ammonia precipitation. *Journal of Alloys and Compounds*, 2012, vol. 513, p. 230-235.

[109] RAMANATHAN, S. et ROY, S. K. Ceria powders by homogeneous precipitation technique. *Transactions of the IndianCeramic Society*, 2003, vol. 62, no 2, p. 88-91.

[110] FLEMING, P. G., HOLMES, J. D., OTWAY, D. J., *et al.* The complex synthesis and solid-state chemistry of ceria–lanthana solid solutions prepared via a hexamethylenetetramine precipitation. *Journal of Solid State Chemistry*, 2011, vol. 184, no 9, p. 2595-2600.

[111] CHEN, Huey-Inget CHANG, Hung-Yi. Synthesis of nanocrystalline cerium oxide particles by the precipitation method. *Ceramics International*, 2005, vol. 31, no 6, p. 795-802.

[112] WALTON, Richard I. Solvothermal synthesis of cerium oxides. *Progress in Crystal Growth and Characterization of Materials*, 2011, vol. 57, no 4, p. 93-108.

[113] DEVARAJU, M. Kempaiah, YIN, Shu, et SATO, Tsugio. Morphology control of cerium oxide particles synthesized via a supercritical solvothermal method. *ACS appliedmaterials& interfaces*, 2009, vol. 1, no 11, p. 2694-2698.

[114] Dunn, A. J. A. *The controlled hydro/solvothermal synthesis of ceria-based materials.*PhD thesis. Department of Chemistry, University of Warwick, September 2018.

[115] LI, Qing, HAN, Zhaohui, SHAO, Mingwang, *et al.* Preparation of cerium hydroxycarbonate by a surfactant-assisted route. *Journal of Physics and Chemistry of Solids*, 2003, vol. 64, no 2, p. 295-297.

[116] BAKIZ, Bahcine, GUINNETON, Frédéric, DALLAS, Jean-Pierre, *et al.* From cerium oxycarbonate to nanostructured ceria: relations between synthesis, thermal process and morphologies. *Journal of Crystal Growth*, 2008, vol. 310, no 12, p. 3055-3061.

[117] HE, Hong-Wei, WU, Xiao-Qing, REN, Wei, *et al.* Synthesis of crystalline cerium dioxide hydrosol by a sol-gel method. *Ceramics International*, 2012, vol. 38, p. S501-S504.

[118] MACA, Karel, CIHLAR, Jaroslav, CASTKOVA, Klara, *et al.* Sintering of gadolinia-doped ceria prepared by mechanochemical synthesis. *Journal of the EuropeanCeramic Society*, 2007, vol. 27, no 13-15, p. 4345-4348.

[119] LU, Jun et FANG, Zhigang Zak. Synthesis and Characterization of Nanoscaled Cerium (IV) Oxide via a Solid-State Mechanochemical Method. *Journal of the American Ceramic Society*, 2006, vol. 89, no 3, p. 842-847.

[120] DANIELIS, Maila, COLUSSI, Sara, DE LEITENBURG, Carla, *et al.* The effect of milling parameters on the mechanochemical synthesis of Pd–CeO 2 methane oxidation catalysts. *Catalysis Science & Technology*, 2019, vol. 9, no 16, p. 4232-4238.

[121] AMINZARE, M., AMOOZEGAR, Z., et SADRNEZHAAD, S. K. An investigation on the influence of milling time and calcination temperature on the characterization of nano cerium oxide powder synthesized by mechanochemical route. *MaterialsResearch Bulletin*, 2012, vol. 47, no 11, p. 3586-3591.

[122] HIELSCHER, Thomas. Ultrasonic production of nano-size dispersions and emulsions. *arXiv preprint arXiv:0708.1831*, 2007.

[123] DAPKUNAS, Stanley J., JILLAVENKATESA, A., et LUM, L. H. Particle size characterization. *NIST Recommended Practice Guide. doi: https://doi. org/10.6028/NBS. SP*, 2001, p. 960-1.

[124] Nogowski, A., Stintz, M., &Barthel, H. *Large particle counting for quality control of CMP slurries.* In: International Conference on Planarization/CMP Technology, October 25–27, 2007, Dresden, Germany. Berlin-Offenbach: VDE VERLAG GMBH.

[125] MERKUS, Henk G. *Particle size measurements: fundamentals, practice, quality*. Springer Science & Business Media, 2009.

[126] MERKUS, Henk G. et MERKUS, Henk G. Particle size, size distributions and shape. *Particle Size Measurements: Fundamentals, Practice, Quality*, 2009, p. 13-42.

[127] TRIVEDI, Mahendra Kumar, SETHI, Kalyan Kumar, PANDA, Parthasarathi, *et al.* A comprehensive physicochemical, thermal, and spectroscopic characterization of zinc (II) chloride using X-ray diffraction, particle size distribution, differential scanning calorimetry, thermogravimetric analysis/differential thermogravimetric analysis, ultraviolet-visible, and Fourier transform-infrared spectroscopy. *International Journal of Pharmaceutical Investigation*, 2017, vol. 7, no 1, p. 33.

[128] PARK, Chuljin, KIM, Hyoungjae, LEE, Sangjik, *et al.* The influence of abrasive size on high-pressure chemical mechanical polishing of sapphire wafer. *International Journal of Precision Engineering and Manufacturing-Green Technology*, 2015, vol. 2, p. 157-162.

[129] KIM, Changmin, CHOI, Sungwon, CHOI, Jeongan, *et al.* Development of a single particle sizing system for monitoring abrasive particles in chemical mechanical polishing process. *Journal of Mechanical Science and Technology*, 2023, vol. 37, no 3, p. 1317-1324.

[130] COETSIER, C. M., TESTA, Fabrice, CARRETIER, Emilie, *et al.* Static dissolution rate of tungsten film versus chemical adjustments of a reused slurry for chemical mechanical polishing. *Applied surface science*, 2011, vol. 257, no 14, p. 6163-6170.

[131] BELKHIR, N., BOUZID, D., et HEROLD, V. Wear behavior of the abrasive grains used in optical glass polishing. *Journal of MaterialsProcessing Technology*, 2009, vol. 209, no 20, p. 6140-6145.

[132] HE, Qiang. Experimental study on polishing performance of CeO2 and nano-SiO2 mixed abrasive. *Applied Nanoscience*, 2018, vol. 8, no 1, p. 163-171.

[133] Opila, Robert Leon, ed. "Chemical mechanical planarization in IC device manufacturing III: Proceedings of the International Symposium." The Electrochemical Society, 2000.

[134] LEE, Manhee, KIM, Dongwon, HEO, Tae-Young, *et al*. Universal inherent fluctuations in statistical counting of large particles in slurry used for semiconductor manufacturing. *Scientific Reports*, 2020, vol. 10, no 1, p. 14731.

[135] KIM, Andy, MURAI, Koh, PARKIN, Michael, *et al.* Real-time, continuous large particle monitoring for CMP slurry quality control. In : *2012 SEMI Advanced SemiconductorManufacturingConference*. IEEE, 2012. p. 227-230.

[136] GRANSTROM, Jimmy, OONISHI, Shogo, TADA, Masaki, *et al.* Particle size distribution shift as a predictor of slurry stability. In : *2015 International Conference on Planarization/CMP Technology (ICPT)*. IEEE, 2015. p. 1-4.

[137] KHOSHNEVISAN, K. et BARKHI, M. Information about zetapotential. *Encycl. Membr*, 2015, p. 2063-2064.

[138] TADROS, Tharwat F. *Applied surfactants: principles and applications*. John Wiley & Sons, 2006.

[139] SPRYCHA, Ryszard. Electrical double layer at alumina/electrolyte interface: I. Surface charge and zeta potential. *Journal of colloid and interface science*, 1989, vol. 127, no 1, p. 1-11.

[140] LEVIN, A. D., ALENICHEV, M. K., MASALOV, V. M., *et al.* Developing of standard reference materials of the electrokinetic (Zeta) potential of nanoparticles. *Nanotechnologies in Russia*, 2018, vol. 13, p. 90-95.

[141] HEIMANN, Robert B. Classic and advanced ceramics: from fundamentals to applications. John Wiley & Sons, 2010.

[142] ADAMCZYK, Zbigniew et WEROŃSKI, Paweł. Application of the DLVO theory for particle deposition problems. *Advances in colloid and interface science*, 1999, vol. 83, no 1-3, p. 137-226.

[143] TREFALT, Gregoret BORKOVEC, Michal. Overview of DLVO theory. *Laboratory of Colloid and Surface Chemistry, University of Geneva, Switzerland*, 2014, vol. 304.

[144] LARSSON, Mats, HILL, Adrian, et DUFFY, John. Suspension stability; why particle size, zeta potential and rheology are important. *Annual transactions of the Nordicrheology society*, 2012, vol. 20, no 6.

[145] HUNTER, Robert J. Measuring zeta potential in concentrated industrial slurries. *Colloids and Surfaces A: Physicochemical and Engineering Aspects*, 2001, vol. 195, no 1-3, p. 205-214.

[146] KIRBY, Brian J. et HASSELBRINK JR, Ernest F. Zeta potential of microfluidic substrates: 1. Theory, experimental techniques, and effects on separations. *Electrophoresis*, 2004, vol. 25, no 2, p. 187-202.

[147] CACUA, Karen, ORDOÑEZ, Fredy, ZAPATA, Camilo, *et al.* Surfactant concentration and pH effects on the zeta potential values of alumina nanofluids to inspect stability. *Colloids and Surfaces A: Physicochemical and Engineering Aspects*, 2019, vol. 583, p. 123960.

[148] HABIB, Ishaq Yusuf, KUMARA, N. T. R. N., LIM, Chee Ming, *et al.* Dynamic light scattering and zeta potential studies of ceria nanoparticles. *Solid State Phenomena*, 2018, vol. 278, p. 112-120.

[149] WANG, Li-Pang, CHEN, Yan-Jhang, TSO, Yun-Chen, *et al.* Separation of Cerium Oxide Abrasive and Glass Powder in an Abrasive-Glass Polishing Waste by Means of Liquid–Liquid–Powder Extraction Method for Recovery: A Comparison of Using a Cationic and an Anionic Surfactant Collector. *Sustainability*, 2020, vol. 12, no 11, p. 4662.

[150] APONTE, Álvaro Guzmán, RAMÍREZ, María A. Llano, MORA, Yuliana Cadavid, *et al.* Cerium oxide nanoparticles for color removal of indigo carmine and methylene blue solutions. *AIMS Materials Science*, 2020, vol. 7, no 4.

[151] INSTRUMENTS, Malvern, *et al.* Zeta potential: An Introduction in 30 minutes. *Zetasizer Nano Serles Tech. Note. MRK654*, 2011, vol. 1, no 2, p. 1-6.

[152] LIN, F., NOLAN, L., XU, Z., *et al.* A study of the colloidal stability of mixed abrasive slurries and their role in CMP. *Journal of the Electrochemical Society*, 2012, vol. 159, no 5, p. H482.

[153] PABST, W. et GREGOROVA, E. J. I. P. Characterization of particles and particle systems. *ICT Prague*, 2007, vol. 122, p. 122.

[154] ZAINITH, Prabhakaret MISHRA, Niraj Kumar. Experimental investigations on stability and viscosity of carboxymethyl cellulose (CMC)-based non-Newtonian nanofluids with different nanoparticles with the combination of distilled water. *International Journal of Thermophysics*, 2021, vol. 42, no 10, p. 137.

[155] Chen, G., Ni, Z., Xu, L., Li, Q., & Zhao, Y. (2015). Performance of colloidal silica and ceria based slurries on CMP of Si-face 6H-SiC substrates. *Applied Surface Science*, *359*, 664-668.

[156] Bouzid, D., Belkhir, N., &Aliouane, T. (2012, February). Optical glass surfaces polishing by cerium oxide particles. In *IOP Conf. Materials Science and Engineering, Mahdia* (p. 012007).

[157] Lee, J., Kim, E., Bae, C., Seok, H., Cho, J., Aydin, K., & Kim, T. (2023). Improvement of oxide chemical mechanical polishing performance by increasing Ce3+/Ce4+ ratio in ceria slurry via hydrogen reduction. Materials Science in Semiconductor Processing, 159, 107349.

[158] Murata, J., &Goda, K. (2019). Abrasive-free surface finishing of glass using a Ce film. Journal of Materials Processing Technology, 265, 56-62.

[159] Cook, L. M. (1990). Chemical processes in glass polishing. Journal of non-crystalline solids, 120(1-3), 152-171.

[160] Suda, S., Sugimoto, T., Masuda, A., &Sagane, F. (2014, November). Surface conductivity of ceria abrasives during glass polishing. In Proceedings of International Conference on Planarization/CMP Technology 2014 (pp. 83-86). IEEE.

[161] Sabia, R., & Stevens, H. J. (2000). Performance characterization of cerium oxide abrasives for chemical-mechanical polishing of glass. Machining science and technology, 4(2), 235-251.

[162] Pal, R. K., Garg, H., Sarepaka, R. V., &Karar, V. (2016). Experimental investigation of material removal and surface roughness during optical glass polishing. Materials and Manufacturing Processes, 31(12), 1613-1620.

[163] Zhang, Z., Liu, W., & Song, Z. (2010). Effect of abrasive particle concentration on preliminary chemical mechanical polishing of glass substrate. Microelectronic Engineering, 87(11), 2168-2172.

[164] Wang, H., Zhao, Q., Xie, S., Zhou, H., & He, Y. (2020). Effect of abrasive particle size distribution on removal rate of silicon wafers. ECS Journal of Solid State Science and Technology,

9(12), 124001.
[165] Suratwala, T., Steele, W., Feit, M., Shen, N., Dylla‐Spears, R., Wong, L., ...&Elhadj, S. (2016). Mechanism and simulation of removal rate and surface roughness during optical polishing of glasses. Journal of the American Ceramic Society, 99(6), 1974-1984.
[166] Sampurno, Y., Sudargho, F., Zhuang, Y., Ashizawa, T., Morishima, H., &Philipossian, A. (2009). Effect of cerium oxide particle sizes in oxide chemical mechanical planarization. Electrochemical and Solid-State Letters, 12(6), H191.
[167] Kim, H. J., Kim, H. Y., Jeong, H. D., Lee, E. S., & Shin, Y. J. (2002). Friction and thermal phenomena in chemical mechanical polishing. Journal of Materials Processing Technology, 130, 334-338.
[168] Sreeremya, T. S., Prabhakaran, M., & Ghosh, S. (2015). Tailoring the surface properties of cerium oxide nanoabrasives through morphology control for glass CMP. RSC advances, 5(102), 84056-84065.
[169]Wang, Y. G., Zhang, L. C., &Biddut, A. (2011). Chemical effect on the material removal rate in the CMP of silicon wafers. Wear, 270(3-4), 312-316.
[170] Pal, R. K., Kumar, M., &Karar, V. (2023). Experimental investigation and modeling of friction coefficient and material removal during optical glass polishing. Arabian Journal for Science and Engineering, 48(3), 3255-3268.
[171] Wang, Y., Zhang, B., Wu, P., Xie, M., Li, Y., & Li, H. (2022, June). Study on Preparation and Polishing Performance of Ceria Slurry. In 2022 China Semiconductor Technology International Conference (CSTIC) (pp. 1-3). IEEE.
[172] Liu, M., Zhang, B., Liu, S., Cui, D., Xian, W., Wu, P., & Wang, Y. (2023, June). Research on the Dispersion Stability and Polishing Performance of Ceria Slurry. In 2023 China Semiconductor Technology International Conference (CSTIC) (pp. 1-3). IEEE.
[173] Bakier, M. A., Suzuki, K., &Khajornrungruang, P. (2021). Study on Nanoparticle Agglomeration During Chemical Mechanical Polishing (CMP) Performance. Journal of Nanofluids, 10(3), 420-430.
[174] Wakamatsu, K., Kurokawa, S., Toyama, T., & Hayashi, T. (2019). CMP characteristics of quartz glass substrate by aggregated colloidal ceria slurry. Precision Engineering, 60, 458-464.
distribution during glass polishing. Journal of the American Ceramic Society, 100(7), 2790-2802.
[175] Liang, S., Jiao, X., Tan, X., & Zhu, J. (2018). Effect of solvent film and zeta potential on

interfacial interactions during optical glass polishing. Applied Optics, 57(20), 5657-5665.
[176] Zhang, Z., Yu, L., Liu, W., & Song, Z. (2010). Surface modification of ceria nanoparticles and their chemical mechanical polishing behavior on glass substrate. Applied Surface Science, 256(12), 3856-3861.
[177] Evans, C. J., Paul, E., Dornfeld, D., Lucca, D. A., Byrne, G., Tricard, M., ...&Mullany, B. A. (2003). Material removal mechanisms in lapping and polishing. *CIRP annals*, *52*(2), 611-633.
[178] Suratwala, T., Steele, W., Feit, M., Shen, N., Dylla-Spears, R., Wong, L., ...&Elhadj, S. (2016). Mechanism and simulation of removal rate and surface roughness during optical polishing of glasses. *Journal of the American Ceramic Society*, *99*(6), 1974-1984.
[179] Barany, S., Bohacs, K., Chepurna, I., &Meszaros, R. (2016). Electrokinetic properties and stability of cerium dioxide suspensions. RSC advances, 6(73), 69343-69351.
[180] Lee, Y., Seo, Y. J., Lee, H., &Jeong, H. (2016). Effect of diluted colloidal silica slurry mixed with ceria abrasives on CMP characteristic. *International Journal of Precision Engineering and Manufacturing-Green Technology*, *3*, 13-17.
[181]Moinpour, M., Tregub, A., Oehler, A., &Cadien, K. (2002). Advances in characterization of CMP consumables. *MRS bulletin*, *27*(10), 766-771.
[182] Becker, E., Prange, A., &Conradt, R. (2009). Chemical-Mechanical polishing of optical glasses. *MRS Online Proceedings Library (OPL)*, *1157*, 1157-E03.
[183] Nabavi, M., Spalla, O., &Cabane, B. (1993). Surface chemistry of nanometric ceria particles in aqueous dispersions. *Journal of colloid and interface science*, *160*(2), 459-471.
[184] Gulicovski, J. J., Bračko, I., &Milonjić, S. K. (2014). Morphology and the isoelectric point of nanosized aqueous ceria sols. *Materials chemistry and physics*, *148*(3), 868-873.
[185] Kaszuba, M., Corbett, J., Watson, F. M., & Jones, A. (2010). High-concentration zeta potential measurements using light-scattering techniques. *Philosophical transactions of the royal society a: mathematical, physical and engineering sciences*, *368*(1927), 4439-4451.
[186] Tantra, R., Schulze, P., &Quincey, P. (2010). Effect of nanoparticle concentration on zeta-potential measurement results and reproducibility. *Particuology*, *8*(3), 279-285.
[187] Lowry, G. V., Hill, R. J., Harper, S., Rawle, A. F., Hendren, C. O., Klaessig, F., ...& Rumble, J. (2016). Guidance to improve the scientific value of zeta-potential measurements in nanoEHS. *Environmental Science: Nano*, *3*(5), 953-965.
[188] Xu, J., Harmer, J., Li, G., Chapman, T., Collier, P., Longworth, S., & Tsang, S. C. (2010).

Size dependent oxygen buffering capacity of ceria nanocrystals. Chemical communications, 46(11), 1887-1889.
[189] Mullins, D. R. (2015). The surface chemistry of cerium oxide. Surface Science Reports, 70(1), 42-85.
[190] Dawkins, K., Rudyk, B. W., Xu, Z., &Cadien, K. (2015). The pH-dependant attachment of ceria nanoparticles to silica using surface analytical techniques. Applied Surface Science, 345, 249-255.
[191] Chen, G., Ni, Z., Bai, Y., Li, Q., & Zhao, Y. (2017). The role of interactions between abrasive particles and the substrate surface in chemical-mechanical planarization of Si-face 6H-SiC. RSC advances, 7(28), 16938-16952.
[192] Wang, L. P., Chen, Y. J., Jiang, Y. H., & Tso, Y. C. (2019). Separation of ultrafine ceria-based abrasive particles from glass polishing powder waste through liquid–liquid–powder extraction. Separation and Purification Technology, 211, 63-70.
[193] Buettner, K. M., Rinciog, C. I., &Mylon, S. E. (2010). Aggregation kinetics of cerium oxide nanoparticles in monovalent and divalent electrolytes. Colloids and Surfaces A: Physicochemical and Engineering Aspects, 366(1-3), 74-79.
[194] Gensdarmes, F. (2015). Methods of detection and characterization. In Nanoengineering (pp. 55-84). Elsevier.
[195] CHEN, Yang, LU, Jinxia, et CHEN, Zhigang. Preparation, characterization, and oxide CMP performance of composite polystyrene-core ceria-shell abrasives. *Microelectronic Engineering*, 2011, vol. 88, no 2, p. 200-205.
[196] KONG, Chun et LEONG, Yee-Kwong. On the flocculation and agglomeration of ceria dispersion. *Journal of dispersion science and technology*, 2011, vol. 32, no 9, p. 1235-1238.
[197] WANG, Lin, ZHOU, Ping, YAN, Ying, *et al.* Investigation on nanoscale material removal process of BK7 and fused silica glass during chemical-mechanical polishing. *International Journal of Applied Glass Science*, 2021, vol. 12, no 2, p. 198-207.
[198] OEY, Tandre, HSIAO, Yi-Hsuan, CALLAGON, Erika, *et al.* Rate controls on silicate dissolution in cementitiousenvironments. *RILEM Technical Letters*, 2017, vol. 2, p. 67-73.
[199] YAN, Weixia, ZHANG, Zefang, GUO, Xiaohui, *et al.* The effect of pH on sapphire chemical mechanical polishing. *ECS Journal of Solid State Science and Technology*, 2015, vol. 4, no 3, p. P108.

[200] ZHANG, Zefang, LIU, Weili, et SONG, Zhitang. Particle size and surfactant effects on chemical mechanical polishing of glass using silica-based slurry. *AppliedOptics*, 2010, vol. 49, no 28, p. 5480-5485.

[201] KOUASSI, SekaSimplice, ANDJI, JONAS, BONNET, Jean-Pierre, *et al.* Dissolution of waste glasses in high alkaline solutions. *Ceramics-Silikáty*, 2010, vol. 54, no 3, p. 235-240.

[202] GIN, Stéphane, DELAYE, Jean-Marc, ANGELI, Frédéric, *et al.* Aqueous alteration of silicate glass: state of knowledge and perspectives. *npj Materials Degradation*, 2021, vol. 5, no 1, p. 42.

[203] FOURNIER, Maxime, DUCASSE, Thomas, PEREZ, Anne, *et al.* Effect of pH on the stability of passivating gel layers formed on International Simple Glass. *Journal of Nuclear Materials*, 2019, vol. 524, p. 21-38.

[204] Zhao, Jun, Jinfeng Huang, Rui Wang, HaoRan Peng, Wei Hang, and Shiming Ji. "Investigation of the optimal parameters for the surface finish of K9 optical glass using a soft abrasive rotary flow polishing process." *Journal of Manufacturing Processes* 49 (2020): 26-34.

[205] Shiou, Fang-Jung, and Assefa Asmare. "Parameters optimization on surface roughness improvement of Zerodur optical glass using an innovative rotary abrasive fluid multi-jet polishing process." *Precision Engineering* 42 (2015): 93-100.

[206] Duan, Bo, Jianwei Zhou, Yuling Liu, Mingbin Sun, and Yufeng Zhang. "Surface roughness of optical quartz substrate by chemical mechanical polishing." *Journal of Semiconductors* 35, no. 11 (2014): 116001.